OPIC
OFFICE DE LA PROPRIÉTÉ
INTELLECTUELLE DU CANADA

CIPO
CANADIAN INTELLECTUAL
PROPERTY OFFICE

*Bureau canadien
des brevets*

Certification

*Canadian Patent
Office* CA99/716

Certification

La présente atteste que les documents
ci-joints, dont la liste figure ci-dessous,
sont des copies authentiques des docu-
ments déposés au Bureau des brevets.

This is to certify that the documents
attached hereto and identified below are
true copies of the documents on file in
the Patent Office.

Specification and Drawings, as originally filed, with Application for Patent Serial No:
2,260,572, on January 29, 1999, by **NATIONAL RESEARCH COUNCIL CANADA**
assignee of Roger Guevremont, and Randy W. Purves, for "Apparatus And Method For
Atmospheric Pressure 3-Dimensional Ion Trapping".

PRIORITY
DOCUMENT
SUBMITTED OR TRANSMITTED IN
COMPLIANCE WITH RULE 17.1(a) OR (b)

Agent certificateur/Certifying Officer

September 14, 1999

Date

ABSTRACT OF THE DISCLOSURE

...

Title: Apparatus and Method for Atmospheric Pressure
3-Dimensional Ion Trapping

FIELD OF THE INVENTION

The present invention relates to an apparatus and method for
5   trapping ions, at atmospheric pressure, within a defined 3-dimensional
space, based on the ion focusing principles of high field asymmetric
waveform ion mobility spectrometry, also known as transverse field
compensation ion mobility spectrometry, and as field ion spectrometry.

BACKGROUND OF THE INVENTION

10   High sensitivity and amenability to miniaturization for
field-portable applications have helped to make ion mobility spectrometry
an important technique for the detection of many compounds, including
narcotics, explosives, and chemical warfare agents (see, for example, G.
Eiceman and Z. Karpas, *Ion Mobility Spectrometry* (CRC. Boca Raton, FL.
15   1994); and *Plasma Chromatography*, edited by T.W. Carr (Plenum, New
York, 1984)). In ion mobility spectrometry, gas-phase ion mobilities are
determined using a drift tube with a constant electric field. Ions are gated
into the drift tube and are subsequently separated based upon differences
in their drift velocity. The ion drift velocity is proportional to the field
20   strength at low electric fields (e.g., 200 V/cm) and the mobility, K, which is
determined from this experiment, is independent of the applied field. At
high electric fields (e.g. 5000 or 10000 V/cm), the ion velocity is no longer
directly proportional to the applied field, and K becomes dependent upon
the applied electric field (see G. Eiceman and Z. Karpas, *Ion Mobility
25   Spectrometry* (CRC. Boca Raton, FL. 1994); and E.A. Mason and E.W.
McDaniel, *Transport Properties of Ions in Gases* (Wiley, New York, 1988)).
At high electric fields, K is better represented by K_h, a non-constant high
field mobility term. The dependence of K_h on the applied electric field has
been the basis for the development of high field asymmetric waveform
30   ion mobility spectrometry (FAIMS), a term used by the inventors
throughout this disclosure, and also referred to as transverse field

compensation ion mobility spectrometry, or field ion spectrometry (see I. Buryakov, E. Krylov, E. Nazarov, and U. Rasulev, Int. J. Mass Spectrom. Ion Phys. 128. 143 (1993); D. Riegner, C. Harden, B. Carnahan, and S. Day, Proceedings of the 45th ASMS Conference on Mass Spectrometry and Allied Topics, Palm Springs, California, 1-5 June 1997, p. 473; B. Carnahan, S. Day, V. Kouznetsov, M. Matyjaszczyk, and A. Tarassov, Proceedings of the 41st ISA Analysis Division Symposium, Framingham, MA, 21-24 April 1996, p. 85; and B. Carnahan and A. Tarassov, U.S. Patent Number 5 420 424). Ions are separated in FAIMS on the basis of the difference in the mobility of an ion at high field K_h relative to its mobility at low field K. That is, the ions are separated because of the compound dependent behaviour of $K_{h,}$ as a function of the electric field. This offers a new tool for atmospheric pressure gas phase ion studies since it is the change in ion mobility and not the absolute ion mobility that is being monitored.

One application of this tool is in the area of 3-dimensional ion trapping at atmospheric pressure. To the inventors' knowledge, there are no previously known devices or methods that produce any sort of a 3-dimensional ion trap at atmospheric pressure (about 760 torr). While other 3-dimensional ion trapping mechanisms do exist, these known ion traps are typically designed to operate below 1 torr, in near-vacuum conditions. The efficiency, and thus usefulness of these known mechanisms, degrades extremely rapidly as the pressure increases beyond 10 torr, and there is no experimental or theoretical basis to suggest that any trapping occurs, using these known methods, at 760 torr.

SUMMARY OF THE INVENTION

••••

BRIEF DESCRIPTION OF THE DRAWINGS

Figure 1 shows three possible examples of changes in ion mobility as a function of the strength of an electric field;

Figure 2 illustrates the trajectory of an ion between two

parallel plate electrodes;

Figures 3A and 3B show schematically a prior art FAIMS device;

Figure 4 illustrates two opposite waveform modes, P1 and P2, which may be used with the apparatus of Figures 3A and 3B;

Figures 5A and 5B show schematically the coupling of the FAIMS apparatus of Figures 3A and 3B together with a mass spectrometer;

Figures 6A and 6B show schematically a FAIMS apparatus for measuring the ion distribution between the outer and inner cylinders, referred to as the FAIMS-R1-prototype;

Figures 7A and 7B illustrate the high voltage, high frequency asymmetric waveform applied to the FAIMS apparatus shown in Figures 6A and 6B;

Figure 8 illustrates varying ion arrival time profiles at the innermost ion collector electrode of the FAIMS apparatus in Figures 6A and 6B;

Figures 9A and 9B show schematically a first embodiment of a 3-dimensional atmospheric pressure high field asymmetrical waveform ion trap, referred to as the FAIMS-R2-prototype;

Figures 10A through 10I show the experimental results for extraction of ions trapped using the FAIMS apparatus of Figures 9A and 9B, with voltages ranging from +1 V to +30 V;

Figures 11A-11C show a second embodiment of a 3-dimensional atmospheric pressure high field asymmetrical waveform ion trap, referred to as the FAIMS-R3-prototype;

Figure 11D shows a timing diagram for a voltage applied to the FAIMS apparatus of Figures 11A-11C;

Figure 12 shows an alternative embodiment of the FAIMS apparatus of Figures 11A-11C, having a simplified electrospray ionization chamber, and using the sampler cone as an extraction grid;

Figure 13A is a schematic view of a system comprising an apparatus similar to the FAIMS apparatus disclosed in Figure 12, and a

time-of-flight (TOF) mass spectrometer;

Figure 13B shows a timing diagram for control of the FAIMS apparatus and the TOF mass spectrometer of Figure 13A;

Figure 13C illustrates a typical TOF mass spectrum acquired using the system shown in Figure 13A;

Figure 13D illustrates a compensation voltage spectrum of an ion with a TOF flight time of 27μs;

Figure 13E shows graphically the results of an experiment designed to determine the overall response time of the system shown in Figure 13A;

Figures 13F and 13G illustrate experimental verification of the 3-dimensional ion trap using the system of Figure 13A;

Figures 13H, 13I and 13J, show the intensity of the TOF peak for variable ion trapping periods from 1 ms to 60 ms, at several compensation voltages;

Figures 14A-14C show schematically an alternative embodiment of a 3-dimensional atmospheric pressure high field asymmetric waveform ion trap;

Figure 15 shows the relevant dimensions of a FAIMS apparatus required for calculation of the voltage within the FAIMS analyzer region;

Figure 16 shows the change in the ion mobility of $(H_2O)_nH^+$ for a given K_h/K ratio and an electric field E;

Figures 17A-17C provide a portion of the original data that was used to calculate the high field mobility K_h of $(H_2O)_nH^+$;

Figures 18A-18D show the trajectory of an ion with the high electric field properties shown by the curves in Figure 16;

Figures 19A-19D illustrate ion trajectory calculations near the terminus of an inner electrode, calculated using the FAIMS apparatus and method described in Figures 11A-11D;

Figures 19E-19I illustrate the results ion trajectory calculations near the terminus of an inner electrode, using various sampler cone

voltages in the FAIMS apparatus shown in Figure 13A;

Figure 19J shows an example of an unusual shape of a FAIMS device designed to establish conditions for ion trapping or focusing;

Figures 20A and 20B show examples of a calculation for illustrating the ion focusing and trapping effect near the terminus of an inner electrode, calculated using the FAIMS apparatus and method described in Figures 11A-11D;

Figure 21 is a graph plotting the optimum combinations of CV and DV for $(H_2O)_nH^+$, based on data collected by a series of CV scans as shown in Figure 17A;

Figure 22A illustrates the electric field due to DV radially across the FAIMS analyzer region for a given FAIMS apparatus;

Figure 22B is a graph showing the electric fields due to DV and CV plotted against each other at several radial locations in the FAIMS analyzer region;

Figure 22C is a graph showing the intersection of the actual conditions and optimum conditions for DV and CV;

Figure 23 shows a segmented FAIMS apparatus for transporting ions along the FAIMS analyzer region; and

Figure 24 shows a schematic of a segmented FAIMS apparatus for trapping ions within the FAIMS analyzer region.

DETAILED DESCRIPTION OF THE INVENTION

As an important preliminary note, the discussion below uses the term "ion" to mean a charged atomic or molecular entity. The "ion" can be any electrically charged particle, solid or liquid, of any size. The discussion always refers to the "ion" as positively charged. However, all of the discussion in this document is equally applicable to negative ions, but with the polarity of applied voltages being reversed. This is a trivial issue, and the application of the discussion below, to negative ions, can be understood by anyone skilled in the art.

The principles of operation for FAIMS have been described in

Buryakov *et. al.* (see I. Buryakov, E. Krylov, E. Nazarov, and U. Rasulev, Int. J. Mass Spectrom. Ion Phys. 128. 143 (1993)) and are summarized here briefly. The mobility of a given ion under the influence of an electric field can be expressed by: $K_h(E) = K(1+f(E))$, where K_h is the mobility of an ion at

5   high field, K is the coefficient of ion mobility at zero electric field and "f(E)" describes the functional dependence of the ion mobility on the electric field (see E.A. Mason and E.W. McDaniel, *Transport Properties of Ions in Gases* (Wiley, New York, 1988); and I. Buryakov, E. Krylov, E. Nazarov, and U. Rasulev, Int. J. Mass Spectrom. Ion Phys. 128. 143 (1993)).

10   Referring to Figure 1, three possible examples of changes in ion mobility as a function of the strength of an electric field are shown: the mobility of type A ions increases with increasing electric field strength; the mobility of type C ions decreases; and the mobility of type B ions increases initially before decreasing at yet higher fields. The separation of

15   ions in FAIMS is based upon these changes in mobility at high electric fields. Consider an ion, for example a type A ion 1 in Figure 1, that is being carried by a gas stream between two parallel plate electrodes 2, 4 as shown in Figure 2. The net motion of the ion 1 between the plates 2, 4 is the sum of a horizontal x-axis component due to the flowing stream of gas 6 and a

20   transverse y-axis component due to the electric field between the plates 2, 4. (The term "net" motion refers to the overall translation that the ion 1 experiences, even when this translational motion has a more rapid oscillation superimposed upon it.) One of the plates is maintained at ground potential (here, the lower plate 4) while the other (here, the upper

25   plate 2) has an asymmetric waveform, V(t), applied to it. The asymmetric waveform is composed of a high voltage component lasting for a short period of time t_2 and a lower voltage component, of opposite polarity, lasting a longer period of time t_1. The waveform is synthesized such that the integrated voltage-time product (thus the field-time product) applied

30   to the plate during a complete cycle of the waveform is zero (i.e., $V_1 t_1 + V_2 t_2 = 0$); for example +2000 V for 10 μs followed by -1000 V for 20 μs. Figure 2 illustrates the ion trajectory 8 (as a dashed line) for a portion of

the waveform shown as $V(t)$. The peak voltage during the shorter, high voltage portion of the waveform will be called the "dispersion voltage" or DV in this disclosure. During the high voltage portion of the waveform, the electric field will cause the ion 1 to move with a transverse velocity component $v_1 = K_h E_{high}$, where E_{high} is the applied field, and K_h is the high field mobility under ambient electric field, pressure and temperature conditions. The distance travelled will be $d_1 = v_1 t_2 = K_h E_{high} t_2$, where t_2 is the time period of the high applied high voltage. During the longer duration, opposite polarity, low voltage portion of the waveform, the velocity component of the ion will be $v_2 = K E_{low}$, where K is the low field ion mobility under ambient pressure and temperature conditions. The distance travelled is $d_2 = v_2 t_1 = K E_{low} t_1$. Since the asymmetric waveform ensures that $(V_1 t_1) + (V_2 t_2) = 0$, the field-time products $E_{high} t_2$ and $E_{low} t_1$ are equal in magnitude. Thus, if K_h and K are identical, d_1 and d_2 are equal, and the ion 1 will be returned to its original position relative to the y-axis during the negative cycle of the waveform (as would be expected if both portions of the waveform were low voltage). If at E_{high} the mobility $K_h > K$, the ion 1 will experience a net displacement from its original position relative to the y-axis. For example, positive ions of the type A shown in Figure 1 will travel further during the positive portion of the waveform (i.e., $d_1 > d_2$) and the type A ion 1 will migrate away from the upper plate 2 (as shown by the dashed line in Figure 2). Similarly, ions of type C will migrate towards the upper plate 2.

If an ion of type A is migrating away from the upper plate 2, a constant negative dc voltage can be applied to this plate 2 to reverse, or "compensate" for thistransverse drift. This dc voltage, called the "compensation voltage" or CV in this disclosure, prevents the ion 1 from migrating towards either plate 2, 4. If ions derived from two compounds respond differently to the applied high electric fields, the ratio of K_h to K is different for each compound. Consequently, the magnitude of the compensation voltage necessary to prevent the drift of the ion toward either plate 2, 4 will also be different for each compound. Under

conditions in which the compensation CV voltage is appropriate for transmission of one compound, the other will drift towards one of the plates 2, 4 and subsequently be lost. The speed which the compound will move to the wall of the plates 2, 4 depends on the degree to which its high

5   field mobility properties differ from those of the compound that will be allowed to pass under the selected condition. Thus, a FAIMS instrument or apparatus is an ion filter capable of selective transmission of only those ions with the appropriate ratio of K_h to K.

The FAIMS concept was first shown by Buryakov *et. al.* using

10   flat plates as described above. Later, Carnahan *et. al.* improved the sensor design by replacing the flat plates used to separate the ions with concentric cylinders (see B. Carnahan, S. Day, V. Kouznetsov, M. Matyjaszczyk, and A. Tarassov, Proceedings of the 41st ISA Analysis Division Symposium, Framingham, MA, 21-24 April 1996, p. 85; and B. Carnahan and A.

15   Tarassov, U.S. Patent Number 5 420 424). The concentric cylinder design has several advantages including higher sensitivity than the flat plate configuration (see R.W. Purves, R. Guevremont, S. Day, C.W. Pipich, and M.S. Matyjaszczyk, Rev. Sci. Instrum., 69, 4094 (1998)). An instrument based on the concentric cylinder design has been built by Mine Safety

20   Appliances Company for trace gas analysis, with the name Field Ion Spectrometer (FIS®). For the purposes of this disclosure, this instrument is referred to as FAIMS-E, where E refers to an electrometer detection device.

The term FAIMS, as used in this disclosure, refers to any

25   device which has the capability of ion focusing or trapping using the mechanism based on high electric field ion mobility discussed above and further explained below. FAIMS also refers to any device which can separate ions via this mechanism, whether or not the device has focusing or trapping behaviour. One previous limitation of this cylinderical

30   FAIMS technology (see D. Riegner, C. Harden, B. Carnahan, and S. Day, Proceedings of the 45th ASMS Conference on Mass Spectrometry and Allied Topics, Palm Springs, California, 1-5 June 1997, p. 473; and B.

Carnahan, S. Day, V. Kouznetsov, M. Matyjaszczyk, and A. Tarassov, Proceedings of the 41st ISA Analysis Division Symposium, Framingham, MA, 21-24 April 1996, p. 85) was that the identity of several of the peaks appearing in the FAIMS-E CV spectra could not be unambiguously

5   confirmed due to the unpredictable changes in K_h at high electric fields, and an electrometer detector cannot determine the m/z of the detected ion (i.e. this detector is not a mass spectrometer).

FAIMS-E

Now referring to Figures 3A and 3B, the FAIMS-E apparatus
10 10 is shown schematically. The FAIMS-E apparatus 10 is composed of two inner cylinders or tubes 11, 12 which are axially aligned and positioned about 5 mm apart, and a long outer cylinder 13 which surrounds the two inner cylinders 11, 12. The inner cylinders 11, 12 (12 mm inner diameter, 14 mm outer diameter), are about 30 mm and 90 mm long, respectively,

15 while the outer cylinder 13 (18 mm i.d., 20 mm o.d.) is about 125 mm long. Ion separation takes place in the 2 mm annular space or FAIMS analyzer region 14 between the long inner cylinder 12 and the outer cylinder 13. In experiments conducted by the inventors, a corona discharge needle 15 (shown in Figures 3A and 3B) was placed in the center axis of the shorter

20 inner cylinder 11, terminating about 5 mm from the end of the short inner cylinder 11. The needle 15 was held at approximately +2000 V (1.2 μA).

As explained above, the FAIMS-E device 10 can be considered as an ion "filter", with the capability of selectively transmitting one type of ion out of a mixture. If a mixture of ions is presented continuously to the

25 entrance of the FAIMS analyzer region 14 for example by a corona needle 15, and the ions are carried along the length of the analyzer 14 by a flowing gas under conditions in which no voltages are applied to either the inner cylinder 11, 12 or outer cylinder 13 (i.e. the two are grounded), some finite level of transmission for every ion is expected, albeit without any

30 separation.

In theory, it is expected that the detected current of any

selected ion in this mixture should never exceed the current for that ion when it is transmitted through the device 10 in the no-voltages condition. Application of high voltages (i.e. application of transverse fields, perpendicular to the gas flows) designed to yield ion separation should not

5 increase the ion transmission, but should decrease transmission through collisions with the walls of the cylinder 11, 12, 13. That is, the asymmetric waveform effectively narrows the "width" of the FAIMS analyzer region 14, and therefore should decrease the ion transmission. However, contrary to this prediction, experiments have shown that the sensitivity of

10 ion detection in the cylindrical geometry FAIMS-E 10 increases as the voltage amplitude of the asymmetric waveform DV is increased. These unusual observations suggest that atmospheric pressure ion focusing is occurring in the FAIMS analyzer region 14. To the inventors' knowledge, this phenomenon has never been observed before. This phenomenon

15 could have many practical applications in the manipulation of ions at atmospheric pressure. For example, atmospheric pressure ion focussing could be used to improve the ion sampling efficiency of mass spectrometers that require transport of ions from atmospheric pressure to vacuum. These include atmospheric pressure ionization (API)

20 spectrometers and atmospheric pressure sampling mass spectrometers, most notably those used for electrospray ionization.

In the inventors experiments, electrospray ionization (ESI) was used alternatively, to replace the corona discharge needle 15. ESI is a technique that involves the transfer of ions from solution to the gas phase

25 through a sequence of events. Several related methods for creating gas-phase ions from solution exist. These methods include, among others, ionspray, nanospray, and thermospray. In this disclosure, the term ESI will be used to simplify the discussion, and will encompass any of the techniques named above (and others that are related) that create gas phase

30 ions from solution. Any of these techniques can replace the electrospray hardware that is shown in the diagrams in this documents. In the inventors' experiments, the ESI needle had a 100 μm (i.d.) stainless steel

capillary which liquid samples were pumped through at approximately 1 μL/min. The ESI needle was typically maintained at approximately +1500V (50 nA).

Still referring to Figures 3A and 3B, four gas connections to

5   the FAIMS-E apparatus 10 are shown. Compressed gas (e.g. air or nitrogen) is passed through a charcoal/molecular sieve gas purification cylinder (not shown) into the FAIMS-E 10 through carrier in (C_{in}) and/or sample in (S_{in}) ports. The gas exits the FAIMS-E 10 via the carrier out (C_{out}) and/or sample out (S_{out}) ports. All four gas flow rates can be adjusted ($C_{in} + S_{in} =$

10   $C_{out} + S_{out}$). Volatile analytes are typically introduced into the FAIMS-E 10 through the S_{in} line, and a portion is ionized as the compound(s) pass by the corona discharge needle 15. Alternatively, non-volatile analytes are ionized using ESI. In both cases, positively charged ions, formed in the short inner cylinder surrounding the tip of either type of needle, are

15   driven radially outward by the electric field, whereas neutrals travel down the long inner cylinder 12 and exit via the S_{out} port. Neutrals are prevented from entering the annular FAIMS analyzer region 14 by a portion of the C_{in} flow which is directed radially inward through the 5 mm gap between the inner cylinders 11, 12, and exits via the S_{out} port. This

20   portion of the C_{in} gas flow that travels radially inward functions very much like the curtain gas flows used in the PE SCIEX atmospheric pressure ionization (API) mass spectrometer instrument (not shown). In the PE SCIEX instrument, the orifice into a vacuum is "protected" by a counter-current flow of gas which is travelling in a direction contrary to that of the

25   arriving ions. This counter-current of gas has the effect of removing water and solvent from the gas adjacent to the orifice into the vacuum, and it also has the effect of reducing the level of degree of solvation. A second method, called the "heated capillary" method (not shown), minimizes the solvation by heating the gas and ions as they pass into the vacuum via a

30   narrow bore capillary tube. This property of the FAIMS-E apparatus 10 identified by the inventors, namely the isolation of the ions in a clean dry gas, is very important since it permits the collection of high quality

electrospray CV spectra and ionization mass spectra, without the use of either a curtain gas *per se*, or the use of a heated capillary tube.

Still referring to Figures 3A and 3B, the outer cylinder of the FAIMS-E apparatus 10, and the shorter inner cylinder 11, are typically held
5 at an adjustable electrical potential (V_{FAIMS}). V_{FAIMS} is usually ground potential in FAIMS-E. During operation, a high frequency (200 kHz) high voltage (for example, 4950 V peak to peak) asymmetric waveform is applied to the long inner cylinder 12 to establish the electric fields between the inner and outer cylinders 11, 12, 13. This leads to the separation of ions
10 in the manner discussed earlier.

The FAIMS-E apparatus 10 operates using one of the two waveform modes, P1 and P2 (with the waveform applied to the inner cylinder), shown in Figure 4. Note, however, that these reversed polarity waveform modes P1, P2 do not yield "reversed polarity" CV spectra as
15 might be expected. This is because the reversal of polarity in this manner also creates a mirror image effect of the ion focusing behavior of FAIMS. The result of such polarity reversal is that the ions are not focused, but rather collide with the walls of the cylinders 11, 12, 13. The mirror image of a focusing valley, is a hill-shaped potential surface. While the ions will
20 slide to the center of the bottom of a focusing potential valley (in 2 or 3-dimensions), if the polarity is reversed, the ions will "slide off" of the top of a hill-shaped surface, and hit the wall of an electrode. This is the reason for the existence of the independent "modes" called 1 and 2. In this disclosure, mode 1 used with positive ions is called P1, and mode 2 used
25 with positive ions is called P2. Negative ions are separated in N1 and N2 modes.

As stated earlier the maximum peak voltage (typically +/- 3000 V) applied during the waveform is referred to as the dispersion voltage DV. In addition to the high frequency waveform shown in Figure
30 4, a dc offset voltage (i.e. the compensation voltage CV) is applied to the long inner cylinder 12, of Figures 3A and 3B.

Referring back to Figures 3A and 3B, some of the ions

produced by the corona discharge (or electrospray) ionization are carried by the gas stream along the length of the annular space between the outer cylinder 13 and the long inner cylinder 12, also referred to as the FAIMS analyzer region 14. If the combination of DV and CV are appropriate, and

5   the ion is not lost to the tube walls, a series of openings 16 near the downstream end of the outer cylinder 13 allow the ions to be extracted to an electrometer 17 which is biased to about -100 V. The compensation voltage CV is typically scanned from -50 V to +50 V, and the ions are sequentially transmitted through the FAIMS analyzer region 14 to register

10   as ion current at the electrometer 17.

FAIMS-MS

Now referring to Figures 5A and 5B, the coupling of FAIMS and a mass spectrometer (FAIMS-MS 20) is shown schematically. The FAIMS-MS 20 of Figures 5A and 5B, and the FAIMS-E 10 shown in Figures

15   3A and 3B, differ significantly only at the detection end of the instrument. The electrometer 17 has been replaced by a sampler cone 18, placed at the end of the FAIMS cylinders 11, 12, 13 as is shown in a simplified form in Figure 5B. The diameter of the orifice 19 in the sampler cone 18 is approximately 100 µm. The gas flows in the FAIMS-MS 20 are analogous

20   to those in the FAIMS-E 10 except that the C_{out} is divided into two components, namely the original C_{out} and the flow through the orifice 19 into the mass spectrometer 19A. The electrical waveforms applied to the long inner cylinder 12 are identical to those used in the FAIMS-E apparatus 10. The sampler cone 18 may be electrically insulated from the

25   other components so a separate voltage V_{OR} can be applied to it. Furthermore, a voltage can be applied to the cylinders of the entire FAIMS unit (V_{FAIMS}) for the purpose of enhancing the sensitivity of the FAIMS-MS.

FAIMS-R1-prototype

30   Now referring to Figures 6A and 6B, a special FAIMS

instrument was designed by the inventors and constructed for measuring the ion distribution between the two cylinders of a FAIMS device. This instrument will be referred to in this disclosure as the FAIMS-R1-prototype 30 and is illustrated schematically in Figures 6A and

5   6B. Ions were generated inside of an electrically grounded cylinder 31 approximately 35 mm long and 20 mm i.d.. The tip of the corona discharge needle 15 was typically located near the center of this tube, and at least 15 mm from the end of the FAIMS analyzer region 34. The FAIMS analyzer region 34 in this embodiment is composed of an outer tube 32 70

10   mm long and 6 mm i.d., which surrounds a 2 mm o.d. inner shield electrode 33. The inner shield electrode 33 is an electrically grounded stainless steel tube which is closed at the end that faces the corona discharge ionization chamber. This inner electrode 33 surrounds, and shields, an electrically isolated conductor 35 passing into its center. This

15   innermost conductor 35 (i.e the ion collector electrode) is a collector for ions, and is connected to a fast current amplifier or electrometer 36 (e.g. Keithly model 428) and a digital storage oscilloscope 37 (e.g. LeCroy model 9450).

In the system shown in Figures 6A and 6B, the ions which

20   surround the inner electrode 33 are forced inwards by a pulsed voltage. The ions travel from the FAIMS analyzer region 34 to the innermost conductor 35 through a series of 50 µm holes 38 drilled through the inner shield electrode. The holes drilled in the inner shield electrode 33 are positioned about 2 cm from the end facing the corona discharge, and are

25   spaced about 0.5 mm apart for a distance of 10 mm on the inner shield electrode 33. The holes 38 drilled in the inner shield electrode 33 are located in this manner to minimize the variability in distance between the inner shield electrode 33 and the outer cylinder 32 in the vicinity of these holes 38. It was our objective to measure the ion abundance profiles

30   of the ions located in the annular space (FAIMS analyzer region 34) between the inner shield electrode 33 and the outer electrode 32 by pulsing the ions toward the inner shield electrode 33 and through the holes 38 and

against the innermost ion collector electrode 35. The time-dependent distribution of ions arriving at the innermost conductor 35 is related to the physical radial distribution of ions around the inner electrode 33. Excessive variation in the distance between the two walls of the cylinders

5   33, 34 would have increased the uncertainty of the ion arrival times at the innermost conductor 35, thus decreasing the spacial resolution of the device.

Now referring to Figures 7A and 7B, the high voltage, high frequency asymmetric waveform DV, applied to the FAIMS-R1-prototype

10   of Figures 6A and 6B, is shown. The waveform is divided into two parts, the focusing period and the extraction period. The waveform was synthesized by an arbitrary waveform generator (e.g. Stanford Research Systems model DS340, not shown) and amplified by a pulse generator (e.g. Directed Energy Inc., model GRX-3.0K-H, not shown). The frequency of

15   the waveform, and the relative duration of the high and low voltage portions of the waveform could easily be modified. Because of the high voltages, and steep rise-times of the square waves applied to this FAIMS-R1-prototype 30, the power consumption limits were severe, and waveforms in excess of about 1330 pulses (16 ms at 83,000 Hz) could not be

20   delivered by this system without over-heating electronic components of the high voltage pulse generator.

Note that, in the case of the FAIMS-R1-prototype 30, the high voltage, high frequency asymmetric waveform was applied to the outer cylinder 32 of the FAIMS-R1-prototype 30 shown in Figures 6A and 6B.

25   Since all other forms of FAIMS discussed in this disclosure have the waveform applied to the inner tube or electrode, confusion may arise from the "polarity" of the waveform and the polarity of CV. In the FAIMS-R1-prototype 30 shown in Figures 6A and 6B, ions of type A (shown in Figure 1) are focussed during application of the opposite

30   polarity waveform and CV than that shown for the devices in Figures 3A, 3B, 5A and 5B. Nevertheless, for simplification, the polarity will be written to be the same as if the device was constructed in the same way as

those of the more conventional configuration. In other words the ions of P1 modes will appear with DV positive and with CV negative. (Please note, however, that the actual voltages used on the device in Figures 6A and 6B are P1 mode with DV negative and CV positive).

5   As was observed in the conventional parallel plate FAIMS apparatus (Figure 2), the application of a high voltage asymmetric waveform DV will cause ions to migrate towards one of the FAIMS electrodes 2, 4 because of the changes in ion mobility at high electric fields (shown in Figures 1 and 2). This migration can be stopped by applying an

10   electric field or compensation voltage CV in a direction to oppose the migration. For the FAIMS-R1-prototype 30 of Figures 6A and 6B, this CV was applied to the same electrode as the high voltage asymmetric waveform (i.e. the outer electrode 32), and was added to the waveform as a small dc bias (up to ± 50 V). At an appropriate combination of DV, and

15   compensation voltage CV, a given ion will pass through the FAIMS device 30. The unit therefore acts like an ion filter. It is possible to fix conditions such that a single type of ion flows uniformly out of the exit of the FAIMS 30 although a mixture of ions are presented to the inlet of the FAIMS analyzer region 34.

20   The second part of the waveform shown in Figures 7A and 7B (i.e. the extraction period) was used to pulse the ions out of the FAIMS analyzer region 34 between the outer electrode, and the inner shield electrode (shown in Figures 6A and 6B). At the end of the focusing period, i.e. after 16 ms of waveform, the asymmetric waveform was replaced by a

25   constant dc bias of approximately +30 V. This caused the ions from the annular space between the outer electrode and the inner shield electrode to move in the direction of the inner shield electrode 33. A detector bias of -5 V, applied to innermost ion collector electrode 35, helped to carry the ions from the vicinity of the holes 38 in the inner shield electrode,

30   through the holes 38 and into contact with the innermost ion collector electrode 35. The +30 V bias created an electric field of approximately 150 V/cm across the FAIMS analyzer region 34 and most ions located within

this region 34 travelled across the 2 mm space in about 1 ms. The ion current due to the arrival of ions at the center inner shield electrode 33 can be predicted. For example, if only one type of ion, with mobility of 2.3 cm^2/V-s, e.g., $(H_2O)_nH^+$ at ambient temperature and pressure conditions,

5 was located in the FAIMS analyzer region 34, and if this ion was distributed evenly in the space, an approximately square-topped signal lasting approximately 0.6 ms should be observed. The signal should be generally square-topped, although the electric fields between the tubes are not uniform, because the first ions to arrive are located near the center

10 electrode, and are driven by a higher electric field than their more numerous counterparts (ions per volume) at greater radial distance, which arrive later, but in larger numbers. Deviation from this expected ion arrival profile would suggest that the ions were distributed in non-uniform profile across the FAIMS analyzer region 34 between the

15 outer and inner cylinders of the FAIMS 30.

Still referring to Figures 6A, 6B, 7A and 7B, the FAIMS-R1-prototype 30 was operated as follows. A 2L/min flow of purified air was passed into the chamber 31 housing the corona discharge needle 15. Approximately 2000 V was applied to the needle 15, and the

20 voltage was adjusted to produce a stable corona discharge. The high voltage asymmetric waveform was applied to the outer FAIMS cylinder 32 for approximately 16 ms; this was followed by a 2 ms extraction pulse (Figure 7A). The ion current striking the innermost ion collecting electrode 35 was detected and displayed on a digital oscilloscope 37. A

25 measurement would typically consist of 100 averaged spectra, collected at a rate of approximately 5 Hz. Many experimental parameters were varied, including gas flow rates, the voltages of the asymmetric waveform DV, the dc voltage applied to the outer electrode CV, and the extraction voltage. Figure 8 illustrates the ion arrival times at the innermost ion collector

30 electrode 35 observed by conducting these experiments. Each trace was recorded with 2500 V applied DV, but with variable CV voltages. As can be seen, during application of DV and CV, the radial distribution of ions is

not uniform across the annular space of the FAIMS analyzer region 34. For example, at CV near -11 V, the ions are focused into a narrow band near the inner electrode 33, and therefore are detected as a high intensity pulse occurring very early after the extraction voltage has been applied. At low CV, for example at -5.6 V, the ions are much more uniformly distributed between the walls of the concentric cylinders 32 33 making up the FAIMS analyzer region 34. Near -2.5 V applied CV, the ions should be almost uniformly distributed across the FAIMS analyzer region 34. When no electrical voltages are applied to the cylinders 32, 33, the radial distribution of ions should be approximately uniform across the FAIMS analyzer region 34. This experiment is evidence that the ion focusing is indeed occurring in FAIMS instruments. This focusing results in the ions being focused in a uniform "sheet" or band around the inner cylinder 33 of the FAIMS analyzer.

The 3-Dimensional Atmospheric Pressure Ion Trap

The gas flows between the cylinders of the FAIMS devices described above serve to carry the ions from one end of the device to the other end. In every case the action of the electric fields is perpendicular to the transporting motion of the gas flow. This is the reason the early devices were referred to as "transverse field" ion spectrometers. The present invention is the result of attempts to convert the 2-dimensional ion focusing action of the FAIMS-E 10 and FAIMS-R1-prototype 30 into a 3-dimensional trap by ensuring that the ions are caught in a physical location in which the gas flows and the electrical fields are not perpendicular, but rather act in opposition to each other. This creates the situation in which the ion cannot progress in any direction whatsoever. This is the 3-dimensional atmospheric pressure ion trap.

Note that, in this disclosure, the term "ion focusing" is restricted to a 2-dimensional configuration. That is, if the ions are "focused", they will be restricted to a sheet-like structure, and the thin, flat sheet can extend in any direction, for any distance. For example, if ions are

"focused" around the external surface of a long metallic cylinder, this will mean that they are restricted to be within a cylindrical space (composed of the ions) which is coaxial to, or surrounding the metallic cylinder. This sheet of ions will extend as far as the cylinder, and all around it

5 continuously. On the other hand, in this disclosure the term "ion trapping" is restricted to the condition that an ion cannot move freely in any direction in 3-dimensional space. This is more restrictive than "focusing", in which the ion is free to move anywhere in the 2-dimensions e.g. along the length of the cylinder described in the example

10 noted above or around the cylinder at a fixed radius.

3-dimensional ion traps for operation in vacuum chambers of mass spectrometers are well known, and several geometry's exist. However, the mechanism and operation of these vacuum-ion-traps is vastly different from that of the atmospheric pressure (760 torr) version of

15 the ion trap described in this document. The physical geometry, the layout of the hardware components, and the electrical voltages applied in known 3-dimensional ion traps are in no way related to the present atmospheric version of the ion trap. Several embodiments of the 3-dimensional atmospheric pressure ion trap of the present invention will

20 be considered below.

FAIMS-R2-Prototype

Referring to Figures 9A and 9B, the device which will be referred to as the FAIMS-R2-prototype 40 is shown. Here, the asymmetric waveform DV and the compensation voltage CV are applied to the inner,

25 solid, electrode 42, having a diameter of about 2 mm. The outer, electrically grounded electrode 43 has an inner diameter of about 6 mm, thereby allowing an annular space of about 2 mm between the electrodes. This annular space has been referred to as the FAIMS analyzer or FAIMS analyzer region 14, 34, 44 in the discussion above, and for simplicity we

30 will continue to use this terminology. The ions are created by corona discharge using a corona needle 15 in a closed cell (not shown) located

adjacent to a 0.5 mm hole through the wall of the outer cylinder. As shown in Figure 9A, ions are driven by the high electric field generated by the corona discharge needle 15 (held at about + 2000 V), through the 0.5 mm hole 45, and into the FAIMS analyzer region 44 (only those ions travelling directly toward the hole 45 are shown for simplicity). Inside the FAIMS analyzer region 44, near this hole 45, the electric fields and the gas flow (shown to be flowing from right to left in Figures 9A and 9B) are perpendicular to each other and the ions experience the 2-dimensional focusing effect described in the sections above in relation to the FAIMS-R1-prototype 30. However the inner electrode 42 in the device shown in Figure 9A, terminates about 5 mm from the end of the outer electrode 43. The inner surface of the outer electrode 43 at the downstream end is contoured in such a way as to maintain approximately the same electric fields (i.e. created by the application of DV and CV) as would be experienced along the length of the FAIMS analyzer region 44. The end of the outer electrode has an exit grid 46 comprising a hole (about 2 mm) which is covered with a fine, high transmission metallic screen. The gas flowing through the device 40 also flows freely through the grid 46 and exits from the space between the outer electrode 43 and a collector plate 47. In the absence of any applied voltages (i.e. DV and CV) the ions will travel through the device very much as shown in Figure 9A. The ions enter the analyzer region 44, flow with the gas out through the exit grid 46 of the outer electrode 43, and the few remaining ions are attracted to an ion collector plate 47 biased at about -5 V. The collector plate 47 was connected to a high gain current amplifier or electrometer 36 (e.g. Keithly 428) and an oscilloscope 37.

The application of an asymmetric waveform of the type shown in Figures 7A and 7B resulted in the ion focusing behavior described above for the conventional FAIMS-E 10 and FAIMS-R1-prototype 30, except that the focusing action extends around the generally spherically shaped terminus 42T of the inner electrode 42, as shown in Figure 9B. This means that the ions cannot escape from the region

around the terminus 42T of the inner electrode 42. This will only occur if the voltages applied to the inner electrode 42 are the appropriate combination of CV and DV as described in the discussion above relating to 2-dimensional focusing. If the CV and DV are suitable for the focusing of

5   an ion in the FAIMS analyzer region 44, and the physical geometry of the inner surface of the outer electrode 43 shown in Figures 9A and 9B does not disturb this balance, the ions will collect near the terminus 42T as shown in Figure 9B. Several contradictory forces are acting on the ions in this region near the terminus 42T of the inner electrode 42. The ion cloud

10   shown near the terminus 42T of the inner electrode 42 in Figure 9B would like to travel from right to left to the exit grid 46 in the manner shown in Figure 9A, because of the force of the gas flow. This also means that the ions cannot migrate back from left to right, toward the corona ion source 15. The ions that get too close to the inner electrode 42 are pushed back

15   away from the electrode 42, and those near the outer electrode 43 will migrate back towards the inner electrode 42, because of the application of the negatively polarized CV. The ions are captured in every direction, either by forces of the flowing gas, or by the electric fields (electric potential well) of the FAIMS mechanism.

20   Note that, while the above discussion refers to the ions as being "captured", in fact, the ions (and neutrals) are subject to 'diffusion'. Diffusion always acts contrary to focusing and trapping. The ions will always require an electrical, or gas flow force to reverse the process of diffusion. This means that although the ions may be focused into an

25   imaginary cylindrical zone in space (with zero thickness), or within a 3-dimensional ion trap, in reality it is well known that the ions will actually be dispersed in the vicinity of this idealized zone in space because of diffusion. This means that ions will always be "distributed" over some region, rather than all precisely located in the same place. This is

30   important, and should be recognized as a global feature superimposed upon all of the ion motions discussed in this document. This means that, for example, a 3-dimensional ion trap will actually have real spacial width,

and leak for several physical, and chemical reasons.

Expanding on the chemical effects in FAIMS, if an ion collides with a neutral molecule and temporarily forms a stable complex, this complex may drift out of the FAIMS focusing or trapping region 5 because this new complex has high field mobility properties which are different from the original ion. This means that the complex may have behavior at high electric field (see Figure 1) which differs from the original simple parent ion. For example (at the extreme) the original ion may be of type A, and the new complex of the type C shown in Figure 1. If this is the 10 case, the new complex will not be trapped at the prevailing DV and CV conditions. The collision of any of these ions with the walls of the device will soon result in loss of the ions from the trap. Although the original ion itself may continue to be trapped, the removal of this ion via "chemical" effects is entirely possible, and is the reason the FAIMS 15 analyzer will fail in the presence of significant water vapor or contaminants in the gas flows. The FAIMS analyzer works best in very clean conditions.

Now referring to Figures 10A through 10I, experimental results with the FAIMS-R2-prototype 40 are shown. The dimensions of 20 the electrodes were described above, for Figures 9A and 9B. DV was approximately 2000 V, CV was -12 V, and the gas flow through the device was 0.9 L/min. The DV and CV were applied to the inner electrode for about 16 ms, then these voltages were replaced by an extraction voltage applied to the inner electrode. The DC extraction voltage applied to the 25 inner electrode 42 pushes the ions away from the inner electrode 42 towards the exit grid 46, whereby the gas flow carries these ions through the grid 46 (with some percentage of the ions lost in a collision with this grid 46). The traces in Figure 10A through 10I represent results for the ions extracted with voltages ranging from +1 V (Figure 10A) to +30 V (Figure 30 10I), and measured using an electrometer detector. The extraction of trapped ions results in a positive pulse 48 recorded in Figures 10A-10I. The negative pulse 49 shown in the figures is the electronic transient noise

that occurs when the DV and CV voltage are removed and replaced by the extraction voltage. It is clear from the data shown in Figures 10A-10I that an increase in the extraction voltage will yield a shorter, more intense ion signal 48. This occurs since the ions are pulsed out of the trap more

5   vigorously with the +30 V than the +1 V. The experimental results shown in Figures 10A-10I verify the hypothesis that a cloud of ions accumulates near the terminus 42T of the inner electrode 42. A pulse of ions, as shown in Figure 10I, could not be extracted from the FAIMS-R2-prototype 40 unless some ions were available near the terminus 42T of the inner

10 electrode 42.

FAIMS-R3-Prototype

Now referring to Figures 11A through 11C, the FAIMS-R3-prototype 50 is shown. This device is configured for detection by mass spectrometry, and a sampler cone 18, through which gas and ions

15 are pulled into the vacuum chamber of a mass spectrometer is shown on the left side of Figures 11A-11C. The right side of the vacuum housing, and sampling cone 18, is at atmospheric pressure. The left side of those components is labelled "Mass Spectrometric Vacuum Housing", and is typically below 1 torr pressure. In most systems a second orifice (not

20 shown) leads the actual mass analyzer region of the mass spectrometer which is usually below 10^{-5} torr pressure.

The FAIMS-R3-prototype analyzer 50 shown in Figure 11A consists of an inner, solid, cylindrical electrode 52 of about 2 mm diameter, and an outer electrode 53 which is about 6 mm inner diameter. The center

25 electrode 52 is powered, through an electrical connection, by an RF asymmetric waveform generator power supply 55. Both DV and CV are supplied by this generator 55. The waveforms, and the timing diagram are shown in Figure 11D. As shown in Figure 11D, the asymmetric waveform is applied continuously to the inner electrode 52. No other

30 variation of the voltage (other than manual selection of various CV and DV settings) is applied to the inner electrode 52.

- 24 -

Referring back to Figure 11A, gas enters the FAIMS-R3-prototype 50 from the right side and flows along the annular space comprising the FAIMS analyzer region 54, and out through the open end of the outer electrode 53. Adjacent to the open end (left side) of the outer

5 cylinder 53 is an exit grid 56 comprising a fine, thin-wired metallic grid which is electrically isolated from the outer electrode 53, and has an electrical connection to a grid electric pulse generator power supply 57. The voltage on the grid 56 can be changed step-wise using this power supply. The grid voltage and timing diagram is shown in Figure 11D. The

10 grid is typically maintained between -5 and +5 V during the ion storage time shown in Figure 11D. The grid will then be stepped (100 ns transition) to between -5 V and -50 V in order to extract the ions from the 3-dimensional atmospheric pressure trap which is located at the spherical terminus of the inner electrode. Figure 11B shows schematically the

15 approximate location of the ions during the storage period. It should be kept in mind that the ions trapped here must have the correct high field ion mobility (see Figure 1) so that their "net" motion is zero at the combination of CV and DV being applied to the storage device (the term "net" is used because the ion is constantly moving back-and-forth due to

20 the application of the asymmetric waveform: if the ion returns to the same location repeatedly, then the "net" motion caused by the application of DV and CV is zero). For example, the ions of type $(H_2O)_nH^+$ will be stored in the geometry shown in Figure 11A-11C at a DV of about +2000 V and a CV of approximately -10 V (typical of P1 mode). At conditions very different

25 (e.g. at DV 2500 and CV -5 V) from this combination of DV and CV the $(H_2O)_nH^+$ ions will not assemble into one physical location as shown in Figure 11B. Instead, these ions will collide with the walls in the FAIMS analyzer region 54. At a second set of DV and CV conditions, such as the DV 2500 and CV -5 V noted above, another ion (e.g.(Leucine)H^+) may be

30 able to collect at the tip 52T of the inner electrode 52 as shown in Figure 11B.

As explained earlier, near the terminus 52T of the inner

electrode 52 shown in Figure 11B, the ions are restricted in motion because of several contrary forces. The gas flowing along the FAIMS analyzer region 54 applies a force which will prevent migration of ions from the left to right (Figure 11B) back toward the ion source, and this force will also

5   tend to pull the ions out of the trap towards the exit grid shown at the left end of the outer electrode. The electrical forces characteristic of FAIMS maintain the ions at a fixed distance from the sides of the inner electrode 52: (1) the ions which are too distant from the inner electrode 52 are attracted to the inner electrode 52 because of the negative polarity of the

10   applied dc offset, i.e. a negative CV; and (2) the ions close to the inner electrode 52 are pushed away because of the increase of the ion mobility at high field (see Figure 1) assuming the ions are of type P1. Details of the ion motions are presented below.

Figure 11C illustrates the removal of ions from the

15   3-dimensional atmospheric pressure trap via a stepwise change to the voltage applied to the grid electrode 56. If the voltage applied to the grid 56 is decreased from, say, 0 V to -15 V as shown in the timing diagram Figure 11D, the ion trap is reduced or eliminated, and the ions are free to escape under the influence of the gas flow, or by the electric field which might

20   pull the ions toward the exit grid 56.

The FAIMS-R3-prototype 50 shown in Figures 11A-11C is appropriate for detection of ions produced by electrospray ionization (ESI). FAIMS is highly sensitive to moisture and contaminants in the gas entering the analyzer region. It is usual that contaminants, or too much

25   water vapor, will result in complete loss of signal, and failure of the FAIMS to function in the manner described in this document. Since electrospray ionization involves the high-voltage-assisted-atomization of a solvent mixture, the amount of water and other volatile solvents is far too high to be tolerated in the FAIMS. This will mean that the ESI-FAIMS

30   combination will always require a type of gas-isolation, curtain gas, or counter-current gas flow, to prevent neutral solvent molecules from entering the FAIMS analyzer. One method to accomplish this is shown in

Figures 11A-11C. The FAIMS is separated from the ESI chamber 60 by a small chamber 61 which has provision for gas inlets 62 and gas outlets 63. If a flow of gas enters this intermediate chamber 61, and a portion of the gas flows toward the ESI chamber, then the neutral solvent molecules will

5   exit via the port on the ESI chamber, and will be prevented from entering the vicinity of the entrance to the FAIMS. The electrospray needle 15A, shown in Figures 11A-11C is more likely to be in a horizontal plane or lower than the FAIMS analyzer region 54, rather than the higher, vertical position shown. This minimizes the tendency for very large droplets to

10   fall via gravity, into the FAIMS analyzer region 54. In a horizontal or lower configuration the large droplets will fall into the bottom of the ESI chamber 60, which could (optionally) have a drain for removal of excess solvent.

       The counter-current of gas can be achieved in a second way

15   shown in Figure 12 (gas flows are emphasized, and most of the ions are omitted). If the FAIMS analyzer gas flow is adjusted so that some of the gas will exit the FAIMS analyzer region 34 into the ESI chamber 60, the entrance of neutral contaminants can be avoided. This may result in higher ion transmission than that for the device shown in Figures 11A-

20   11C, but the device may not be user-friendly since accidental gas flow adjustment such that the gas from the ESI chamber 60 is passed into the FAIMS analyzer region 54 may compromise FAIMS performance for some period of time (hours) after the accident. Note also that the exit grid electrode 56 (Figures 11A-11C) has not been shown in Figure 12. In this

25   embodiment the 'extraction' pulse that destroys the ion trap is applied to the mass spectrometer sampling cone 18.

FAIMS for Ion Trapping Experiments: Instrumental Overview

       Now referring to Figures 13A-13J, a system of using a time-of-flight (TOF) mass spectrometer, in conjunction with the FAIMS-R3-

30   prototype 50, is discussed. As shown in Figure 13A, the assembly of the FAIMS, the ion production, and gas controls are the same as shown in

Figure 12. For the purposes of further elucidation of the operating details of this system, and the experimental results, the diagram has been extended to show the internal components of the time-of-flight (TOF) mass spectrometer 70 used for this work. The timing diagram for control

5   of the dispersion voltage, compensation voltage, sampler cone voltage V_{OR}, and the TOF acceleration pulse appears in Figure 13B.

Figure 13A shows that there is an electrical connection to the sampler cone. This electrical connection is used to control the sampler cone voltage V_{OR}, the voltage used to gate the ions out of the ion trap. For

10   example, in a typical experiment, the V_{OR} may be set at +40 V during trapping of the ions and at +1 V for ion extraction (e.g., at FAIMS offset voltage +20 V, and compensation voltage -3 V). These voltages would be applied for time periods, for example, 40 ms for trapping and 10 ms for ion extraction. After the initiation of the ion extraction, a cloud of ions, which

15   was located near the terminus 52T of the inner electrode 52, would move towards the sampler cone 18. Because of the electric field between the sampler cone 18 and the FAIMS 50, and the high flow of gas through the sampler cone orifice 18A and into the vacuum system, some ions would be transported into the low pressure (1 torr) region between the sampler

20   cone 18 and the skimmer cone 71. The skimmer 71is typically held at ground potential. The 1 V difference between the sampler cone 18 and the skimmer 71 is sufficient to draw the ions through the skimmer 71, after which they enter a low pressure region (9×10^{-5} torr) and are transported to the entrance of the TOF acceleration region 72 via an octopole ion guide

25   73. The octopole guide 73 is operated at low pressure so that the delay and broadening of the pulse during transport of the pulse through the octopole 73 is minimized. The octopole 73 is typically operated using a DC offset of -4 V, and a 1.2 MHz applied waveform of 700 V (peak-to-peak) to confine the ions. An exit aperture lens of the octopole ion guide (not shown) is

30   held at -5.5 V. The ions pass through the octopole exit lens and through a series of grids which compose the ion acceleration region 72 of the TOF mass spectrometer 70.

Still referring to Figure 13A, the acceleration region 72 of the TOF is connected to two high voltage pulse generators 74A, 74B, and operates as follows. The device includes 3 fine mesh metal grids 72A, 72B, 72C. The grid 72C which is located closest to the flight tube is held at
5   constant ground potential. The other two grids 72A, 72B are each connected to a high voltage pulse generator 74A, 74B. The grids 72A, 72Bare found at two possible voltage states, controlled by external pulse generator digital logic 75. In one voltage state both of the grids 72A, 72B are held at one voltage, our experiments used -5.5 V. In this state, the ions
10   that travel from the exit lens of the octopole ion guide 73, will pass through the grids 72A, 72B. The grids 72A, 72B are also held at a second, high voltage condition obtained by applying a very rapid pulse (less than 0.1 µs risetime) of about 50 µs duration. There will be some ions which are located in the regions between these grids 72A, 72B when the pulse is
15   applied, and these ions will be accelerated in the direction of the flight tube 76 and the detector 77 shown in Figure 13A. These ions pass through the second grid 72B and are further accelerated because of the high electric field between the second grid 72B and the third grid 72C, which is at ground potential. Once these ions have passed out of the acceleration region 72,
20   and are travelling along the flight tube 76, the voltages on the two variable grids 72A, 72B in the acceleration region 72 are returned to the low voltage condition, and new ions can enter the space between the grids 72A, 72B. The grids 72A, 72B are typically maintained at high voltage for about 50 µs.

In principle, the ions which pass down the flight tube 76
25   separate according to mass because all of the ions have the same energy (as a first approximation), defined by the voltage drop between the pulsed voltage grids 72A, 72B and the fixed grounded grid 72C. The ion energy is defined by $E_i = mv^2/2$, therefore changes in ion mass, m, are accompanied by changes in the ion velocity, v, in order to keep E_i, the energy, constant.
30   The ions arrive at the TOF detector 77 in sequence of ion mass. The lowest mass ions have the highest velocity and arrive at the detector 77 first, and the highest mass ions arrive last.

In practice, however, not the all of the ions leaving the acceleration region 72have identical voltages. The ions have energy in part dictated by their starting location between the two pulsed acceleration grids. This difference in energy allows the device the capability of 'spacial' focusing, which means that all of the ions with a given m/z, regardless of their starting position in space, will reach the detector 77 simultaneously. This use of the word 'focusing' in this context is much like the focusing of light in an optical system (e.g., camera). Ions accelerated from between the second grid 72B and the grounded grid 72C have a wide range of energy and contribute to unwanted 'background' noise. This is minimized by locating the second grid 72B very close (2 mm) to the grounded grid 72C.

The TOF acceleration region 72 is pulsed at fixed delay times following the pulse applied to the sampler cone 18 (V_{OR}). There will be a finite delay time for the pulse of ions to be extracted from FAIMS 50, pass through the vacuum interface 18, 71, through the octopole 73, and into the acceleration region 72. TOF mass spectra are collected at a series of delay times after the extraction pulse is applied to the sampler cone 18. The arrival of the pulse of ions is characterized by the appearance of a strong, transient signal, followed by a decay of signal intensity down to a constant signal which corresponds to the uniform signal which would be detected if the sampler cone was held at the low voltage (i.e., +1 V) state continuously.

TOF Mass Spectra, and CV Spectra for the Study of Ion Trapping

An experimental condition was selected for the study of ion trapping in FAIMS. The low mass ions produced by corona discharge ionization, particularly protonated water ions were at very high ion density (abundance), and were therefore expected to either fill the trap too rapidly, or have too short lifetimes for the present study. Therefore, it was decided to look for higher mass ions in P2 mode. The abundance of these ions were expected to be low since they were only formed from trace contaminants in the carrier gas. No additional sample compounds or

gases were added to the system. The ions studied here were formed by corona discharge ionization in the clean nitrogen atmosphere. The ion source, and the FAIMS device were operated in as clean a condition as possible.

5   Figure 13C illustrates a typical mass spectrum acquired for this study. The exact mass was not determined, since this would require a known calibration compound, however the approximate mass was determined using the flight times for some lower mass ions including the protonated water ions. Several impurity ions 81, 82 appear in the

10   spectrum, however only the ion 83 of highest abundance (flight time 27 µs) was considered for the present study. This ion 83 has a m/z of about 380 (±10 m/z).

Figure 13D illustrates the compensation voltage scan for detection of the ion 83 with flight time of 27 µs (m/z about 380) at an

15   applied dispersion voltage of -3500 V. This polarity of DV is referred to as P2 mode, and the ions typically passing through FAIMS in P2 mode usually have mass above m/z 300. The ions that are usually apparent in P2 mode have ion mobilities that decrease as the electric field increases (ion type C, Figure 1). One limitation of P2 mode is that the ions are

20   typically found at low CV, and therefore the strength of the ion trapping is weak. On the other hand, one advantage of higher mass ions is that the ion mobility is usually lower, and therefore the distances travelled during the application of the high voltage asymmetric waveform are reduced, and the rate of ion loss to the walls via diffusion is expected to be minimized.

25   The ion intensity at each experimental point in Figure 13D was acquired by averaging the spectra recorded from 5000 repeat TOF acceleration pulses. The compensation voltages were adjusted manually, with a digital voltmeter used to read out the voltages set by a power supply. Three traces appear in Figure 13D, corresponding to the collection

30   of compensation voltage sweeps in three operating methods including: (1) pulsed sampler cone with detection at 4.5 ms after the 'down' edge of the V_{OR}; (2) continuous ion transport from FAIMS through to the TOF with

the V_{OR} set at +1 V; and (3) continuous ion transport from FAIMS to the TOF with V_{OR} at +15 V. The compensation voltage corresponding to the maximum detected ion transmission was comparable for these three methods of data acquisition. The detection of the m/z 380 ion therefore required a compensation voltage between about -2.5 V and -4 V.

Ion Transport Delays within the Ion Optics of the TOF

Now referring to Figure 13E, the results of an experiment designed to determine the response time of the entire system are shown. The V_{OR} was stepped between two values, one (+15 V) which was suitable for ion transmission through the FAIMS and into the vacuum system, and the second voltage (-10 V) which was unsuitable for either trapping or ion transmission. Typical examples of V_{OR} were +15 V for transmission, and -10 V for non-transmission. Figure 13E illustrates the intensity of mass spectra collected at a series of time delays between the V_{OR} transitions of both possible types, namely from high to low voltage, and also from low to high voltage. For the discussion below, these transitions will be considered the 'down' and 'up' edges of the change in V_{OR}, respectively. The origin of the delay, and the length of delay, is different for the two cases. The reasons are considered next.

In the case of high to low voltage transition, 'down', which occurs at 40 ms in Figure 13E, the low voltage sampler cone 18 will prevent any (positively charged) ions from passing between the sampler cone 18 (i.e., V_{OR} at -10 V) and the skimmer cone 71 (at 0 V), and thus create an extremely abrupt decrease in ion flux passing into the octopole ion guide 73. At one extreme it might therefore be expected that the intensity of spectra taken by the TOF might decrease to zero abruptly. Experimentally, the abrupt decrease in ion density will be 'blurred' due to ions moving back into the low ion density region. This broadening is expected: (a) because not every ion will have identical kinetic energy, and those ions with slightly less energy will fall behind, and (b) because collisions between the ions and the residual gas within the octopole housing 73 will affect the

kinetic energy of some fraction of the ions. Since the octopole 73 is an ion guide, this longitudinal spreading will be accentuated since ions which have undergone collision with the residual gas will remain contained within the octopole 73. Because of their lowered kinetic energy, these ions

5 will travel through the octopole 73 and arrive at the acceleration region 72 of the TOF with long delay times. Figure 13E shows that the ions continue to arrive at the TOF acceleration grids for about 2 ms after the V_{OR} is shifted from +15 V down to -10 V. Note that this 'down' transition occurs at 40 ms on Figure 13E.

10 The 'up' voltage transition of the sampler cone from low to high voltage has a slightly different effect. This transition occurs at time 0 ms in Figure 13E. As shown in Figure 13E, the time required for the intensity of the TOF spectra to reach a plateau is about 10 ms. Several delays are expected. When V_{OR} is raised, the relatively low density of ions

15 which are located in front of the terminus 52T of the inner cylinder 52 of FAIMS 50 must be augmented by newly arriving ions which have been passing along the annular region 54 of the FAIMS cylinders 52, 53. Secondly those ions must start to pass through the sampler cone 18-skimmer 71 region, and subsequently through the octopole 73. From

20 the discussion of the 'down' edge of the V_{OR} pulse described above, it requires a minimum of 2 ms for changes in ion density (of the ion which is monitored) to be transmitted through the octopole 73. The additional time delays required prior to ion abundance increases in the TOF spectra (i.e., the difference between 2 ms and 10 ms) are therefore attributed to

25 delays in appearance of ions in front of the sampler cone 18, and secondly due to the transmission through the sampler cone 18-skimmer 71 region.

Experimental Verification of Ion Trapping in FAIMS

Now referring to Figures 13F and 13G, the experimental verification of the 3-dimensional ion trap located near the spherical

30 terminus 52T of the inner electrode 52 of the FAIMS 50 are illustrated. The experimental conditions for collection of the data for Figure 13F and

13G were identical, except that the carrier gas flow into FAIMS 50 was decreased for collection of Figure 13G. The data for these plots were collected in independent experiments, about 1 week apart.

5   The plots in Figure 13F and 13G show the measured intensity of the ion (about m/z 382) collected at various times after the 'down' transition of the sampler cone 18. The timing of these pulses is shown at the bottom of Figure 13F. Time zero represents the time at which the sampler sone 18 is pulsed from the high voltage state (V_{OR} = +40 V) to its low voltage state (V_{OR} = +1 volt), thereby extracting ions from the FAIMS

10   trap. The ions require about 5 ms to travel through the system to the TOF acceleration region 72. The pulse of ions is widened during passage, and appears to be about 3 ms wide (at half height) when detected by the present system. Considering the system response times determined in an earlier experiment, and shown in Figure 13E, a peak that is 3 ms wide has been

15   very poorly characterized in this system, and the absolute ion intensity is probably greatly underestimated.

Figures 13F and 13G also include two horizontal lines corresponding to collection of non-pulsing mode data at two different settings of V_{OR}. The lower intensity data was collected with V_{OR} = +1 V,

20   which corresponds to the 'low' state of the sampler cone 18 when operating in pulsed mode. The higher intensity, horizontal trace, was collected at an experimentally optimized setting for the sampler cone 18 (at V_{OR} = +15 V). At this setting the dc level of the sampler cone 18 resulted in the maximum possible TOF spectrum intensity. Note that the intensity

25   of signals for V_{OR} = +15 V for Figures 13F and 13G are comparable although the data was collected on different occasions and with different FAIMS gas flow conditions. Ion trajectory modelling has shown that the ions passing around the terminus 52T of the inner electrode 52 will be focused towards the center channel as they pass by the end of the electrode

30   52. In this way the ions will tend to be transmitted into the sampler cone orifice 18A leading to the vacuum with maximum sensitivity. An example of this trajectory calculation that indicates that this ion focusing

will occur is shown in Figure 19C and 19D (below). Nevertheless, considering the long response time of this system, probably requiring between 5 and 10 ms to reach maximum signal, the absolute amplitude of the signal of the short pulse of ions in pulsed mode is probably

5   substantially higher than the uniform flow of ions detected in continuous mode.

Ion Storage Time Period

An experiment was performed to determine the effect of the ion storage period on the intensity of the detected pulse of ions resulting

10 from extracting the ions from the storage zone near the end of the inner FAIMS electrode. The intensity of the TOF peak for the ion at flight time 27.0 μs, plotted as a function of the length of the storage time period is shown in Figures 13H, 13I and 13J. The waveform applied to the sampler cone 18 was composed of a constant period of time (10 ms) at low voltage

15 (V_{OR} = +1 V) during which the ions were permitted to enter the TOF. The signal intensity was measured by activating the TOF acceleration grids 72A, 72B about 4.5 ms after the sampler cone grid voltage V_{OR} was lowered. V_{OR} was held at a high value (V_{OR} = +40 V) for periods of time shown on the x-axis of Figures 13H-13J. Three traces appear in Figures 13H, 13I and

20 13J, corresponding to data collected at various settings of compensation voltage CV. The ion intensity for a non-optimum compensation voltage, CV = -4 V (Figure 13J), suggests that the ion trap is relatively inefficient, and the maximum number of ions which can be held in the trap is reached relatively rapidly, i.e., about 10 ms. On the other hand, at CV =

25 -3 V (Figure 13H) and -3.5 V (Figure 13I), the intensity rises for over 30 ms. This suggests that the lifetime of the ion, i.e., with drift time 27 μs, within the FAIMS ion trap is at least 5 ms. At high trapping times it is assumed that the trap has filled and that the influx of ions is balanced by losses by diffusion and gas flows. This experiment can be considered to be a simple

30 kinetics problem. The influx of ions is X ions/sec. The loss of ions, Y ions/sec, is proportional to the number of ions in the trap. The increase in

the number of ions in the trap, Z ions total, will continue until steady state is reached and $X = Y = kZ$, where k is the rate constant for the function describing the rate of ion loss from the trap. At a short delay time Z is small and kZ is small. It therefore can be assumed that $Z = Xt$ where t is

5   the time. The solution to the differential equation $dZ/dt = X - kZ$ is $Z(t) = X(1-e^{-kt})/k$, if Z at time zero is zero. The data set can be fit to this function to determine X and k. Figures 13H, 13I and 13J show the experimental data, and calculated curves based on the equation above used to fit the data. The k values were 0.06, 0.12 and 0.34 for the CV curves -3, -3.5 and -4

10   V respectively. The corresponding X values were 0.4, 0.72 and 0.8 respectively. High values of k represent conditions wherein the rate of ion loss is high. High values of X correspond to a high rate of ion input into the trap. It is not known how these parameters are related to each other. For example, the curve at CV -4 V corresponds to a high input rate of ions

15   into the trap, as shown by the very rapid rise of the curve during the first 10 ms. Despite this rapid rise, the final ion population in the trap may not be high because the rate of ion loss, k, is also high for these conditions.

FAIMS-R4-prototype

Now referring to an alternative embodiment shown in

20   Figures 14A-14C, referred to as FAIMS-R4-prototype 80, a FAIMS 3-dimensional atmospheric pressure ion trap is shown in which the electrospray (or other ionization) occurs within the radius of the inner electrode 82. This is the configuration preferred in the Mine Safety Appliances Company version of the FAIMS shown schematically in

25   Figures 3A and 3B. In general, ions may be introduced to the FAIMS analyzer region 84 either from outside (external) to the outer electrode 83, or from inside (internal) the inner electrode 82. The latter is less convenient because the dimensions are small, and the radius of the inner electrode 82 must be much larger than can be used in devices using the

30   external ion source. Moreover, the ionization source (e.g. corona discharge needle) may be susceptible to the influence of the high voltages

applied in the asymmetric waveform. The electrode immediately surrounding corona discharge ion source, or electrospray source is electrically grounded in the Mine Safety Appliances Company version of the FAIMS shown schematically in Figure 3A and 3B.

5   In the device shown in Figures 14A-14C, the inner electrode 82 would be about 14 mm outer diameter, and the outer electrode 83 about 18 mm inner diameter, with about 2 mm annular space (FAIMS analyzer region 84) between these two concentric cylinders 82, 83. The end of the inner cylinder 82T (left end in Figures 14A-14C) is closed, and shaped

10   either spherically, or cone shaped as appropriate to maintain the electric fields suitable for FAIMS ion trapping in all locations near the end of the electrode 82T. The inside of the outer cylinder electrode is shown to be uniform in diameter in Figures 14A-14C, but with wide diameter inner electrodes 82 such as shown in Figure 14A-14C, it is very likely that the

15   FAIMS analysis conditions will be better maintained if the inner surface of the outer electrode is contoured very much like that shown in Figures 9A and 9B. This will maintain substantially constant distance between the inner electrode, and the outer electrode near the spherically shaped (or conical etc.), closed end 82T of the inner electrode 82. Computer modelling

20   of the behavior of ions at the ends of these electrodes is feasible, and will be discussed below.

      Gas flows enter the end of the FAIMS analyzer region 84 shown in Figures 14A-14C (right hand side of the FAIMS in the figure), and flow toward the closed end or terminus 82T of the inner electrode 82.

25   Beyond the terminus 82T of the inner electrode 82 the gas flow passes through an exit grid 85 comprising a high transparency, fine-wire grid, and exits through the space between the mass spectrometer sampler cone 18 and the exit grid 85. A portion of the gas flows into the sampler cone orifice 18, drawn by the vacuum of the mass spectrometer. Some of the

30   ions which have passed through the exit grid 85 during the extraction time period will also be drawn into the mass spectrometer, by gas flows and by electrical fields.

Some of the gas entering the FAIMS analyzer region 84 shown in Figures 14A-14C must be permitted to flow inwards (i.e. the counter current gas flow) from the analyzer region 84 into the ionization region 86, thereby preventing neutral molecules, large liquid droplets and

5   other unwanted non-charged components from passing into the FAIMS analyzer region 84.   These components would contaminate the gas in the analyzer 84, and the ion focusing and trapping described elsewhere in this document will be degraded.   The device therefore may fail if the gas flow from the FAIMS analyzer into the ionization region is reversed during

10   electrospray experiments.   If the ionization occurs in a very clean non-contaminated gas, then this restriction on the gas flow direction may be relaxed (e.g. ionization of clean gas with radioactive ^{63}Ni foil, corona discharge ionization, ionization by UV light radiation etc.).   During operation in P2 mode the requirement for high purity gas is somewhat

15   relaxed.

The device shown in Figures 14A-14C operates in a manner analogous to that described previously.   The ions pass radially out of the ionization region 86, transported by electric fields against the radially inward flowing gas.   Having passed into the FAIMS analyzer region 84 the

20   electric fields will either confine the ion inside the analyzer region 84 (focusing or trapping) of the ion, because of application of DV and CV which are not appropriate, will collide with the walls of the device. Assuming that the DV and CV are appropriate for one of the ions in the sample, that ion will be focused in the FAIMS analyzer region, and flow

25   with the gas (since in the analyzer region the gas and electric fields act perpendicularly to each other) toward the closed, dome-shaped terminus 82T of the inner electrode 82.   If the trapping fields (electrical potential well) remain appropriate, the ions will assemble near the terminus 82T of the inner electrode 82 as shown in Figure 14B.   This will occur because the

30   ions cannot return toward the ion source against the flow of gas, and the ions cannot flow with the gas out of the grid 85 because of the confining action of the electric fields near the terminus 82T of the inner electrode.

- 38 -

As long as the following conditions are maintained, this trap will exist: (1) the DV and CV must be applied, and the voltages remain appropriate for the ion being trapped; (2) the voltages on the outer electrode and the grid remain fixed, e.g. near 0 V, as appropriate for the ion being trapped; and (3) 5 the gas flow is maintained. If any condition changes the ions may leave the trap. If it is desired to have the ions travel to the sampler cone 18 of the mass spectrometer after passing out of the trapping region, and through the grid 83 as shown in Figure 14C, then one of the above conditions may be optionally changed to achieve this result. This could 10 occur in a number of ways:

(1) The grid 85 voltage may be dropped (from its value during trapping) relative to the inner electrode 82, and relative to the outer electrode 84. This will have the effect of attracting (positively charged ions) away from the FAIMS trapping region (near the terminus 82T), and 15 thereby breaking the hold of the trap. The ions will leave the trap, and travel toward the grid 85. Some ions will strike the grid wires, and some will travel through (assisted by the gas flow). Since all of the voltages in the device must be considered relative to each other, somewhat the same effect can be achieved by changes in the voltages 20 applied to the outer electrode, and to the inner electrode 82. For example, an increase in voltage applied to both the outer electrode 84 and to the inner electrode 82, will have exactly the same effect as a decrease in the voltage applied to the grid 85.

25 (2) The DV or CV can be changed in many ways which alter the ion motion in the vicinity of the FAIMS trapping region. If the CV is made more negative the ions (positive ions) will tend to collide with the inner electrode 82, and if the CV is more positive the ions will be positioned farther from the inner electrode 82, and at some voltage 30 the FAIMS trap will no longer exist for this ion and the ion will travel with the gas flow and under the influence of the average dc

electric field, to the grid, as noted in (1) above. If DV is removed the trap will no longer function. If CV is altered, e.g. more positive, and DV is removed, (positively charged) ions will be repelled from the inner electrode 82, and may travel to the grid.

5   (3)   The gas flow can be changed. If the gas flow is sufficiently high to overcome the trapping action of the electric fields near the closed end of the inner electrode 82T, the ions will be pushed out of the trap and toward the grid 85, as described above. If the gas flow is decreased, or stopped, the ions will move via diffusion, and via chemical changes.

10   The diffusion will permit the ions to return back toward the ion source, thereby de-populating the FAIMS trapping region near the terminus 82T of the inner electrode 82. Even in the presence of gas flows the ions may soon de-populate the trap because of chemical effects. If the ion collides with a neutral molecule and temporarily

15   forms a stable complex, this complex may drift out of the FAIMS trapping region because this new complex has high field mobility properties which were different from the original ion. This means that the complex may have behavior at high electric field (see Figure 1) which differs from the original simple parent ion. For example (at

20   the extreme) the original ion may be of type A, and the new complex of the type C shown in Figure 1. If this is the case, the new complex will not be trapped at the prevailing DV and CV conditions. The collision of any of these ions with the walls of the device will soon result in loss of the ions from the trap. Although the original ion

25   itself may continue to be trapped, the removal of this ion via "chemical" effects is entirely possible, and is the reason the FAIMS analyzer will fail in the presence of water vapor or contaminants in the gas flows. The FAIMS analyzer works best in very clean conditions.

30   *Other Versions of FAIMS-Rx-prototypes*

The primary objective of the atmospheric pressure FAIMS ion trap is to collect, confine and increase the concentration of ions in some location in space. This can be achieved using the devices described in the paragraphs above. Several simple variations on these devices can
5   be visualized.

(1)   The geometry of the end of the inner electrode has been assumed to be spherical, but the surface may be conical, or some variation on these shapes. The shape will be selected to establish the non-uniform electric fields which are necessary to create the FAIMS focusing of
10   ions and FAIMS trapping of ions that is described above.

(2)   The geometry of the inside of the outer electrode may be varied. Most of the examples shown have simple cylindrical geometry, for ease in mechanical fabrication. A non uniform surface is more difficult to fabricate, but will be advantageous in some cases, especially
15   if the inner electrode has an inner diameter in excess of approximately 4 mm.

(3)   The inner and outer electrodes have been shown to have walls that are parallel to the central longitudinal axis, but this is not essential. The inner electrode may have an outer diameter which varies
20   linearly or non-linearly along its length. The outer electrode may have an inner diameter which varies along its length. This will be advantageous in those geometries in which the ionization source is located within the radial distance of the inner electrode, for example, as shown in Figures 3A, 3B, 14A, 14B and 14C.

25   (4)   The gas flows shown in the devices illustrated in this document serve two independent and identifiable purposes. First, the gas flow serves to carry the ions along the length of the FAIMS analyzer region since the electric fields are acting perpendicularly to the length of the

region, and therefore cannot help to transport the ions along the length of the device. Secondly the gas flows are always arranged to maintain the FAIMS analyzer and FAIMS trapping regions clean, and relatively free of gas phase water and chemical contaminants. Where possible, the ions must travel upstream, counter-current, to the flowing gas prior to entering the FAIMS analyzer region, in order to avoid entrance of neutrals and droplets into the FAIMS analyzer region. The embodiments of the atmospheric pressure, 3-dimensional ion traps that have been described above may permit the replacement of one or another function of the gas flow. For example, the transport of ions along the length of the FAIMS could be accomplished via electrical means. For example, if an electrical gradient is established along the length of the FAIMS analyzer which will serve to carry the ions along its length, this would replace one of the functions of the gas flow noted above. The electrical gradient can be created in two ways. First, the inner and/or outer electrodes can be segmented, with a slightly different constant, dc, voltage applied to each segment in such a way as to create another voltage gradient from one end of the device to the other. This is entirely feasible if the device can simultaneously maintain the DV and CV and geometric conditions which are necessary to maintain the ion focusing or trapping conditions. Secondly, one or more of the electrodes may be fabricated in such a way as to permit a voltage gradient to be established along the length of the device. The has been accomplished using insulating electrodes coated with a semiconductive layer. If a different voltage is applied to each end of such an electrode, the electrode acts like a resistive device, and the voltage gradient sits along its length. The voltage gradient can be linear, or non-linear depending on the application of the semi-conducting layer. The methods for ion motion modelling described below permit evaluation of such approaches without construction of prototypes. Modelling has shown that these devices are feasible.

orifice itself at the apex of the cone. The ions are generally attracted toward the pointed surface, and the ion transmission across the space between the grid, and through the orifice may be improved.

(8) The applied asymmetric waveform may be operated with small transient changes in voltage, phase shifts, and polarity. For example, if an ion is focused or trapped with DV 2500 V, and CV -11 V in a certain geometry, short (ms) changes of DV will affect the capability for ion separations. The voltage of DV may be changed for millisecond periods, the polarity reversed for millisecond periods, and the relative time periods of high and low voltage can be changed for small periods of time. This will create conditions whereby ions which are focused or trapped in a marginal way will be rapidly rejected from the FAIMS. For example, two ions which have almost the same high field ion mobility properties, my co-exist in the FAIMS analyzer region or the FAIMS trapping region. Unless steps are taken to selectively remove one of the ions, both will reach the detector (electrometer or mass spectrometer). Small voltage changes to DV or CV, and transient changes in voltages and phases of the waveform may help to eject one of the ions.

(9) The exit grid electrode can take many forms, and in some cases will not be necessary. The exit grid electrode serves 3 functions, including (1) completing the electric fields around the inner electrode, so that the ion trap is formed, (2) forming the electrode described in (1) but simultaneously permitting the gas flow to pass through this region unimpeded and (3) allowing a mechanism by which to form, and destroy the trap without modification to the voltages applied to the inner electrode. Clearly these functions can be carried out by other parts of the device. For example in Figure 9, the ion trap is controlled via the voltages applied to the inner electrode. The extraction voltage used to eliminate the ion trap may be applied to the outer

electrode, or to the inner electrode. Moreover, the grid can be totally eliminated if the sampler cone of the mass spectrometer is placed substantially near the end of the outer cylindrical of the FAIMS. This is the case shown in Figure 13.

5   *Modelling the Ion Motion in the FAIMS-E, FAIMS-MS, 2-dimensional and 3-dimensional ion traps:*

The ion motion in the FAIMS was modeled using a combination of experimental and theoretical considerations. First, consider the two cylinders used in FAIMS shown in Figure 15. When a

10   voltage is applied to the inner cylinder, the voltage at any point between the two cylinders can be calculated using the following formula: $V = V_a (\ln(r/b)/\ln(a/b))$ where V is the potential at radial distance r (assuming that r falls in the space between the two conductors), V_a is the potential applied to the inner electrode, the outer diameter of the inner cylinder is

15   "a" (cm), and the inner diameter of the outer cylinder is "b" (cm). The outer electrode is electrically grounded, i.e. 0 V applied. The annular space (called the FAIMS analyzer region) falls in the radial distance between a and b. This is shown in Figure 15. The voltage between the tubes is not linear, and the electric field (which is the derivative of the voltage i.e.

20   dV/dr) is also non-linear. The electric field between the tubes (at location r) can be shown to be: $E = -V (1/(r \ln (a/b))$ where E is the electric field (V/cm) and V is the voltage applied to the inner electrode, while the outer electrode is at 0 V. Variables a and b (cm) are defined above, and shown in Figure 15.

25   The motion of an ion in an electric field at atmospheric pressure is described by: $v = KE$ where v is the ion velocity (cm/sec) and E is the electric field (V/cm). The constant (almost constant) of proportionality for a given set of conditions is called the "ion mobility constant" K. Note however that many changes in conditions can change

30   the value of K. The obvious conditions that change the velocity of an ion in an electric field include: (1) temperature and (2) gas pressure. As

- 45 -

discussed above, K also varies with the electric field, but only at electric fields that are too high to be normally present in instrumentation used for conventional ion mobility measurements.

Although it will not be shown here, the ion mobility at high
5 field (called K_h in the discussion above) can be estimated using the FAIMS-E 10 instrument built by Mine Safety Appliances Company. Figure 16 shows the change in ion mobility of one type of ion, $(H_2O)_nH^+$, at very high electric field. The word "terms" in Figure 16 refers to the cyclic refinement of correction factors for the ion mobility during the low field
10 portion of the asymmetric waveform. In practice, during a waveform at DV 3000 V, the low voltage portion of the waveform is at about -3000/2 or -1500 V. Even at this lower voltage, the electric field is sufficiently high that the ion mobility cannot be assumed to be at it's "low field" value that is shown at the left axis of Figure 1. This requires a correction, that can be
15 repeated in a cyclic manner to get the best estimates of the ion mobility ratio K_h/K at very high electric field.

Figures 17A through 17C provide a portion of the original data (Figure 17A) that was used to calculate the high field mobility, and the spreadsheet calculations (Figure 17B and 17C) which were used to produce
20 the curves shown in Figure 16. The details will not be discussed here. Note also that the calculations are based on a square wave while the actual wave is shown in Figure 4.

Assuming that the high electric field change in the ion mobility of $(H_2O)_nH^+$ is represented by the curve shown in Figure 16, the
25 trajectory of this ion within the cylindrical geometry shown in Figure 15 can be easily calculated. As a first approximation, it can be easily shown that: $R_{final} = sqrt(2tK(V/ln(a/b)) + R_{initial}^2)$ where R_{final} is the radial location of the ion after a time period of length t, and $R_{initial}$ was the radial location before the time period t. The sqrt() is the square root function.
30 Again, this equation only applies if the ion spends all of its time between the radial distances a and b shown in Figure 15. Moreover the equation only gives useful values of final radial distance if the electric field does not

vary significantly between $R_{initial}$ and R_{final}. The voltage applied to the inner electrode is V, and the ion mobility is K. For this calculation K is assumed to be constant for the trajectory distance (distance the ion travels), but recall that K is calculated from the high field behavior shown in Figure

5   16. For example, if the ion is located at a distance r, and at some selected time (during application of the asymmetric waveform) that the voltage applied to the inner electrode results in an electric field of about 10,000 V/cm, then the ion mobility is calculated to be about K*1.01 where the 1.01 is the value taken from Figure 16. The value of K is about 2.3 cm^2/V-s

10 for $(H_2O)_nH^+$ at room temperature. This mobility, K, cannot be easily determined using the FAIMS instrument, but can be found in the conventional ion mobility spectrometry (IMS) literature.

With the information shown above, calculation of the motion of the ion in the annular space between the two cylinders is

15 relatively easy. Figures 18A-18D show the trajectory of an ion with the high field properties shown by the curve in Figure 16. Figure 18A shows very few oscillation motions caused by the applied asymmetric waveform of the type shown in Figure 2.

By way of illustration, the cylindrical geometry shown in

20 Figure 15 may have an inner cylinder having an outer radius of 0.1 cm and an outer cylinder having an inner radius of 0.3 cm. This means that all of the calculations giving rise to the trajectory must be done with a=0.1 and b=0.3 cm, and the trajectory must not extend past these limits. The ion trajectory shown in Figure 18A is calculated with the ion initially at 0.11

25 cm radial distance. This is shown as the left-most point in Figure 18A. The ion will oscillate as a result of the applied waveform and this is shown as an increase and decrease in the radial distance of the ion. The gas flow which transports the ions in the FAIMS analyzer region is simulated (for figure clarity) by showing the trajectory as a function of time

30 (x-axis) in Figure 18A. The applied voltages for the trajectory simulation were: DV=2500 V, CV=0 V, frequency=83000 Hz, relative ratio of low voltage to high voltage (t_1 and t_2 in Figure 2) was 5 to 1. It is clear that the

ion does not travel exactly the same distances during the low field, and high field portions of the waveform, and the ion experiences a "net" drift. The "net" drift refers to the general motion of the ion radially outward (in the case of Figure 18A). The simulation was repeated several times, and
5 the results shown in Figures 18B through 18D. Figure 18B was simulated in exactly the same manner as Figure 18A, except that the number of oscillations of the waveform, and thus of the ion motion, are significantly higher in Figure 18B. This shows that the ion will eventually cross over the FAIMS analyzer region, and collide with the outer wall which is
10 located in Figure 18B at the top of the Figure, at radial distance of 0.3 cm. Therefore, the DV and CV conditions that were used to simulate the motion of ion $(H_2O)_nH^+$ in Figures 18A and 18B, would not be suitable for the focusing or trapping in an FAIMS with the physical geometry described above. The condition which would be suitable for ion storage is shown in
15 Figure 18C. The conditions are: DV=2500 V, CV=-11 V, frequency=83000 Hz, relative ratio of low voltage to high voltage (t_1 and t_2 in Figure 2) of 5:1. The only change in conditions was the application of a more negative CV to the inner electrode. This could have been predicted from Figure 18B, since the outward drift of the ion might be expected to be retarded by
20 the application of a negative dc potential to the inner electrode. Figure 18C shows that the ion will experience a net drift from its starting position of 0.1 cm radial distance outwards, but quickly the drift stops and the ion oscillates because of application of the asymmetric waveform, but progresses neither inward nor outward. Figure 18D shows the calculated
25 ion trajectory for the same conditions except that the original radial starting point for the ion motion was selected to be about 0.26 cm. It is clear that the ion experiences a drift toward the inner electrode, and stabilizes at exactly the same radial distance as the ion shown in Figure 18C. This means that a ion, irrespective of its starting position will fall into
30 the ion focusing region. The focusing characteristics of the FAIMS are therefore easily demonstrated by ion trajectory calculations.

The radial location of the optimum focusing of an ion

depends on the high field mobility properties of the ion, and the DV and CV and geometry of the FAIMS analyzer region.   For the example shown above, the ion $(H_2O)_nH^+$ was selected because the high field ion mobility behavior of this ion had previously been established.   The optimum

5 combination of DV and CV for the ion $(H_2O)_nH^+$ can be calculated for various FAIMS hardware geometries.   The trajectory of the ion can be calculated easily based upon the principles described in the paragraphs above.

Figures 19A-19D show the ion trajectory for a geometry that is

10 shown in Figures 11A-11C, the device referred to as the FAIMS-R3-prototype (one of the 3-dimensional, atmospheric pressure ion trapping devices).   Because the geometry is not a simple cylinder the ion trajectory calculation is more complex.   The calculation is composed of two independent calculations.   In the first, the mechanical geometry of the

15 device is entered into a computer program which then calculates the strength of the electric fields around the components.   This is done by a method called "relaxation" (Jacobi iteration Richardson method), and involves a repetitive series of approximations of the field at every point in the physical space.   The field at a given point is calculated as the 'average'

20 of the points in each direction around it.   This is repeated for every point in the space.   Once this calculation has been completed for every point in the entire space, then the process is started again at the first point, now using the estimations from the previous calculation.   This is very easy to show in 1-dimension.   Let us assume that the following are the voltages at

25 several adjacent points in an imaginary 1-dimensional world (before the 'relaxation' calculation has begun).   The point at the left most of the array is an electrode at 100 V, and that at the right most point is an electrode at 0 V.   We begin by assuming every point is at zero V, except the electrode at 100 V.   The array is shown in the next line:

30 100 0   0   0   0   0   0   0

Signal enhancement using ion focusing at the spherical terminus of the inner electrode of FAIMS

Figures 19E-19I illustrate the results of ion trajectory calculations using a FAIMS consisting of a cylindrical outer electrode 93 of

5 about 6 mm id, and an inner electrode 92 of about 2 mm o.d.. The annular FAIMS analyzer region 94 is about 2 mm wide along the sides of the device. The inner electrode 92 terminates in a spherical shape 92T which is about 2 mm from the flat, front plate of the sampler cone 18. At the center of the sampler cone 18 is a small orifice 18A leading into the

10 vacuum system. In Figure 19E, the sampler cone 18 is held at 0 V, i.e., V_{OR} = 0 V. The conditions used for the ion trajectory simulation appear in Figure 19E. Figures 19F through 19I were prepared in exactly the same manner as Figure 19E, except that the V_{OR} was changed to -2.5, -5, -7.5 and -15 V respectively. This low applied V_{OR} had the effect of drawing the

15 ions out of the 3-dimensional trapping region. If this extraction occurs at voltages very close to the normal 'trapping' conditions (i.e., indefinite ion trapping), then the ions tend to be focused to near the center axis of the inner electrode 92, and therefore are focused to regions very close to the exit orifice 18A. The detected signal intensity will be maximized at the

20 V_{OR} which confines the ions as closely as possible to the center axis.

Although not shown in the Figures, it is possible that further improvements to the 'compactness' of the ion beam can be achieved by modification of the sampler cone 18. This might involve addition of extra lenses with voltages applied, or the modification of the shape of the front

25 of the sampler cone 18. Additional improvements might also be achieved by 'shaping' the inside surfaces of the outer FAIMS cylinder 93 at the end of the cylinder that is adjacent to the sampler cone 18. A previous version of the trapping experiments, shown in Figures 9A and 9B, did use a device with an outer cylinder which had a curved inner surface to maintain an

30 (approximately) constant distance between the outer cylinder and the inner electrode at the spherical end of the inner electrode.

Several experimental parameters will affect the focusing described above, and are shown to be optimized near $V_{OR} = -5$ V in Figure 19G. These include the gas flow rate, the spacing between the spherical end of the inner electrode and the sampler cone, and the applied DV and

5 CV. It is expected that optimization of the detected ion intensity will depend mainly on these parameters. The gas flow will control at least two factors, namely the rate that ions flow into the trapping region from the length of the FAIMS annular space, and secondly the turbulence at the end of the inner electrode. The simulations shown in Figures 19E through 19I

10 do not take into account gas turbulence and ion diffusion. The effectiveness of the focusing action will require a gas flow that maximizes the ion transport rate into the 'trapping region', and simultaneously minimizes ion loss through turbulence. The trajectory calculations shown in Figures 19E through 19I also do not account for gas flows in

15 directions non-parallel to the x-axis. If the experimental system includes gas flowing, for example, radially outward from the FAIMS trapping region, as would occur in the system shown schematically in Figure 13A, the locations of the maximum ion intensity would have to be determined experimentally. The modelling serves to suggest that this ion focusing

20 can enhance sensitivity in some set of optimized experimental conditions.

Several possible hardware designs can achieve the effects shown in Figures 19E through 19I. These embodiments require some essential components:

(1) the electrodes must have curved surfaces, including cylindrical, or

25 spherical, but also including surfaces that do not simply fall into one of these categories. An example of an unusual shape which would serve to establish conditions for trapping or focusing, is a cylindrical rod which has a bend in it, somewhat like a hairpin turn, shown in Figure 19J. With appropriate gas flows, a trapping region can be

30 created.

(2) the ions must be transported to the trapping region by gas flows, or by electric field gradients. All of the previously described embodiments

of FAIMS take advantage of gas flows, since these function quite independently of the voltages applied, especially DV and CV. The use of gas flows is relatively simple to visualize, and easy to create experimentally.

5   The behavior of ions within a selected geometry can be determined without repetitive calculation of individual trajectory paths as shown in Figures 18A-18D and 19A-19D. An example of this calculation is shown in Figures 20A and 20B. This is better illustrated in color, but black and white is shown for simplicity. The hardware geometry is the same as 10 has been considered in Figures 18A-18D and 19A-19D. The inner electrode 52 is a solid, with a substantially cylindrical end 52T which appears near the center of Figure 20A. There is a black zone around the electrode 52, but this is not part of the electrode. The outer electrode 53 is along the length of the top and bottom edges of Figure 20A, and the grid electrode 56 15 appears along the entire left edge of Figure 20A (other than the corner points). Trajectory calculations in Figure 20A were based on the following conditions: DV=2500 V, CV=-11 V, frequency = 83000 Hz, relative ratio of time periods at low voltage and high voltage (t_1 and t_2 in Figure 2) was 5:1, outer electrode 0 V, grid electrode 0 V. These are the same conditions as 20 Figure 19A and 19B. Unlike Figures 18A-18D and 19A-19D the individual trajectory is not drawn, rather the 'net' motion of the ion at a point in space is represented by a dot at that point in the calculated physical space. For Figures 20A-20B, a smaller 'net' motion, or smaller net velocity is represented by a darker grey colored spot in the space between the 25 electrodes 52, 53, whereas the regions of higher net motion are colored by spots of a lighter shade of grey. The ion cannot ever occupy some of the regions 101 near the electrodes because of the oscillations caused by the application of the asymmetric waveform. The locations wherein the oscillation caused by the waveform will cause the ion to immediately 30 collide with a surface will be left black 101 (unoccupied space) in Figures 20A-20B. The region around the inner electrode 52 is therefore surrounded by a black zone 101 that is approximately equal to half of the

back-and-forth distances the ions are moving while in the immediate vicinity of the inner electrode. This distance can also be estimated from the trajectory motions shown in Figures 18A-18D and 19A-19D. No ions will occupy the black zones around any of the electrodes shown in Figures

5 20A-20B.

A dark grey colored zone extends around the spherical termination 52T of the inner electrode 52 as shown in Figure 20A. This is the location where the net ion motion will be near zero. In Figure 20A this grey area is just beyond the dark black, non-allowed region which is

10 just adjacent to the electrode. Also note that a very light area is located directly next to the black, non-allowed region. In this very light area, the ions have high net motion, but the net motion is away from the electrode 52. This is seen in Figure 19A at the beginning of the trajectory at the right hand side of the Figure. Under the DV, CV and geometry considered in

15 this example the ion $(H_2O)_nH^+$ will be strongly pushed away from the immediate region of the inner electrode. Similarly, comparison of the motions shown in Figure 19B, at larger radial distances, shows that the lightly grey colored regions of Figure 20A which are close to the outer electrode and to the grid represent regions in which the $(H_2O)_nH^+$ ion will

20 have a net motion, and this net motion will take the ion in a direction TOWARD the inner electrode. This ion motion diagram therefore graphically illustrates the physical location of the stable, ion focusing and ion trapping regions around the inner electrode 52.

Figure 20B is closely related to 20A, except the grid electrode is

25 held at -7 V. The diagram shows that the region of trapping is not clearly defined (and may have disappeared). It also shows that the region of highest, outward motion in the vicinity of the inner electrode has been de-compressed away from the terminus 52T of the inner electrode 52. This illustrates the importance of the geometry around such surfaces in

30 determining the exact location of the FAIMS focusing or trapping conditions. This indicates that for certain geometric arrangements, notably that shown in Figures 14A-14C, the inner surface of the outer electrode

may be required to 'track' the shape of the inner electrode in such a manner to maintain the 'trapping' well in the optimum position relative to the inner electrode (if that is the requirement for the geometry in question).

5   *Qualitative, Simple Method for the Understanding of Ion Focusing and Ion Trapping*

There exists an optimum condition of DV and CV at which an ion is transmitted through the FAIMS analyzer. This condition is easy to determine. Referring back to Figure 17A, a set of repeat sweeps of the

10   CV at a series of DV values ranging from 2100 V to 3000 V is shown. The location of the peak maximum for some ion (in this case $(H_2O)_nH^+$) represents the condition where the compensation voltage CV is just strong enough to balance the net ion drift towards the wall of the FAIMS analyzer. Consider therefore that the ion $(H_2O)_nH^+$ can be transmitted

15   through the FAIMS analyzer region at a number of ideal combinations of CV and DV. If the ion experiences a combination of CV and DV that is different from the ideal, then the ion collides with a surface. A plot showing the ideal combinations of CV and DV for $(H_2O)_nH^+$ is shown in Figure 21. The ideal combination of DV and CV might be called

20   "balanced" because the ion experiences no 'net' motion. The plot shown in Figure 21 illustrates this balanced condition in terms of electric field, rather than the applied voltage DV and CV, moreover each data point on the Figure is an experimentally acquired combination of DV and CV, collected much as shown in the traces of Figure 17A. Each point is the CV

25   with the maximum efficiency of transmission (peak maximum shown for each trace in Figure 17a) for that setting of DV. Since the annular FAIMS analyzer region of the FAIMS-E is about 2 mm wide, a voltage of DV 2000 will result in a field of about 2000/0.2= 10,000 V/cm. Similarly an applied CV of -10 V will result in a field of about -10/0.2 = -50 V/cm. The x- and

30   y- axes of Figure 21 are displayed as electric field (V/cm) (absolute values, unsigned).

Figure 21 also shows a trace for the best fit third order regression to this data. This regression will help to determine the best combination of CV and DV under conditions which fell between the experimentally determined points. The fit to the data is very good, and a

5   small deviation only appears for the last points at high DV field (electric field which results from the application of DV, at the maximum applied voltage). Note that the 'DV field' is intermittent, since a part of the asymmetric waveform has a lower, opposite polarity time period. This maximum will be used as a 'reference point', for the purposes of this

10   description.

We will address the following question. Assume that an ion is located in the center of the FAIMS analyzer region (radially) and assume it is at a balanced condition at optimum DV and CV for the given hardware geometry. This means that the electric fields due to CV and DV

15   fall directly on the line drawn in Figure 21. The cylindrical geometry shown in all of the FAIMS diagrams in this document will have electric fields that are not constant along the radial direction in the FAIMS analyzer region. (The field may or may not be constant in the longitudinal direction, depending on the geometry of the particular

20   device.) If the electric field is not constant, will the optimum conditions shown by the curve in Figure 21 be maintained everywhere in the FAIMS analyzer region?

Figure 22A illustrates the actual fields due to DV (2500 V) radially across the FAIMS analyzer region of the FAIMS-E which has

25   approximate dimensions of 0.7 cm radius of the inner electrode (cylinder) and approximately 0.9 cm radius at the inside surface of the outer electrode. Figure 22B illustrates both the actual fields due to DV (2500 V) and CV (-13 V) that are found radially across the FAIMS analyzer region of the FAIMS-E, but unlike Figure 22A, the fields will be plotted against each

30   other in the manner used in Figure 21. The points corresponding to some of the physical, radial positions are noted on the diagram. At the right side of Figures 22A-22B, the field is highest, and corresponds to the surface

of the inner electrode, at radial distance of 0.7 cm. Similarly the left side of the Figure 22B corresponds to the inner edge of the outer electrode.

Compare Figures 21 and 22B. During an FAIMS experiment DV and CV are applied to the inner electrode. The DV field is not

5 constant, but rather falls within a small range of values (Figure 22B, x-axis), which in turn is only a small portion of the range of fields described by Figure 21. The curve in Figure 22B can be superimposed on the graphic shown in Figure 21. This is shown in Figure 22C. It is clear from Figure 22C that the real, physical conditions of electric fields within FAIMS

10 analyzer region do not all correspond to points with a balance of DV and CV. Recall that the short curve of 'actual' conditions reflects the conditions at a set of different radial distances (i.e. the left most point of the short curve is the condition of fields at 0.9 cm, near the outer electrode, and the right most point is physically located near the inner electrode

15 surface). Naturally at least at one point, corresponding to the center of the FAIMS analyzer region in this 'selected' combination of DV and CV, there exists the so-called balance where the ion migrates (net drift) neither toward the inner or outer electrode. Note also, there are many combinations of DV and CV which will result in the entire line shown for

20 'actual conditions' in the FAIMS analyzer will not cross the optimum balance curve at any point. For example if the DV is reduced to 50% of that shown in Figure 22B, the short trace for 'actual conditions' in Figure 22C will move left along the x-axis to fall at a much lower x-axis value of 'DV Electric Field'. If the CV voltage is unchanged the short trace in

25 Figure 22C will not cross over the 'optimum' balance trace, and the ions will not be able to be transmitted through the FAIMS.

The comparison of the two traces in Figure 22C also introduces one further question. If the ions, which are at the radial distance wherein the 'optimum' and 'actual' traces intersect, experience no

30 'net' motion radially, i.e. are at a balance point, what is the behavior of ions at larger radial distances, and at smaller radial distances? They must experience a net drift. For the conditions shown in Figure 22C, the ions at

radial distances larger than the crossing point, i.e. to the left of the intersection, will drift towards the intersection point i.e. toward smaller radial distances. The ions which are at small radial distances, will also drift toward the intersection point i.e. toward larger radial distances. If

5 ions from every radial location other than the 'balance' or focus point (intersection of the traces in Figure 22C) drift toward this focus point, then the device has the FAIMS ion focusing property that was described above. If the motions are divergent, i.e. away from the 'balance' point, then no ions can pass through the FAIMS. In mode 1 (P1, positive ions) the ions

10 drift toward the focus point when DV is positive, and CV is negative polarity (CV and DV applied to the inner electrode). If both of these polarity values are reversed, then the ion motion (type A, Figure 1) is divergent instead of convergent. This is the reason that the ions of the two types are automatically separated in the FAIMS. This is the reason

15 the spectra of modes 1 and 2 are always different, and must be always considered as independent spectra. The ions (to a first approximation) which appear in P1 do not appear in P2 type spectra, and vice versa. The same applies to ions of types N1 and N2.

Now referring to Figure 23, it is possible to visualize the
20 transport of ions in FAIMS using electric fields. A possible embodiment would require that the FAIMS unit be segmented, much in the same way that Javahery and Thomson (J.Am.Soc.Mass Spectrom. 1997, 8, 697-702) used a segmented rf-only quadrupole to create a longitudinal electric field to draw ions along the length of a set of quadrupole rods which were

25 operating with the usual applied high frequency, high voltage ac voltage applied to them. The segments in either the case of segmented quadrupole rods, or FAIMS, are held at slightly different dc potentials, which creates a field superimposed on the other non-constant fields. A possible way to do this is shown in Figure 23.

30 Based on a similar concept, a device for 3-dimensional trapping using only electric fields in a segmented FAIMS may be developed, and is described below.

3-Dimensional Trapping using only Electric Fields in a Segmented FAIMS

This segmented FAIMS version of the 3-dimensional trap is novel because it does not use gas flows as one of the trapping components. In the trapping of ions at the spherical end of the inner electrode, as previously described, the ions are held by a combination of the motion of the gas sweeping the ions towards the end of the inner electrode, and the FAIMS focusing action caused by the asymmetric waveform. In that device, upon stopping of the gas flows, the ions can begin to make their way back along the length of the FAIMS inner cylinder. The driving force for this migration would be diffusion and ion-ion repulsion which creates a so-called space-charge in the zone where the ions are congregated.

In the present description of a segmented FAIMS ion trap, the ions are held entirely because of the combination of the asymmetric waveform and the gently rising dc voltages applied to the adjacent segments which prevents ion motion in either direction along the length of the segmented FAIMS device. The stopping of the gas flow will have only a minor affect on the ions caught in the ion trap, and there exists no escape even if the gas flow is zero. Consider this new version of 3-dimensional trapping in more detail.

Figure 24 shows the segmented cylindrical outer 113 and inner 112 electrodes of FAIMS. The high voltage asymmetric waveform of FAIMS is applied to the inner electrode 112. The ions will be focused between these cylinders 112, 113 given the correct combination of DV and CV, and the cylindrical geometry. In normal operation all of the segments 112A or 113A would be at identical voltages, i.e., the inner electrode 112 is one conductor, and the outer electrode 113 is also one conductor. Assume that typical conditions for some ion to be focused between the cylinders are DV=2500 V and CV= -12 V. This is the condition shown in Figure 24. If the electrodes were not segmented, the outer electrode would be at e.g., 0 V. Similarly the inner electrode would be only at one condition i.e., asymmetric waveform DV=2500 V with plus -12 V offset compensation

voltage. Under these conditions if the ions were carried into the annular space between the cylinders by a gas flow, they would proceed longitudinally, carried from one end of the FAIMS analyzer to the other end of the device by the flowing gas, simultaneously being focused at some

5   radial distance and between the inner and outer electrodes.

Still referring to Figure 24, this situation can be changed substantially once the inner and outer electrodes 112, 113 are segmented 112A-112E, 113A-113E.   If all of the new dc voltages added to the outer electrodes 113A-113E are 0 V, and all of the new dc voltages added to the

10   inner electrodes 112A-112E are 0 V, then the conditions described in the paragraph above are returned, and no 3-dimensional trap exists, only the 2-dimensional focusing between the cylinders. Visualize next, that a set of new, small, dc voltages are applied to each segment 112A-112E, 113A-113E of this new FAIMS, such that the middle segment of the inner and outer

15   electrodes 112C, 113C have the lowest applied voltage.   Note, however, that each voltage applied to the outer electrode 113 must be matched by the same (approx.) voltage added to the inner electrode 112.   This means that if +5 V extra are added to the first segment 113A of the outer electrode, then +5 must be also added to the same segment 112A of the inner

20   electrode.   If that segment already had -12 V compensation voltage added to it, then the new +5 is added to that CV to give a net dc voltage of -7 V on that segment.   This approach is used to add voltages to the other segments 112B-112E, 113B-113E, in such a way that the middle segment 112C, 113C (in the Figure) has the lowest applied dc voltage.   This means that +ve

25   ions caught somewhere in this assembly will fall to the lowest voltage region, i.e., between the inner and outer electrodes of the middle segment 112C, 113C.   Since the normal FAIMS conditions continue to apply within each segment 112A-112E, 113A-113E, namely the inner electrode has an asymmetric waveform with DV=2500 V and the difference between the dc

30   applied to the inner electrode and the dc applied to the outer electrode within that segment continues to be 12 V (a required compensation voltage in this example), then the ions will be focused in the normal way

in the annular space between the inner and outer electrode. The flow of gas along the length of this FAIMS will not (at low gas flows, 1 L/min) be able to remove the ions which are located in the space within the middle segment 112C, 113C of this trap. For the ions to escape they must climb up the dc potential walls (of about +5 V in the Figure). At high gas flows, and at high ion density in which space charge is high, this escape might be possible. Nevertheless, there exists a trapping region which is totally electrical in nature, and the ions are held in place only by electric fields.
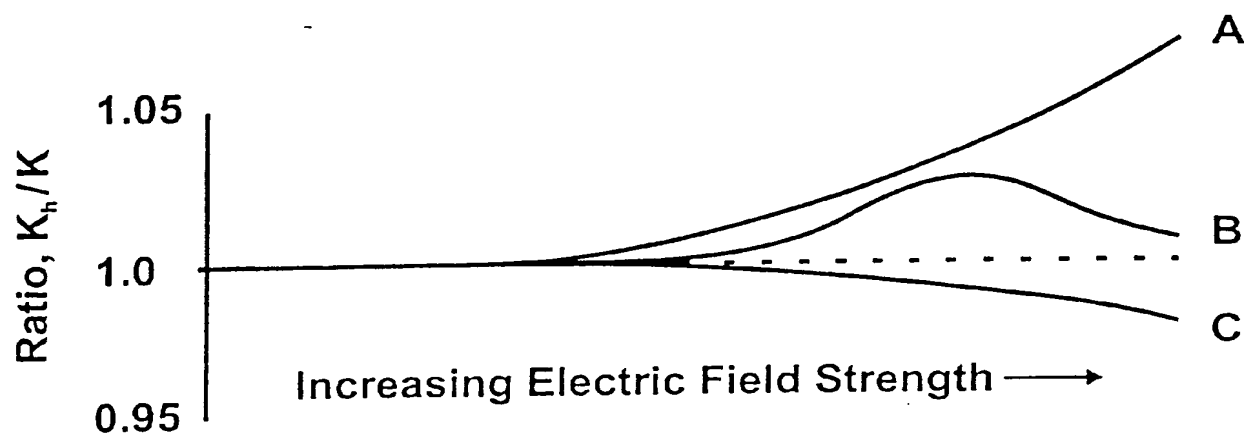
- 64 -
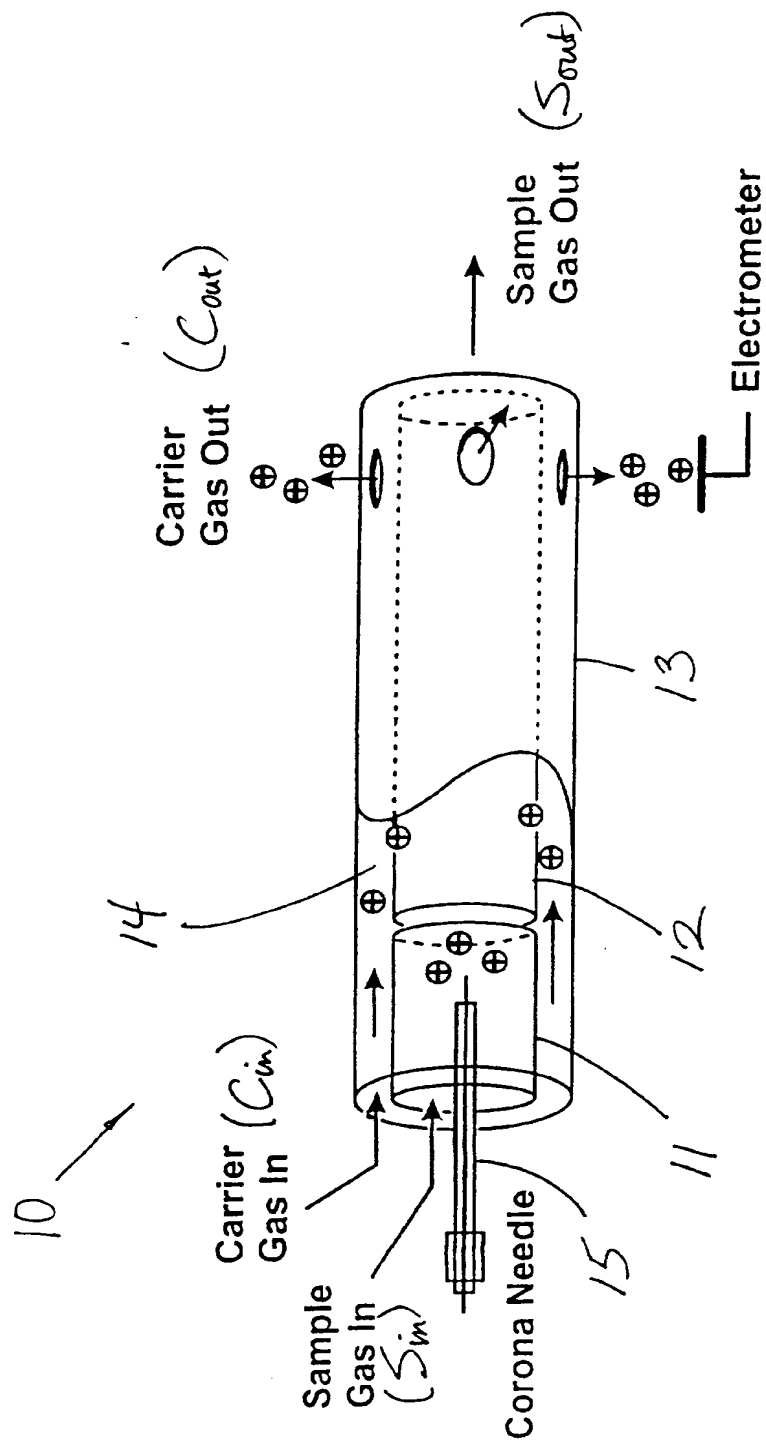
<u>WE CLAIM</u>:

1. •••

FIG. 1

Carrier Gas Out (C_{out})

Sample Gas Out (S_{out})

Electrometer

13

14

12

11

15

10

Carrier Gas In (C_{in})

Sample Gas In (S_{in})

Corona Needle

FIG. 3A (PRIOR ART)

Carrier Gas In (C_{IN})

Sample Gas In (S_{IN})

Corona Needle

Carrier Gas Out (C_{OUT})

Sample Gas Out (S_{OUT})

Electrometer

V(t)

10

15

11

12

14

13

16

17

FIG. 3B (PRIOR ART)

A

P1

DV

0

Waveform #1

B

P2

0

DV

Waveform #2

FIG. 4

Carrier Gas Out (C_{OUT})

Sample Gas Out (S_{OUT})

Roughing Vacuum Pump

Carrier Gas In (C_{IN})

Sample Gas In (S_{IN})

Corona Needle

Sampler Cone

Skimmer Cone

Quadrupole Mass Spectrometer

14

16

13

18

12

11

15

20
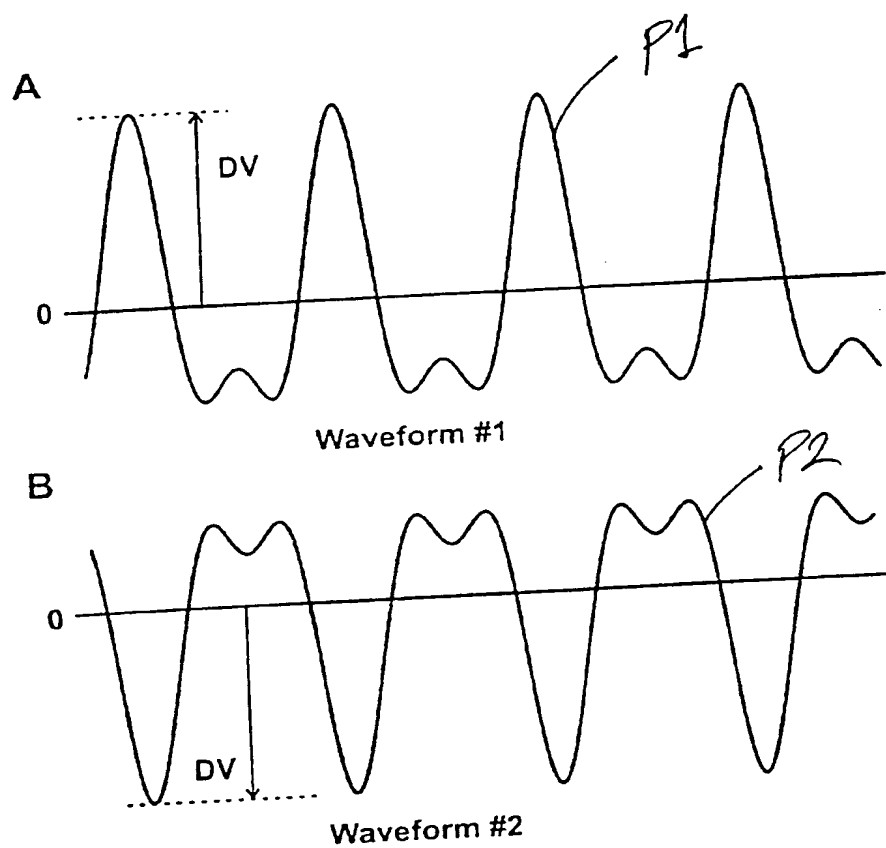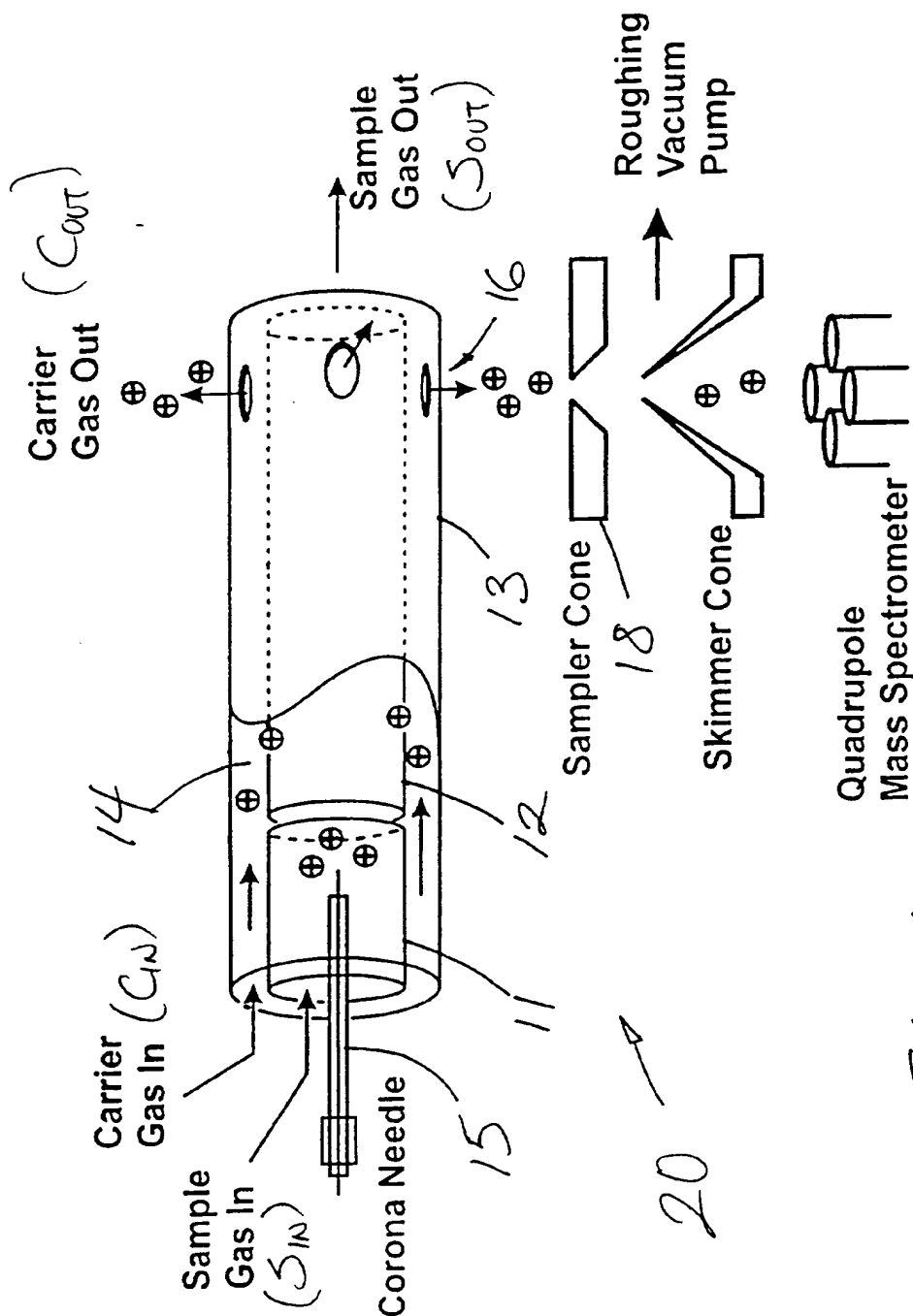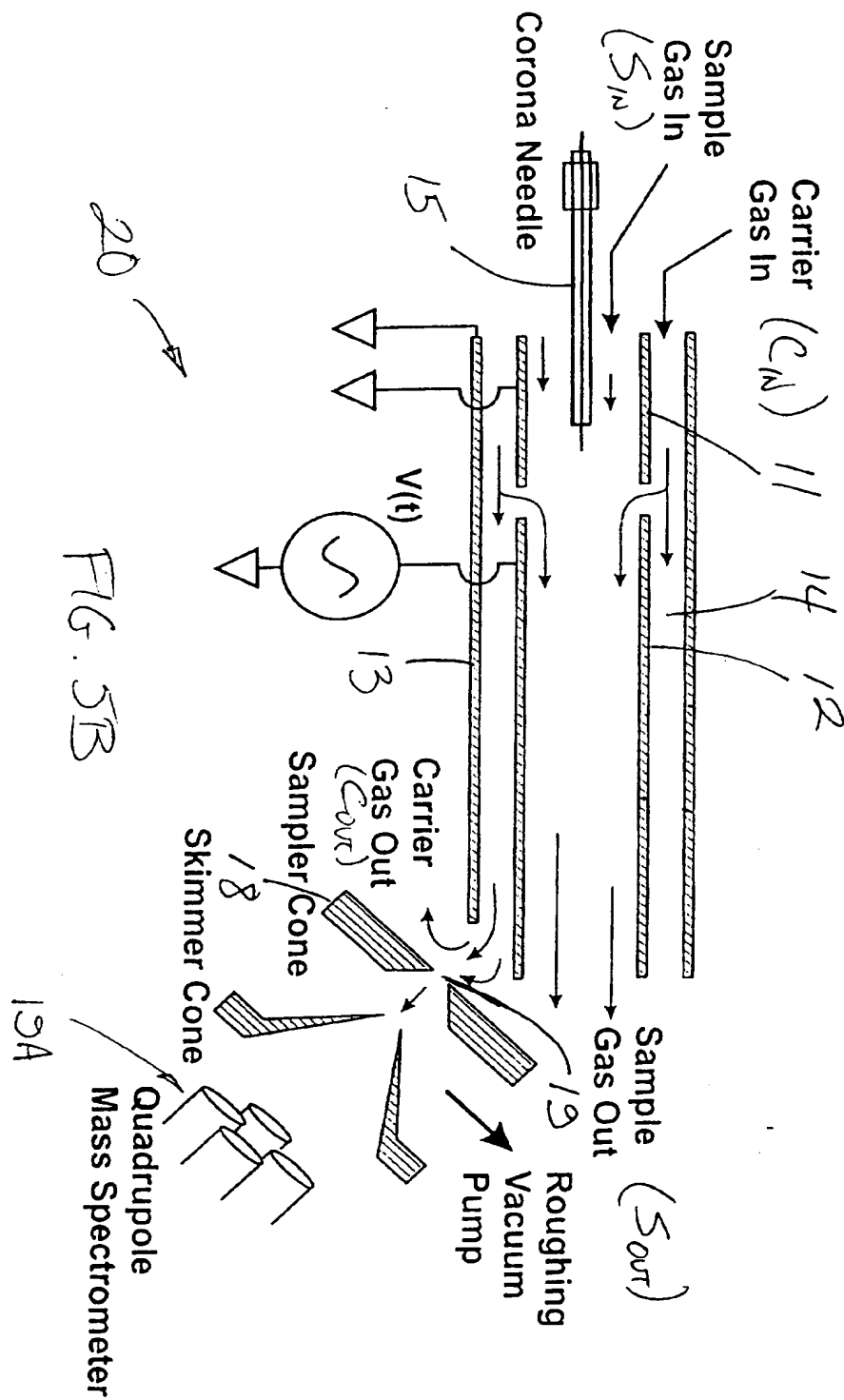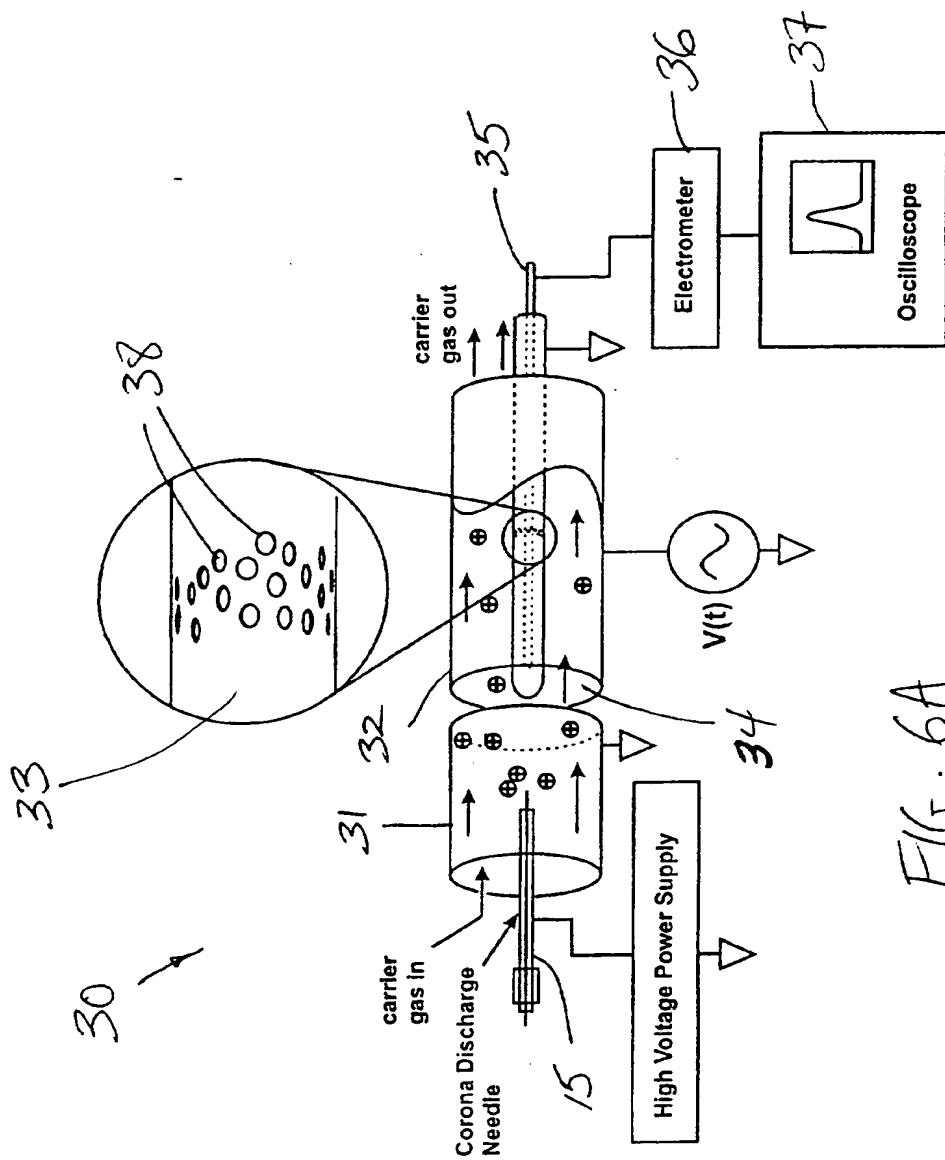
FIG. 5A

FIG. 5B

FIG. 6A

FIG. 6B

FIG. 7A

Timing Diagram for the Application of a High Frequency Asymmetric Waveform,
a DC Voltage, and an Extraction Voltage

The Voltages are all applied to the center electrode.

Time = 0   Time = 16.2 milliseconds   Time = 300 milliseconds

High Voltage Assymetric Wave

DV

CV

DC Voltage (-20 Volts)

(example)

Extraction Voltage (+30 V)

FIG. 7B

Details of the Asymmetric Waveform
(time and amplitude not to scale)

+2000 Volts

DC offset Voltage

Extraction Voltage

0 Volts

-400 Volts

5 microseconds

1 microsecond

Time = 0 milliseconds

Time = 16.2 milliseconds

Detected ion signals with FAIMS-R1-prototype shown in Fig. 6A and 6B

FIG. 8

40

Outer Shell

Exit Grid

46

Inner Electrode

15

45

Corona Discharge
Ion Source

Ion Collector
Plate

Gas Flow In

42T

47

Gas Flow In

43 *44* *42*

High Voltage Asymmetric
Wave Generator

DC voltage Applied

Ammeter (High Gain)

36

37

Oscilloscope

FIG. 9A

40

Outer Electrode

Inner Electrode

15

45

Corona Discharge
Ion Source

Exit Grid

46

Ion Collector
Plate

Gas Flow In

42T

Gas Flow In

47

Gas Flow Out

43   *44*   *42*

High Voltage Asymmetric
Wave Generator

DC voltage Applied

Ammeter (High Gain)

36

37

Oscilloscope

FIG. 9B

FILE OPENED: G:\JUNK\ROGER\FIS_R2\98JA23\98012202.DAT

Ext+1.0 CV-12.0 D=3.11mm DV+2090-343 Gas 0.9L/min Jan23/98

00235OWAVEDESC

Parameter File = 0
Sample id = 0
Vert Gain = 1.220703E-05
Vert Offset = 0.097
Horiz Interval = 0.00002
Horiz Offset = 0.01211
FirstValidPt = 4
WaveArray Count = 1002

FIG. 10A

FILE OPENED: G:\JUNK\ROGER\FIS_R2I98JA23I98012303.DAT

Ext+2.0 CV-12.0 D=3.11mm DV+2090-343 Gas 0.9L/min Jan23/98

002350WAVEDESC

Parameter File = □
Sample id = 0
Vert Gain = 1.220703E-05
Vert Offset = 0.097
Horiz Interval = 0.00002
Horiz Offset = 0.01211
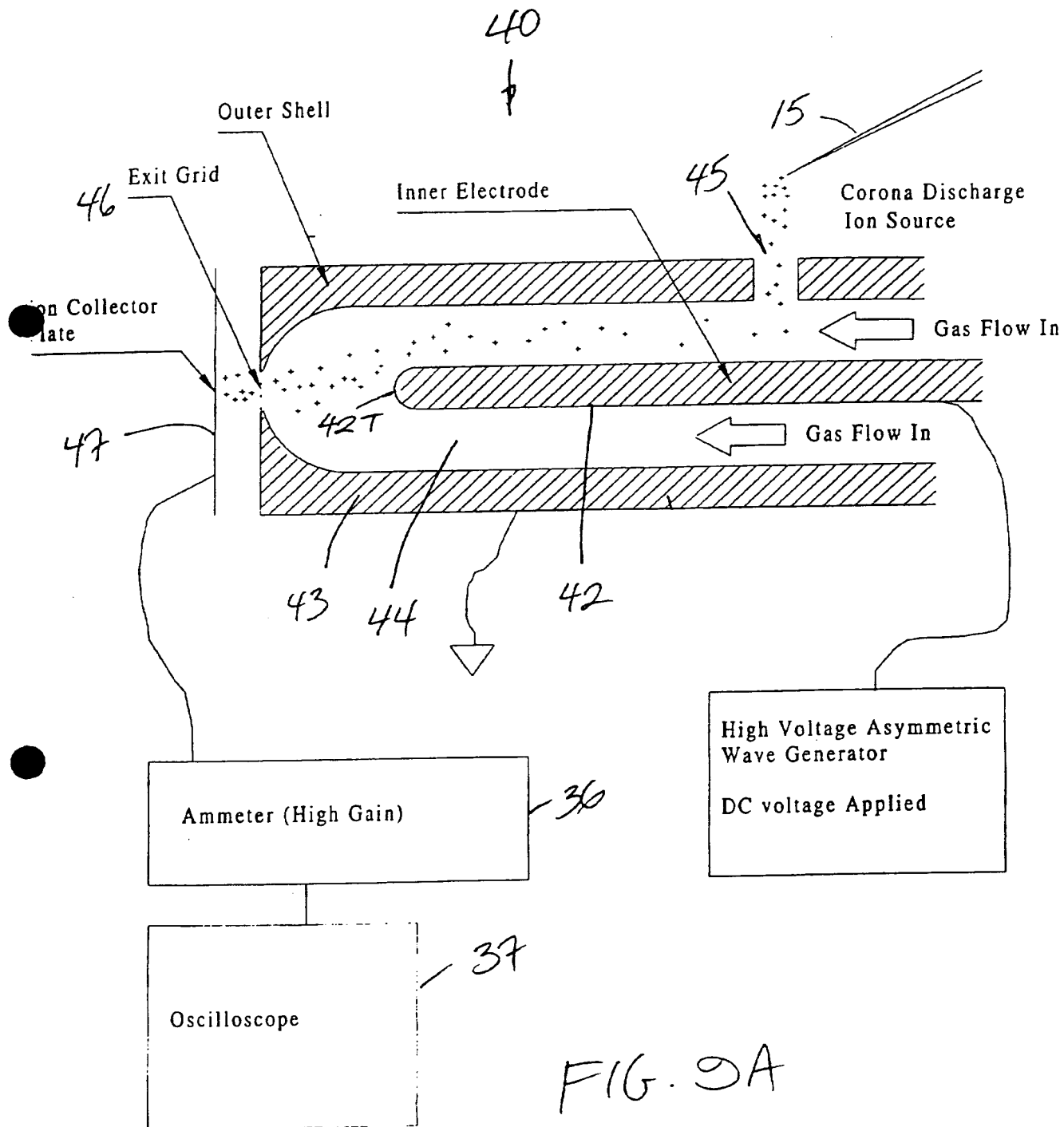FirstValidPt = 4
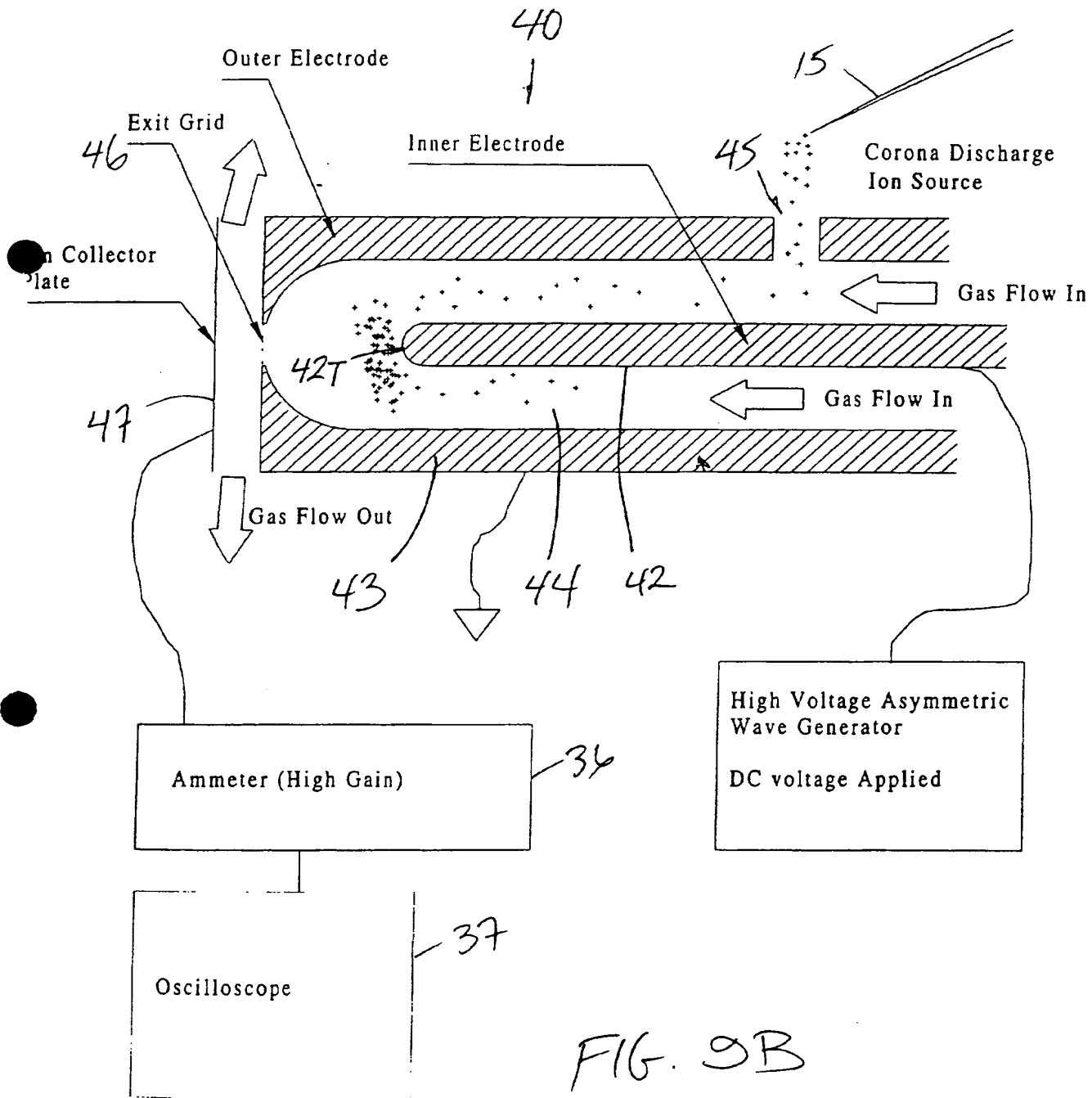WaveArray Count = 1002

FIG. 10B

FILE OPENED: G:\JUNK\ROGER\FIS_R2\98JA23\9801230 4.DAT

Ext+3.0 CV-12.0 D=3.11mm DV+2090-343 Gas 0.9L/min Jan23/98

002350WAVEDESC

Parameter File = □
Sample id = 0
Vert Gain = 1.220703E-05
Vert Offset = 0.097
Horiz Interval = 0.00002
Horiz Offset = 0.01211
FirstValidPt = 4
WaveArray Count = 1002

FIG. 10C

FILE OPENED: G:\JUNK\ROGER\FIS_R2198/A2319801 2305.DAT

Ext+5.0 CV-12.0 D=3.11mm DV+2090-343 Gas 0.9L/min Jan23/98

002350WAVEDESC

Parameter File = 0
Sample id = 0
Vert Gain = 1.220703E-05
Vert Offset = 0.097
Horiz Interval = 0.00002
Horiz Offset = 0.01211
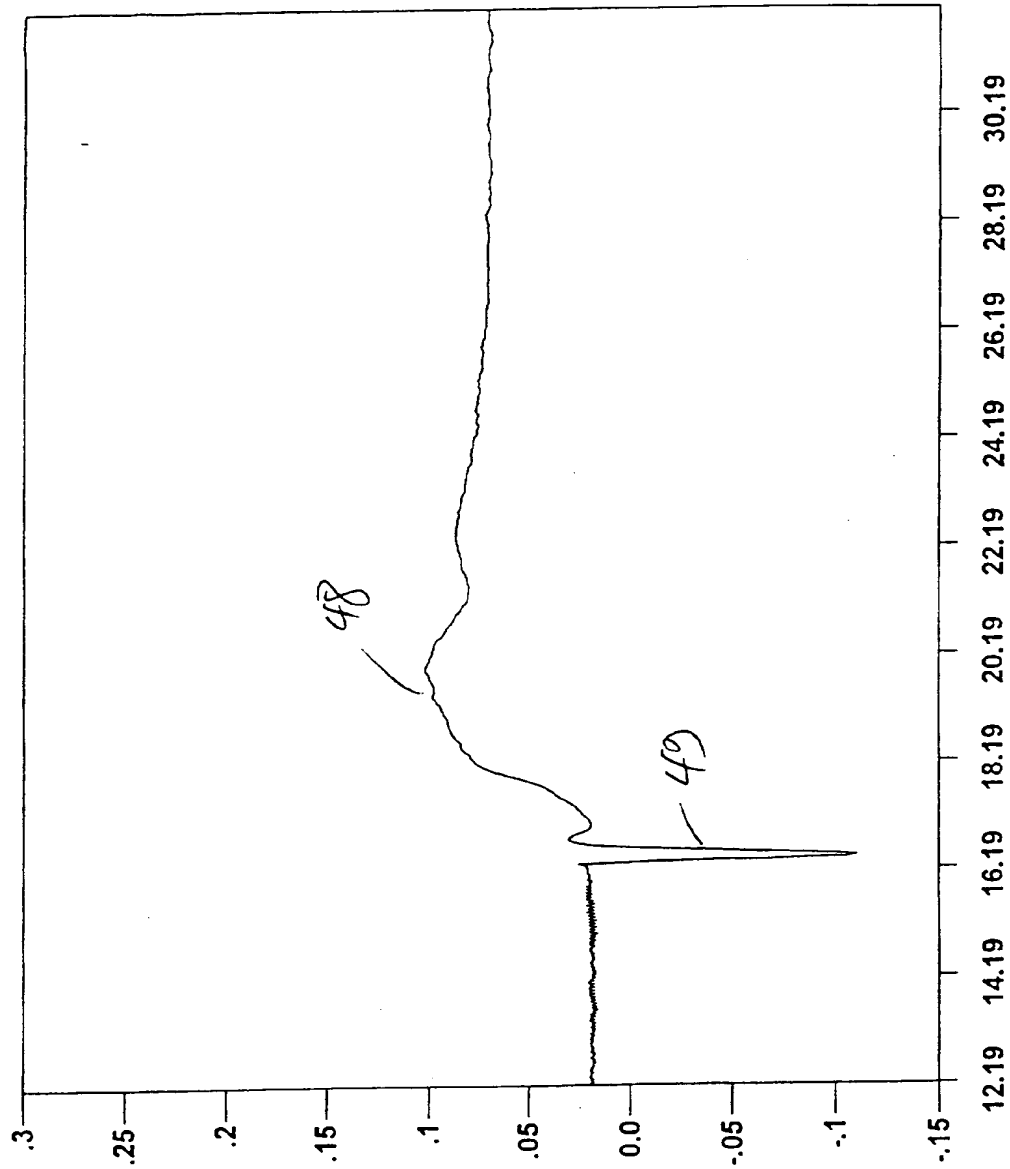FirstValidPt = 4
WaveArray Count = 1002

FIG. 10D

FILE OPENED: G:\JUNK\ROGER\FIS_R2\98JA23\98012306.DAT

Ext+7.5 CV-12.0 D=3.11mm DV+2090-343 Gas 0.9L/min Jan23/98

002350WAVEDESC

Parameter File = 0
Sample id = 0
Vert Gain = 1.220703E-05
Vert Offset = 0.097
Horiz Interval = 0.00002
Horiz Offset = 0.01211
FirstValidPt = 4
WaveArray Count = 1002

48

49

FIG. 10E

FILE OPENED: G:\JUNK\ROGER\FIS_R2198\A2319B012307.DAT

Ext+10.0 CV-12.0 D=3.11mm DV+2090-343 Gas 0.9L/min Jan23/98

002350WAVEDESC

Parameter File = 0
Sample id = 0
Vert Gain = 1.220703E-05
Vert Offset = 0.097
Horiz Interval = 0.00002
Horiz Offset = 0.01211
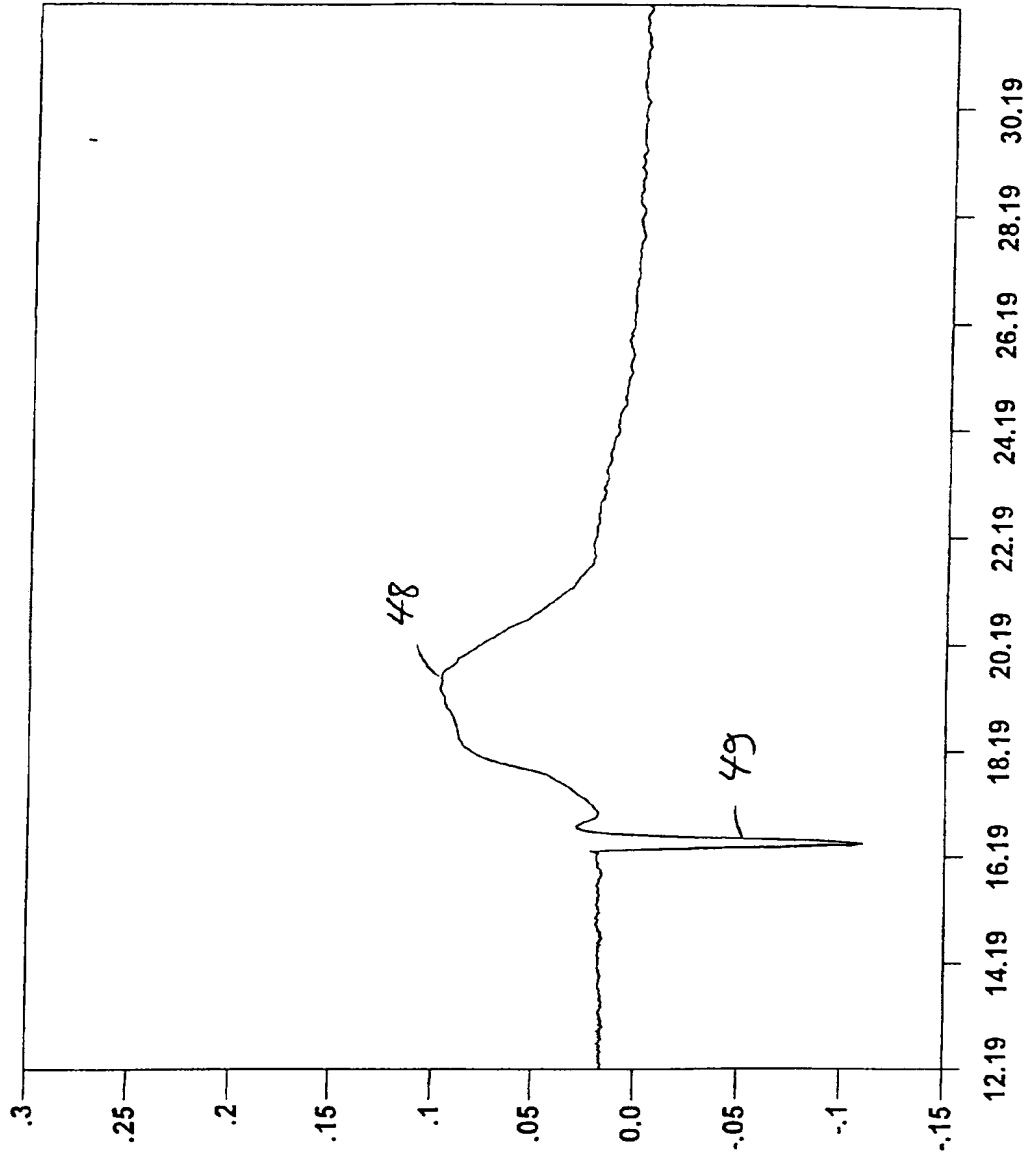FirstValidPt = 4
WaveArray Count = 1002

FIG. 10F

FILE OPENED: G:\JUNK\ROGER\FIS_R2198JA2319801 2308.DAT

Ext+15 CV-12.0 D=3.11mm DV+2090-343 Gas 0.9L/min Jan23/98

002350WAVEDESC

Parameter File = 0
Sample id = 0
Vert Gain = 1.220703E-05
Vert Offset = 0.097
Horiz Interval = 0.00002
Horiz Offset = 0.01211
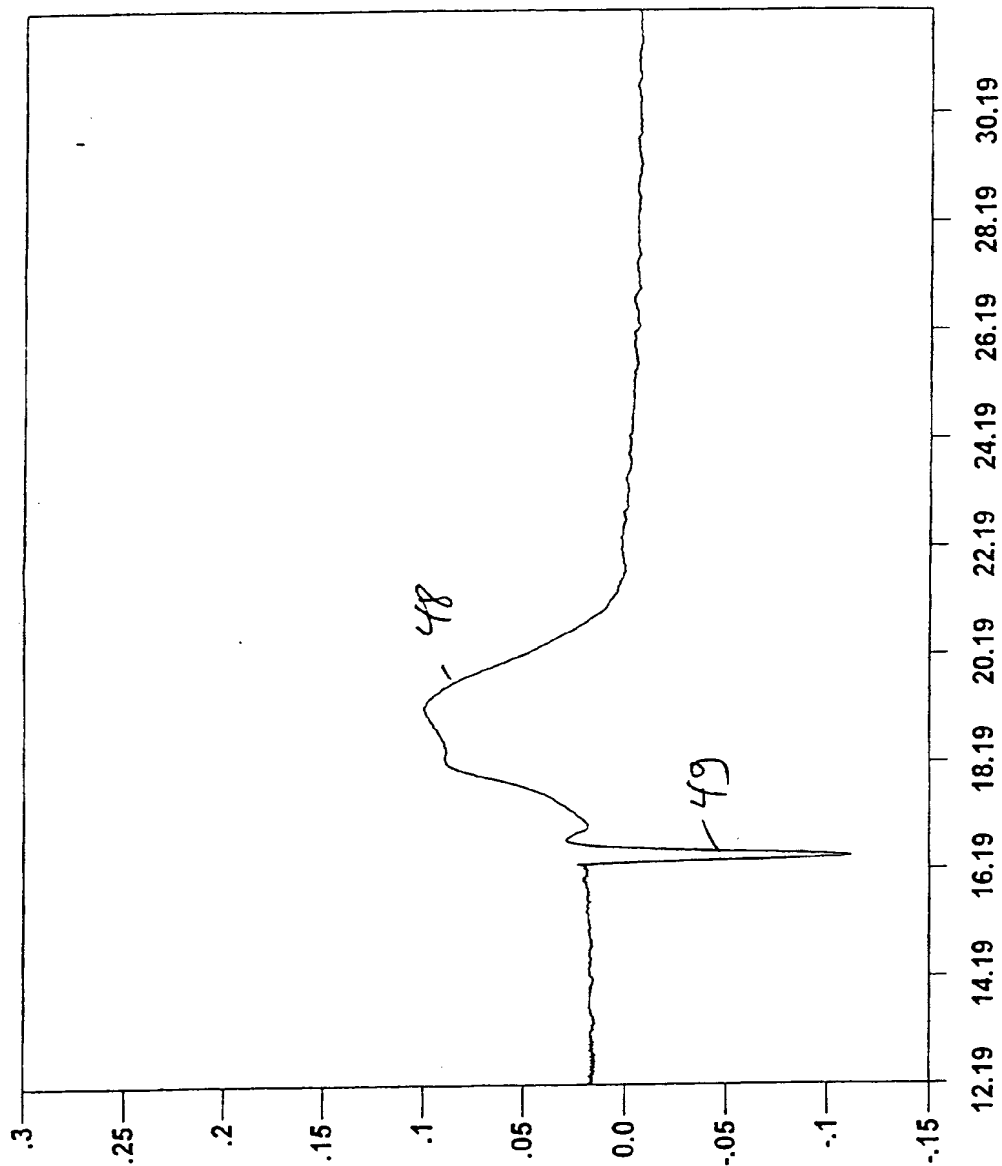FirstValidPt = 4
WaveArray Count = 1002

FIG. 106

FILE OPENED: G:\JUNK\ROGER\FIS_R2198JA23\9801 2309.DAT

Ext+20 CV-12.0 D=3.11mm DV+2090-343 Gas 0.9L/min Jan23/98

002350WAVEDESC

Parameter File = 0
Sample id = 0
Vert Gain = 1.220703E-05
Vert Offset = 0.097
Horiz Interval = 0.00002
Horiz Offset = 0.01211
FirstValidPt = 4
WaveArray Count = 1002

48

49

FIG. 10H

FILE OPENED. G:\JUNK\ROGER\FIS_R2\98\JA23\98012310.DAT

Ext+30 CV-12.0 D=3.11mm DV+2090-343 Gas 0.9L/min Jan23/98

002350WAVEDESC

Parameter File = ▯
Sample id = 0
Vert Gain = 1.220703E-05
Vert Offset = 0.097
Horiz Interval = 0.00002
Horiz Offset = 0.01211
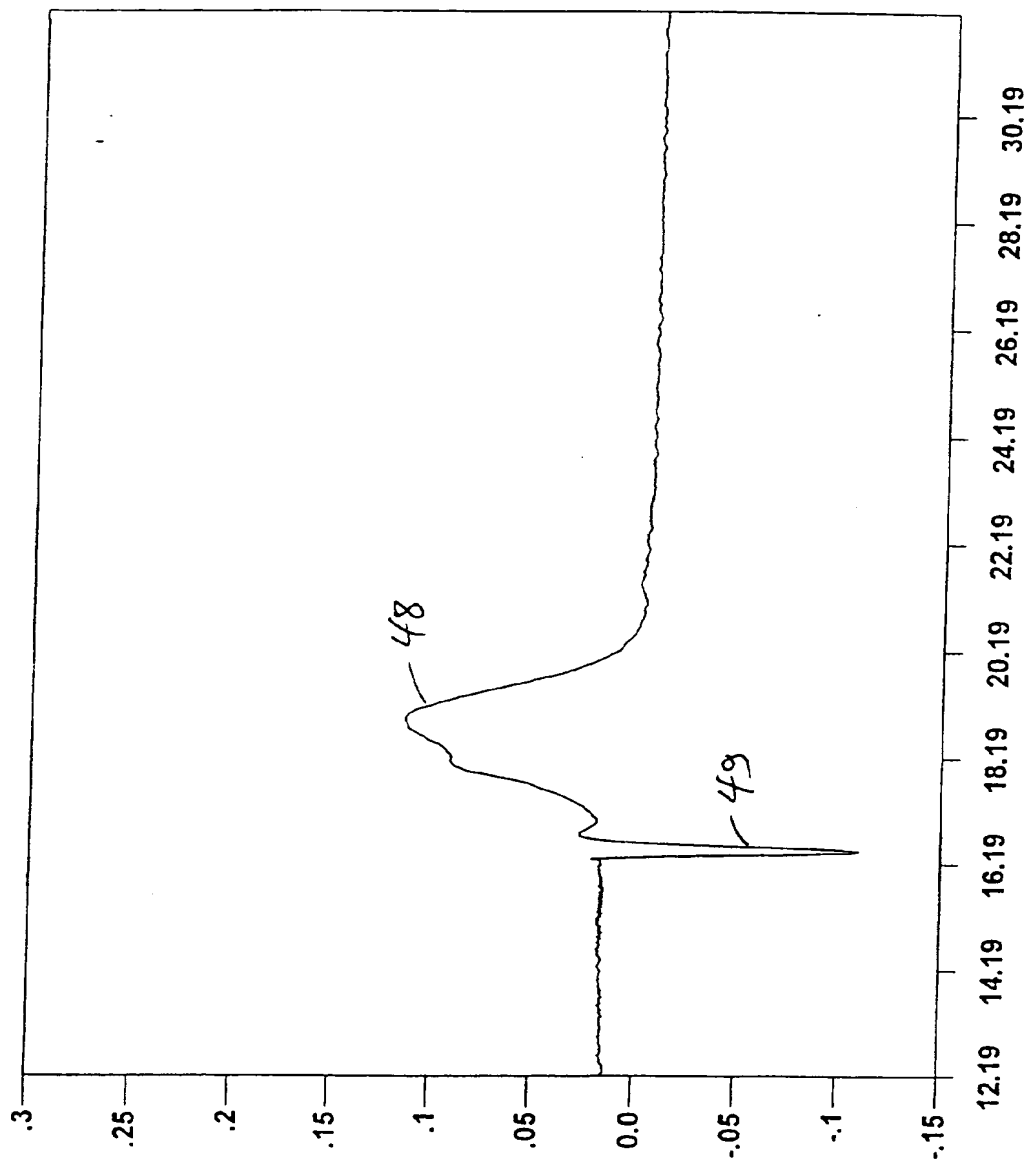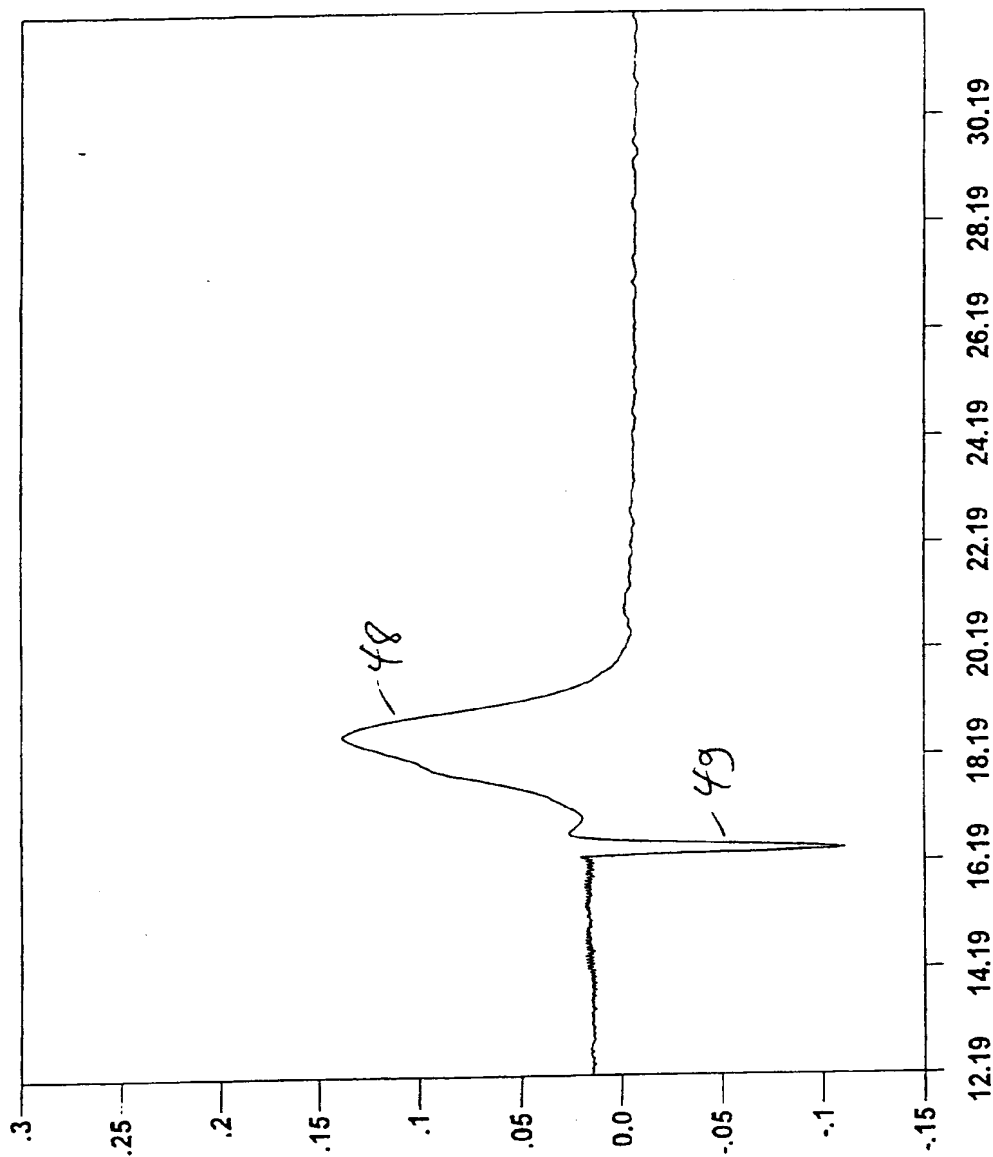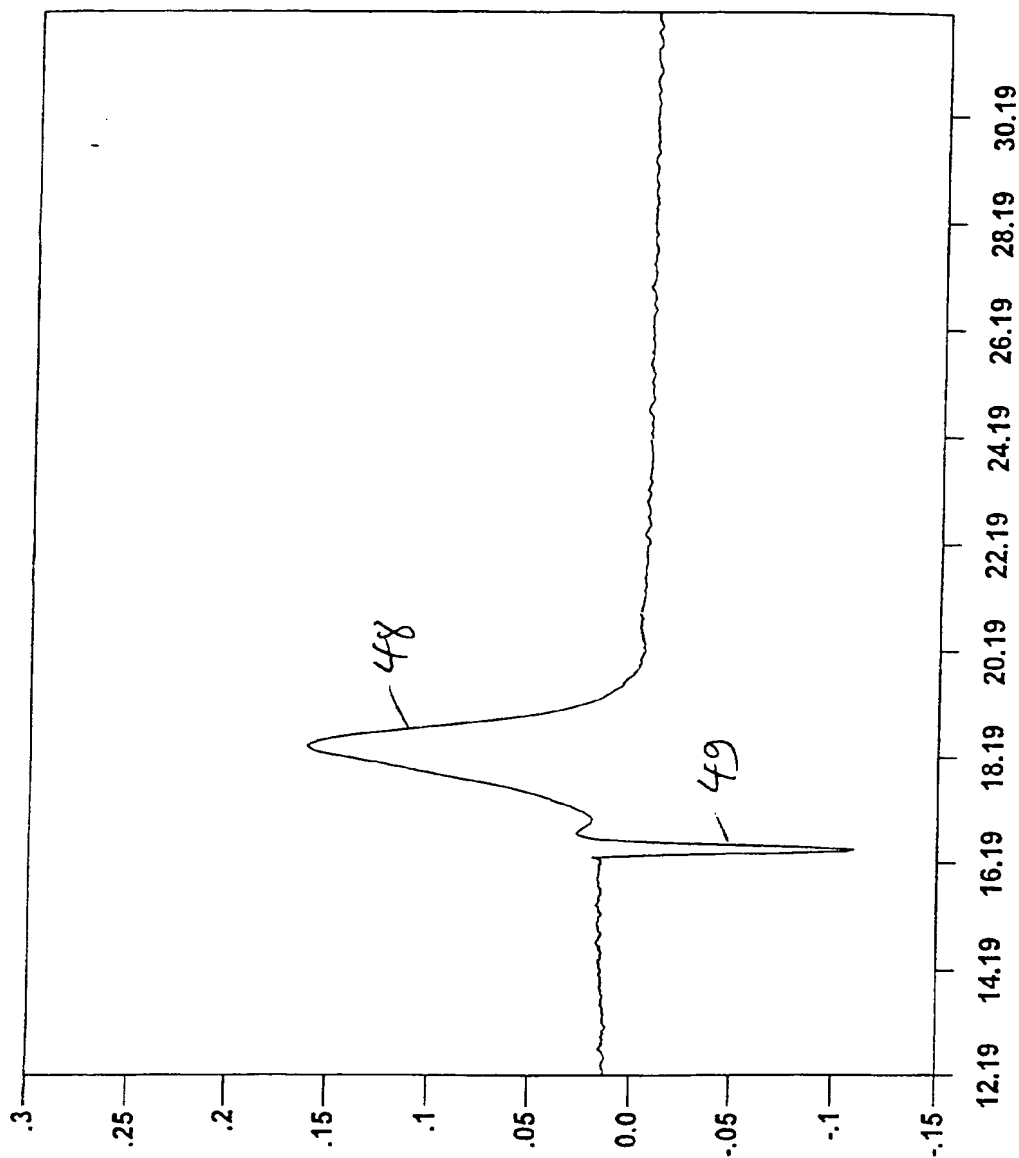FirstValidPt = 4
WaveArray Count = 1002

FIG. 10 I

50

Electrospray Ionization
Chamber (ESI)
60

Sample Delivery Capillary

15E

Ions Generated by
Electrospray Ionization

Electrospray Needle

Mass Spectrometer
Vacuum Housing

→ Purge Gas Out

Gas Out   Purge Gas Out

Purge Gas Out

Outer Ion Aperture

61   62

Mass Spectrometer
Vacuum Chamber

Purge Gas In

63

Ion Trap Aperture

Ion Trap Gas In

Orifice →

52T

Mass Spectrometer
Sampling Orifice

54   53   Ion Trap Gas In

52

18   Grid 56 Ion Trap Outer Electrode

Grid Support Ring

Gas Out   Ion Trap Powered Electrode

55

RF Asymmetric Waveform
Generator Power Supply

Dispersion Voltage +
Compensation Voltage

57

Grid Electric Pulse
Generator
Power Supply

FIG. 11A

50

Sample Delivery Capillary

15E

Ions Generated by
Electrospray Ionization

Mass Spectrometer
Vacuum Housing

Electrospray Needle

60

Purge Gas Out

Outer Ion Aperture

61

63

Purge Gas In

62

Mass Spectrometer
Vacuum Chamber

Ions Trapped

Ion Trap Aperture

Ion Trap Gas In

Orifice

52T

Mass Spectrometer
Sampling Orifice

54

53

Grid

Ion Trap Outer Electrode

52

56

Grid Support Ring

18

Ion Trap Powered Electrode

Grid at 0V,
Closed with
no Ion Transmission

55

57

RF Asymmetric Waveform
Generator Power Supply

Dispersion Voltage +
Compensation Voltage

Grid Electric Pulse
Generator
Power Supply

FIG. 11B

50

ESI Chamber
Electrospray Ionization
Chamber

Sample Delivery Capillary

15E

Ions Generated by
Electrospray Ionization

Electrospray Needle

Mass Spectrometer
Vacuum Housing

Purge Gas Out

60

Outer Ion Aperture

61   62

Purge Gas In

63

Ion Trap Aperture

Mass Spectrometer
Vacuum Chamber

54

Ion Trap Gas In

Orifice

52T

53

Mass Spectrometer
Sampling Orifice

Grid
56

Ion Trap Outer Electrode

52

18

Grid Support Ring

Ion Trap Powered Electrode

Grid at Negative
Voltage and
Extracting Ions

(Inner Electrode)

55

57

RF Asymmetric Waveform
Generator Power Supply

Dispersion Voltage +
Compensation Voltage

Grid Electric Pulse
Generator
Power Supply

FIG. 11C

Timing Diagram for the Application of a High Frequency Asymmetric Waveform,
a DC Voltage, and an Extraction Voltage

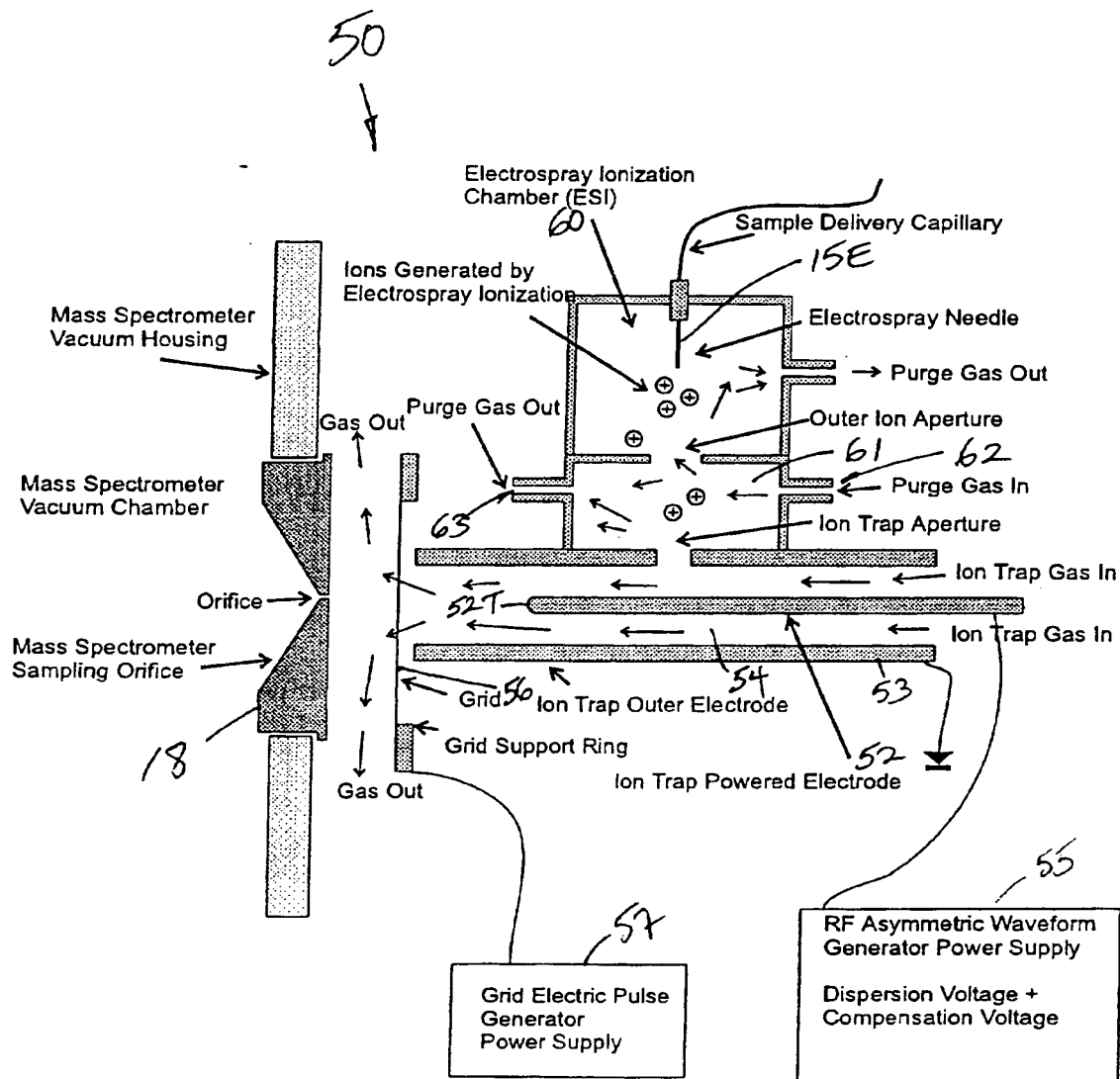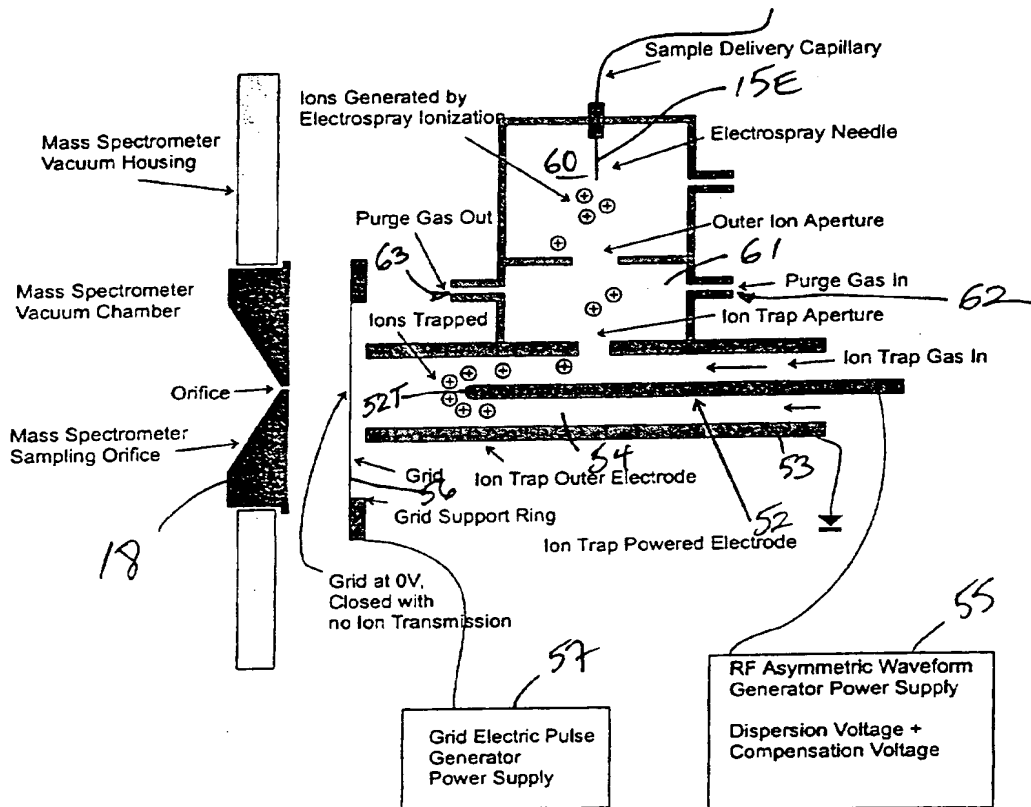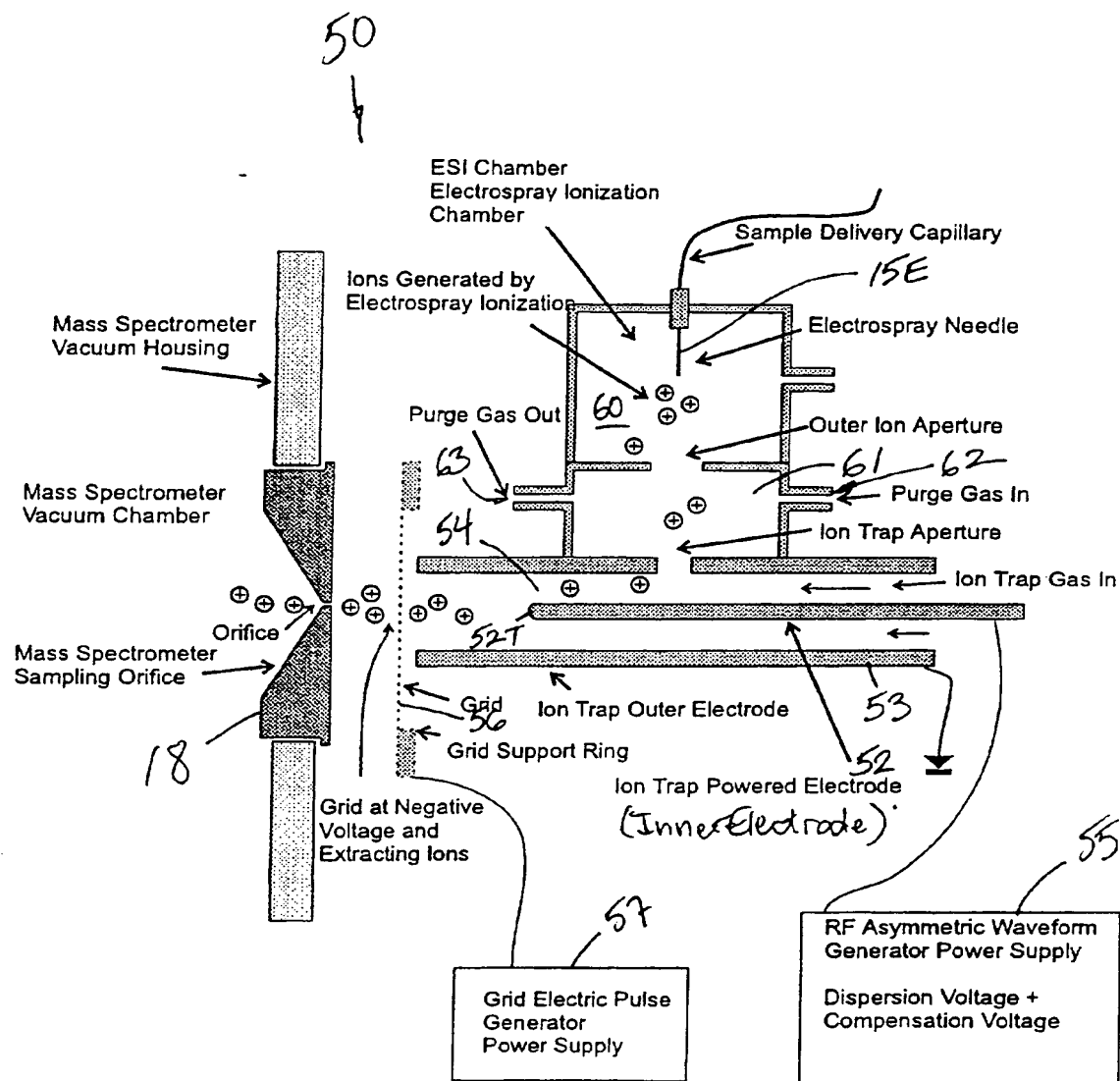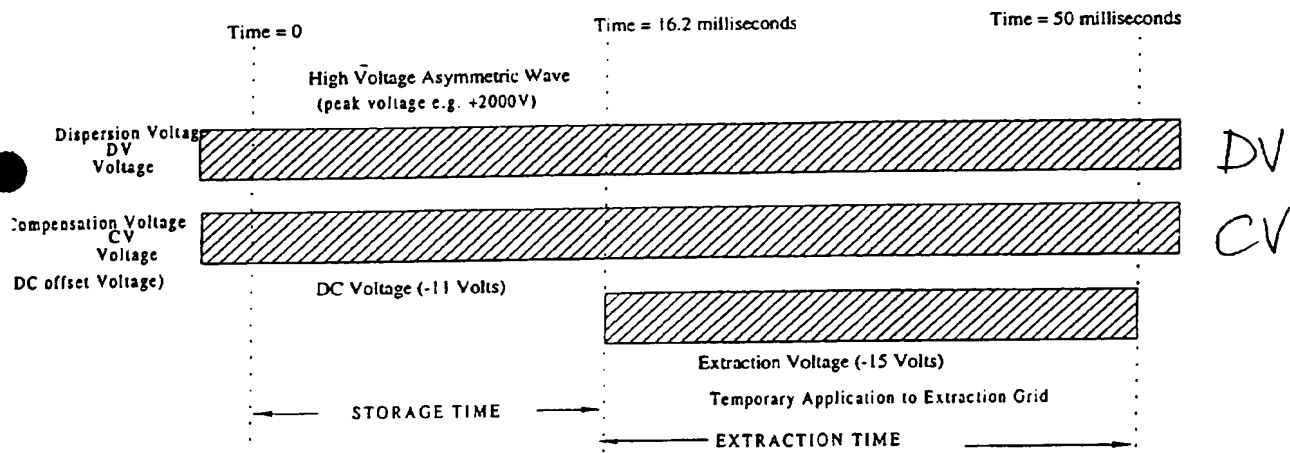The DV and CV Voltages are all applied to the center electrode.
The Extraction voltage is applied to the grid located in front of the
center electrode.

Time = 0   Time = 16.2 milliseconds   Time = 50 milliseconds

High Voltage Asymmetric Wave
(peak voltage e.g. +2000V)

Dispersion Voltage
DV
Voltage   DV

Compensation Voltage
CV
Voltage   CV

DC offset Voltage)

DC Voltage (-11 Volts)

Extraction Voltage (-15 Volts)

Temporary Application to Extraction Grid

⟵ STORAGE TIME ⟶   ⟵ EXTRACTION TIME ⟶

Details of the Asymmetric Waveform
(time and amplitude not to scale)

Dispersion Voltage (DV)
+2000 Volts

Compensation(CV) Voltage = DC offset Voltage

Compensation(CV) Voltage
DC offset Voltage

0 Volts

-400 Volts

5 microseconds

1 microsecond

Time = 0 milliseconds   Time = 16.2 milliseconds   Time = 50 milliseconds

Details of the Extraction Pulse applied to the Extraction Grid

0 Volts

-15 Volts

FIG. 11D

50

Mass Spectrometer
Vacuum Housing

ESI Chamber

Sample Delivery Capillary

Ions Generated by
Electrospray Ionization

Electrical
Insulation

Electrospray Needle

Mass Spectrometer
Vacuum Chamber

→ Purge Gas Out

60

Ion Trap Aperture and
Counter-current gas flow

18A

Ion Trap Gas In

Orifice

Mass Spectrometer
Sampling Orifice

52T

54

Ion Trap Outer Electrode

53

18

Electrical
Insulation

52

Sampling Orifice
serves as the extraction
grid

Ion Trap Powered Electrode

Grid Electric Pulse
Generator
Power Supply

RF Asymmetric Waveform
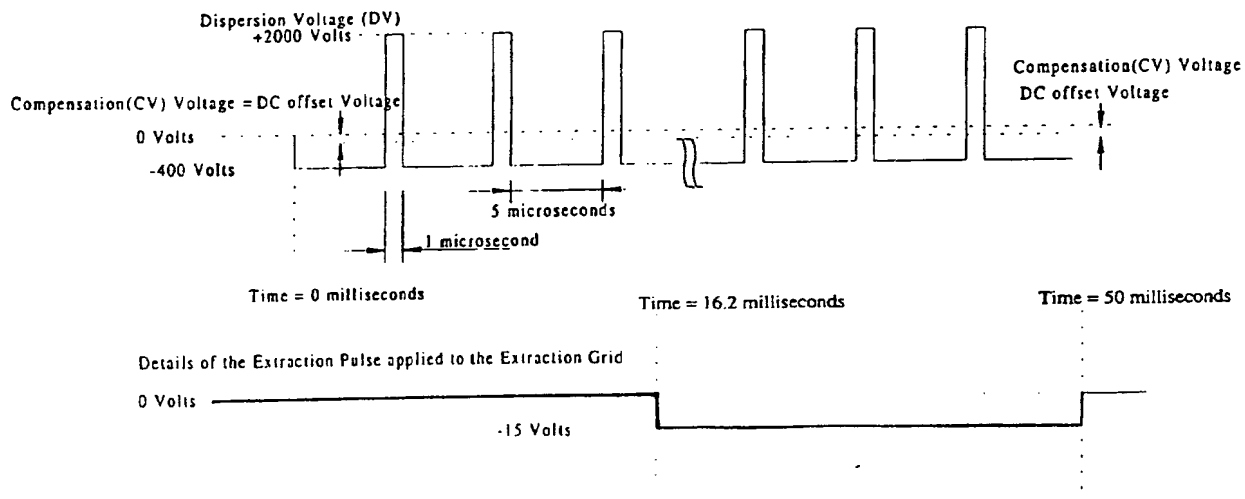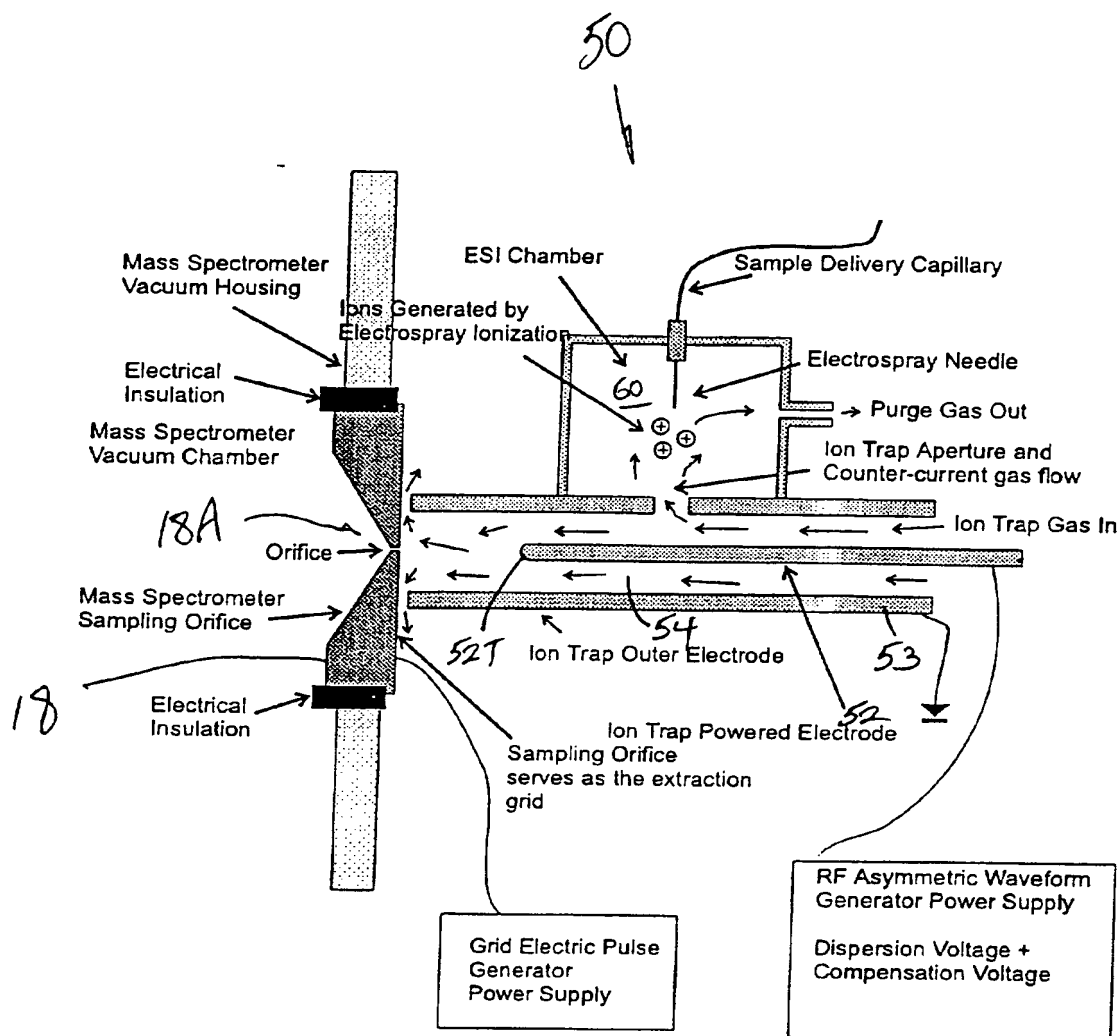Generator Power Supply

Dispersion Voltage +
Compensation Voltage

File: Diag_Trap_CounterGas1.c>r

FIG. 12

FIG. 13A

Timing Diagram for FAIMS Trap - TOF mass spectrometer

FAIMS offset voltage (dc)   +20 V

Asymmetric Waveform (ac)   DV -3500 (P2 mode)

Compensation Voltage (dc)   CV= -3 volts

Sampler Cone (OR) V_OR   +40 V   +1 V

Storage Period (40 msec)

Extraction Period (10 msec)

TOF Acceleration Region High Grid Pulse   -5 V   +1500 V   pulse width 50 usec

TOF Acceleration Region Low Grid Pulse   -5 V   +450V   pulse width 50 usec

FAIMS storage

Delay for ion transfer time (4.5 msec)

PulseTime1.cdr

FIG. 13B

TOF Mass Spectrum
Acceleration +1200 V
Flight 62 cm

27.0 usec

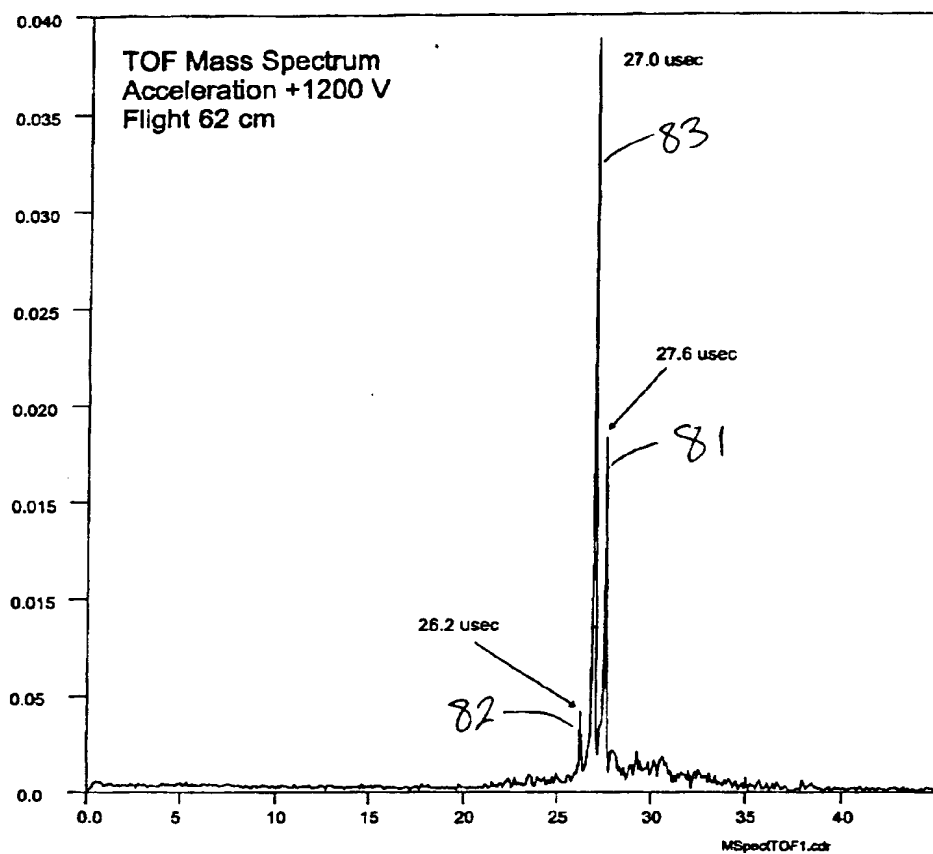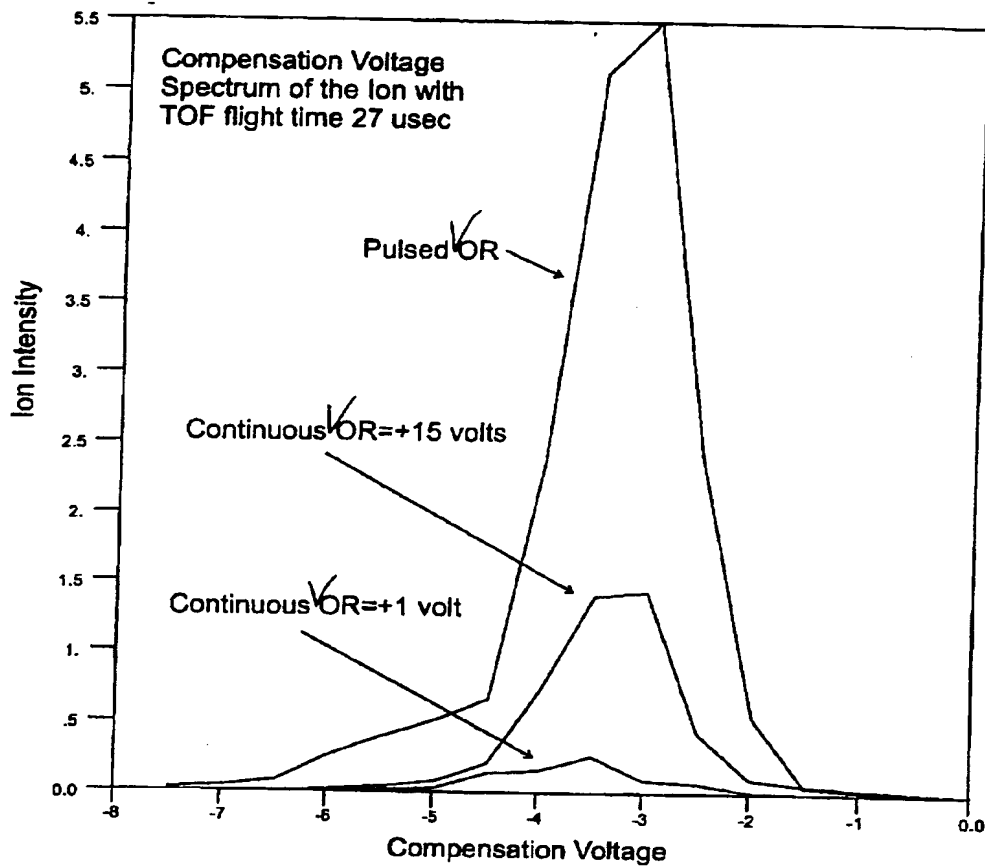83

27.6 usec

81

26.2 usec

82

MSpecTOF1.cdr

FIG 13C

FIG 13D

Response Time of Interface, Octopole, and TOF System

FIG 13E

Response for 27 usec Ion at
several delay times after opening
the Sampler Cone (OR)

Signal of TOF Ion 27 usec

Continuous, +15 V

Continuous, +1 V

Delay (msec)

ChaTOF1

Sampler Cone 'down'   Sampler Cone 'up'

+ 40 V

Storage in
Trap (40 msec)

+1 V

V_{OR}

Extraction from Trap (10 msec)

FIG 13F

Response for 27 usec Ion at
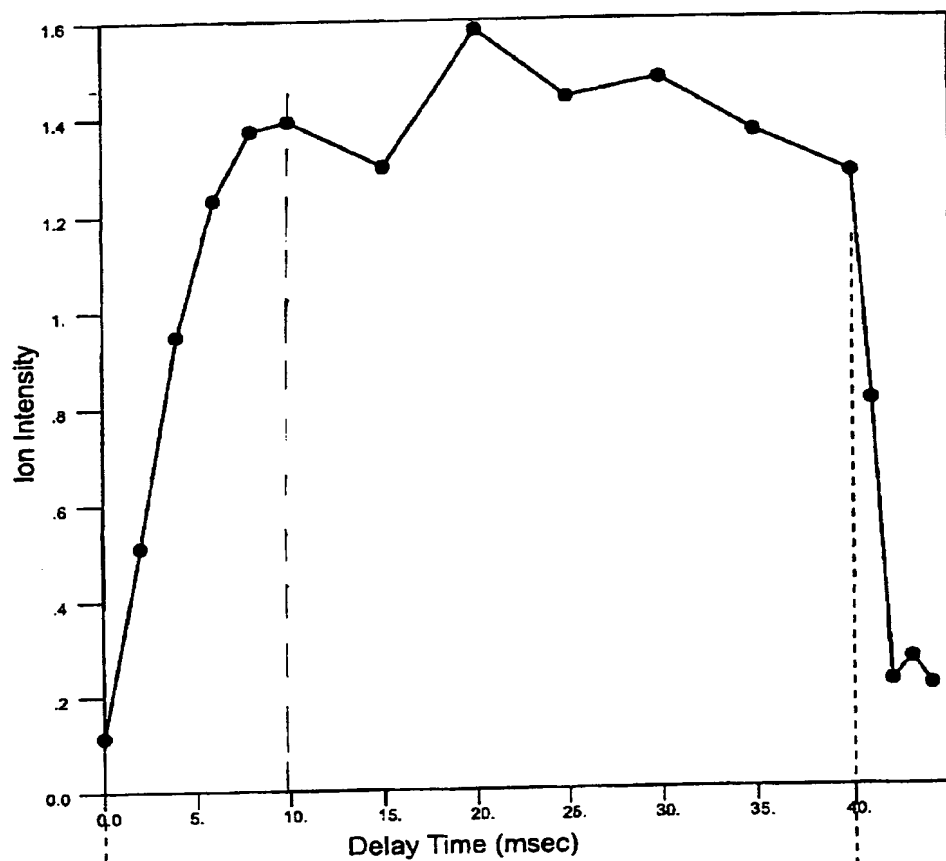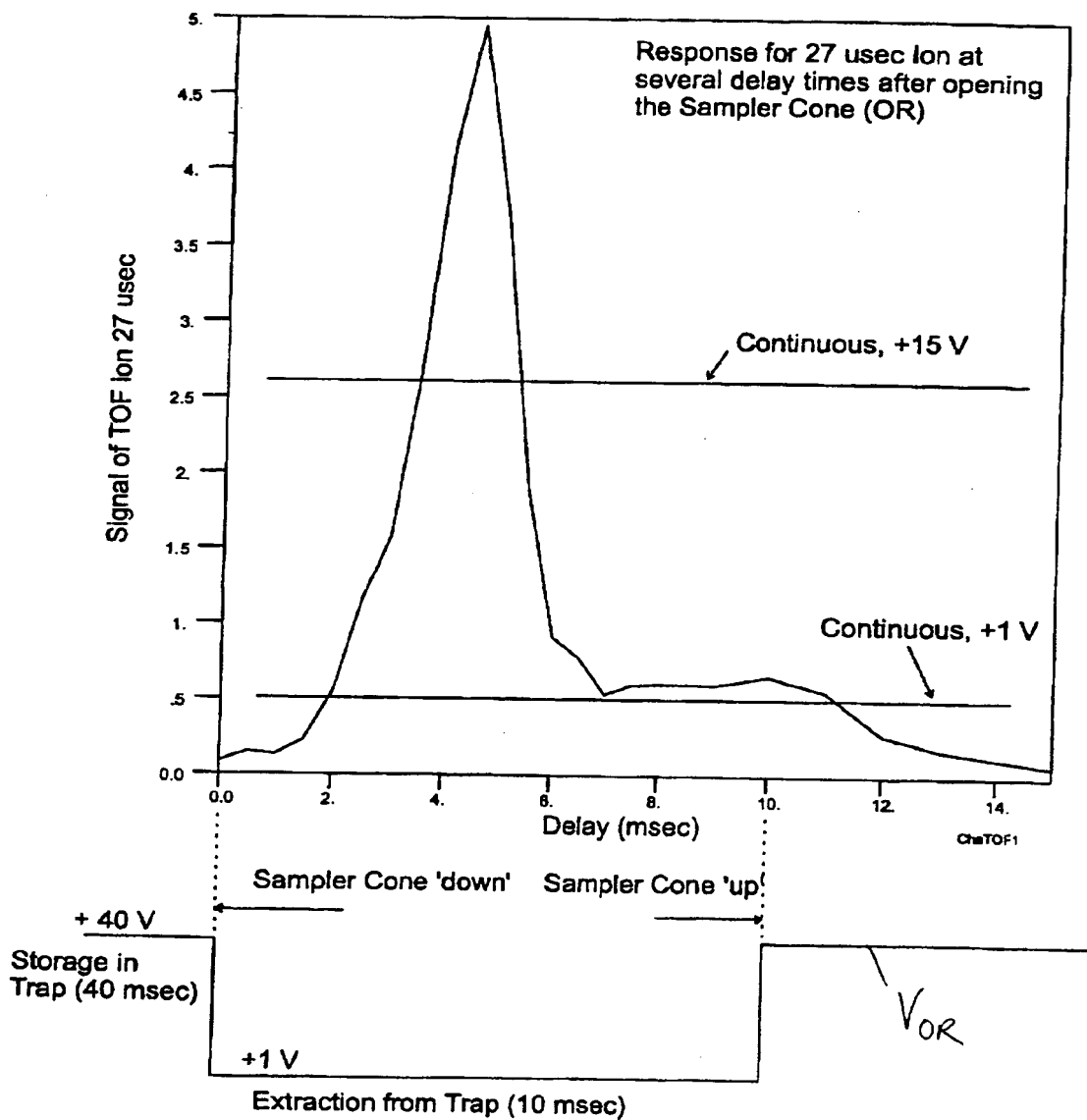several delay times after opening
the Sampler Cone (OR)

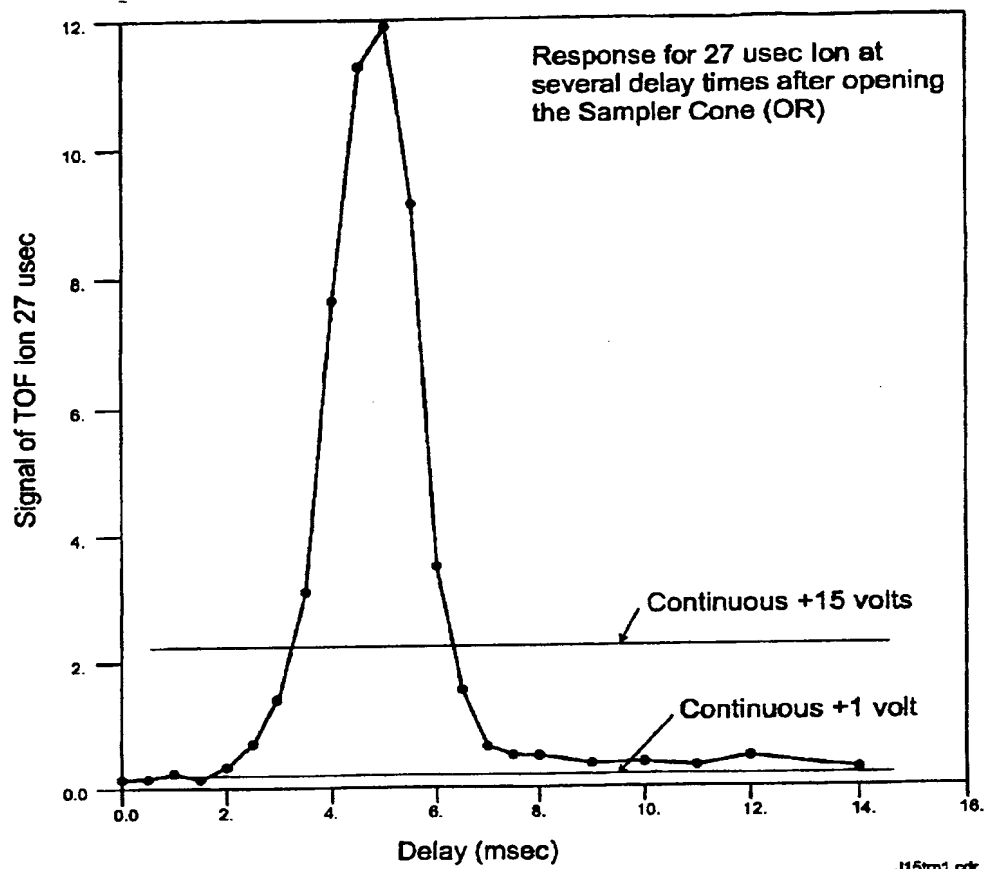FIG 13G

Intensity of TOF ion 27 usec after Storage Times up to 60 msec
Compensation Voltage = -3.0 V, Dispersion Voltage - 3500 V

Calculated with k=0.06, X=0.40

Ion Intensity (TOF ion 27 usec)

Storage Time (msec)

StoCV30.cdr

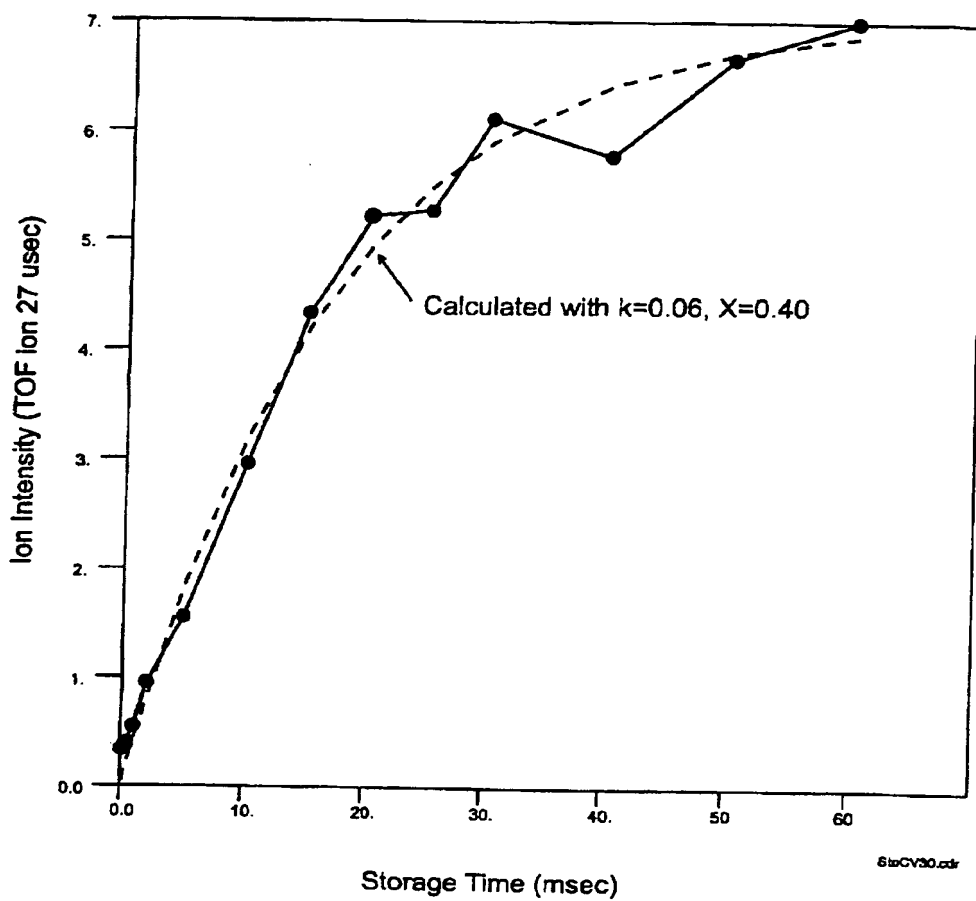FIG 13H

Intensity of TOF ion 27 usec after Storage Times up to 60 msec
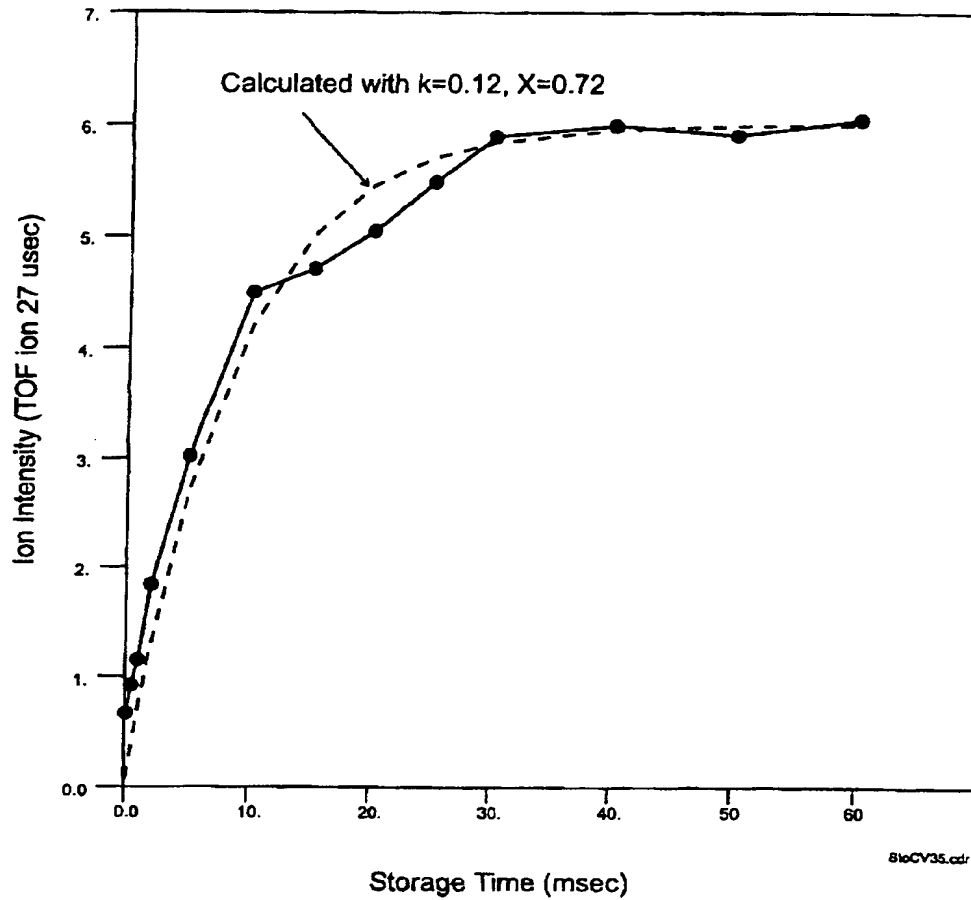Compensation Voltage = -3.5 V, Dispersion Voltage - 3500 V

Calculated with k=0.12, X=0.72

FIG 13 I

Intensity of TOF Ion 27 usec after Storage Times up to 60 msec
Compensation Voltage = -4.0 V, Dispersion Voltage - 3500 V

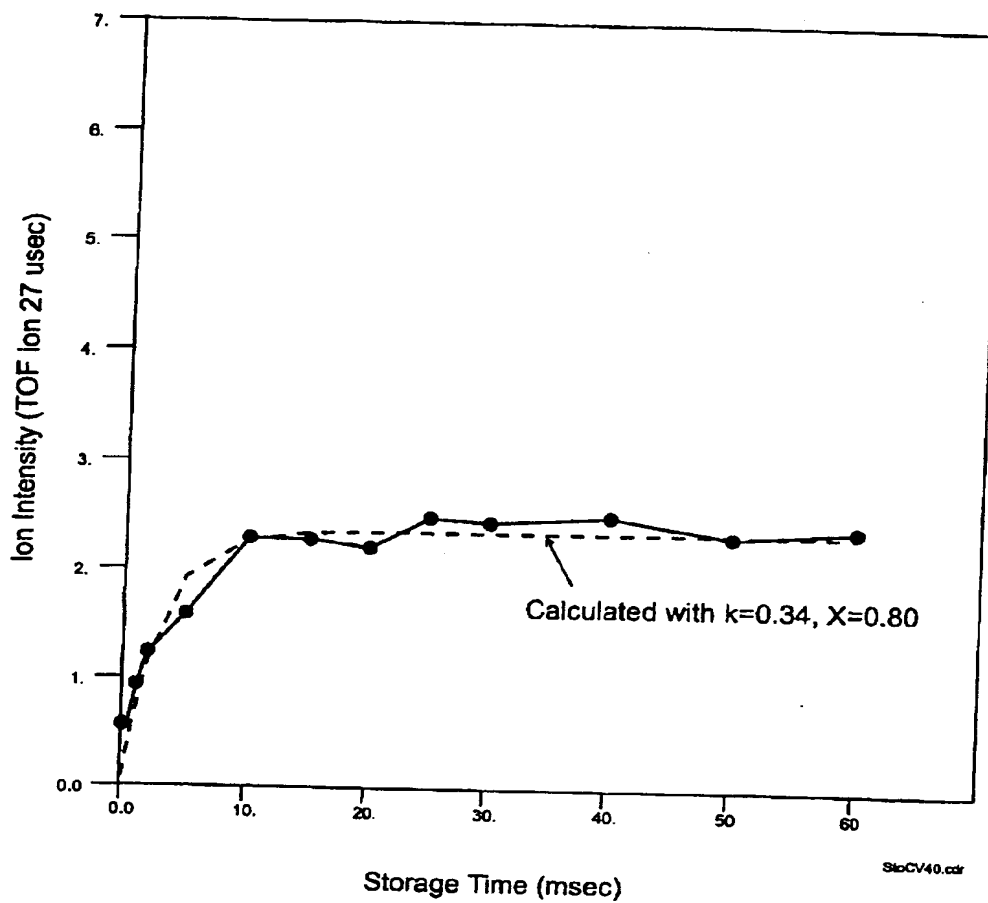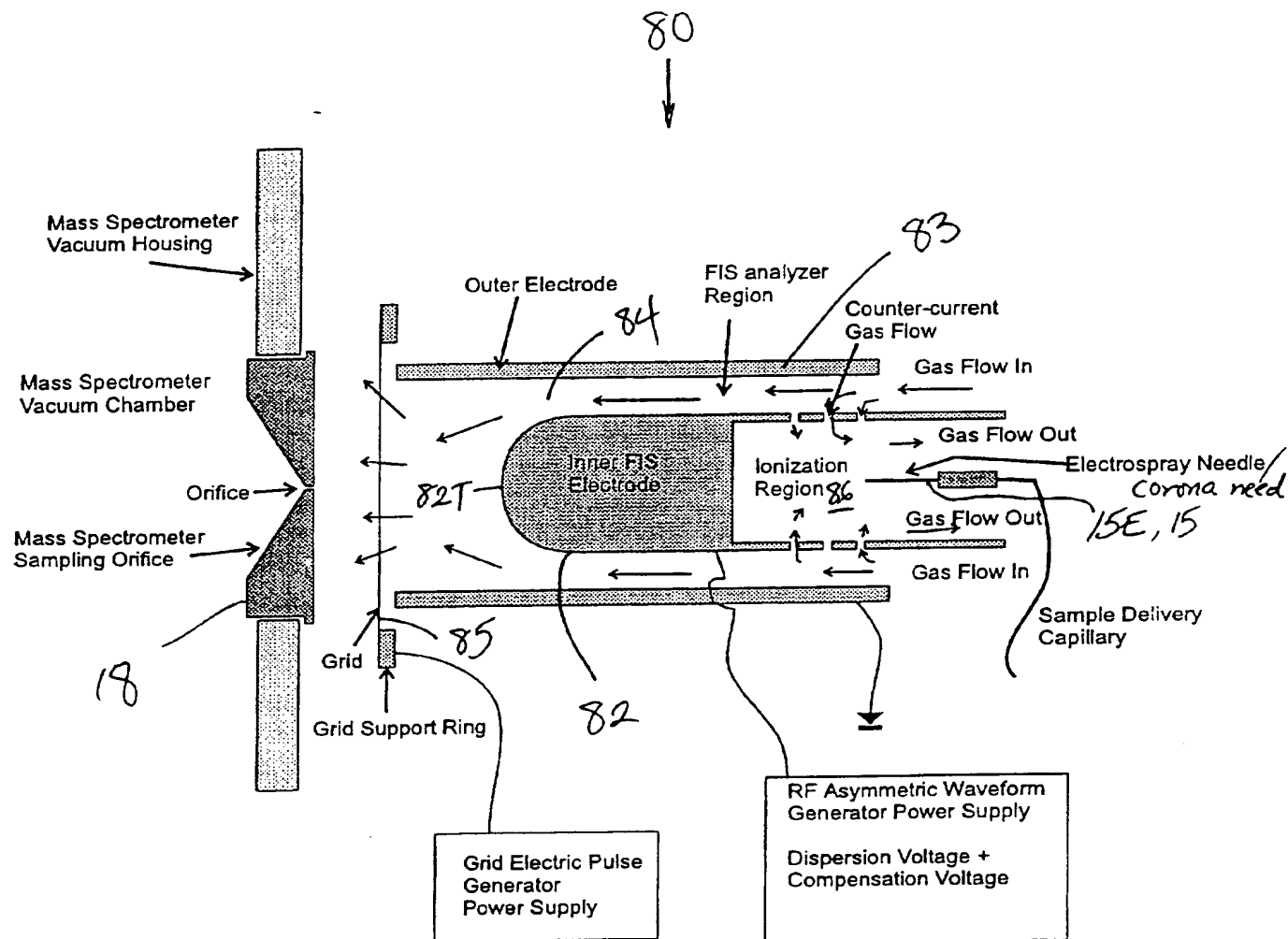Calculated with k=0.34, X=0.80

Storage Time (msec)

StoCV40.cdr

FIG. 13J

80

Mass Spectrometer
Vacuum Housing

Outer Electrode

FIS analyzer
Region

83

Counter-current
Gas Flow

Gas Flow In

84

Mass Spectrometer
Vacuum Chamber

Gas Flow Out

Inner FIS
Electrode

Orifice

82T

Ionization
Region 86

Electrospray Needle/
Corona need

15E, 15

Mass Spectrometer
Sampling Orifice

Gas Flow Out

Gas Flow In

Sample Delivery
Capillary

18

Grid

85

Grid Support Ring

82

RF Asymmetric Waveform
Generator Power Supply

Dispersion Voltage +
Compensation Voltage

Grid Electric Pulse
Generator
Power Supply

FIG. 14A

80

Mass Spectrometer
Vacuum Housing

84

Ions Trapped in front of Dome Shaped Electrode

Mass Spectrometer
Vacuum Chamber

Gas Flow In

Orifice

Gas Flow Out

82T

Ion Trap
Powered
Electrode

86

Electrospray Needle/corona needle

15E, 15

Mass Spectrometer
Sampling Orifice

Gas Flow Out

Gas Flow In

18

Grid

85

Sample Delivery
Capillary

Grid Support Ring

82   83

Grid Electric Pulse
Generator
Power Supply

RF Asymmetric Waveform
Generator Power Supply

Dispersion Voltage +
Compensation Voltage

FIG. 14B

80

Mass Spectrometer
Vacuum Housing

Grid Voltage at -15 V
to Extract ions away from Powered Electrode

84 Outer Electrode 83

Gas Flow In

Mass Spectrometer
Vacuum Chamber

Gas Flow Out

Electrospray Needle/corona needle

ISE, 15

Orifice

82

86

Gas Flow Out

Mass Spectrometer
Sampling Orifice

Gas Flow In

Sample Delivery
Capillary

18

Grid 85

Grid Support Ring

82

Grid Electric Pulse
Generator
Power Supply

RF Asymmetric Waveform
Generator Power Supply

Dispersion Voltage +
Compensation Voltage

FIG. 14C

FIS analyzer Region

Inner Cylinder, radius a

Outer Cylinder
radius b

FIS analyzer
region

a

r

b

Cross Secion
View
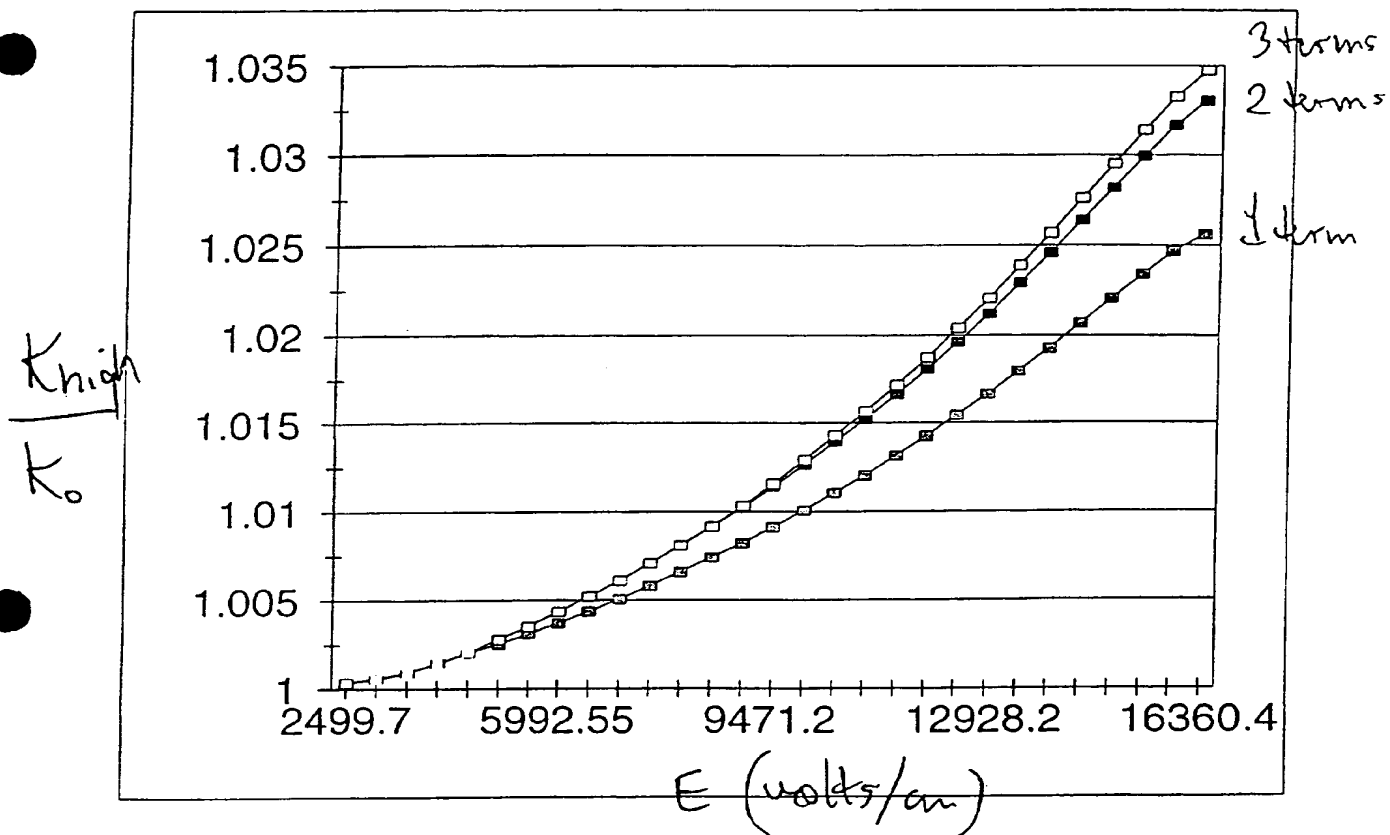
FIG. 15

$(H_2O)_2^+ H$ m/z 37

Best curve: $1.1207(E) + 1.2898 (E^2) + 0.99903$
$\times 10^{-5}$ $\times 10^{-10}$

FIG. 16

+100 volt increments HV = 2500V clea. a.

DV varied in 100 volt steps
CV scanned from -50 to Ø
corona, clean air
each peak = $(H_2O)_n H^+$

major

3000V

2100V

$(H_2O)_n H^+$ ion

Electrometer Output (pA)

Compensation Voltage (V)

(CV)

FIG. 17A

unknown
may be NO^+

$N_2(H_2O_n)H^+$ ions

Processing of DV and CV to get ratio of Mobility at high and low field
June 26/98

DATA of DV and CV of ion m/z 37

RATIO
$\frac{K \text{ high}}{K \text{ low}}$

Experimental Dispersion Voltage Voltage DV	Experimental Compensation Voltage CV	High Voltag Applied Actual	Electric Field volts/cm	Low Voltage Applied Actual	Electric Field volts/cm	RATIO Kmob(high
0	0	0	0	0	0	
500	-0.06	499.94	2499.7	-250.06	-1250.3	1.00036
600	-0.11	599.89	2999.45	-300.11	-1500.55	1.00055
700	-0.21	699.79	3498.95	-350.21	-1751.05	1.0009
800	-0.39	799.61	3998.05	-400.39	-2001.95	1.001463
900	-0.61	899.39	4496.95	-450.61	-2253.05	1.002035
1000	-0.85	999.15	4995.75	-500.85	-2504.25	1.002552
1100	-1.14	1098.86	5494.3	-551.14	-2755.7	1.003112
1200	-1.49	1198.51	5992.55	-601.49	-3007.45	1.00373
1300	-1.9	1298.1	6490.5	-651.9	-3259.5	1.004391
1400	-2.36	1397.64	6988.2	-702.36	-3511.8	1.005066
1500	-2.9	1497.1	7485.5	-752.9	-3764.5	1.005811
1600	-3.51	1596.49	7982.45	-803.51	-4017.55	1.006596
1700	-4.19	1695.81	8479.05	-854.19	-4270.95	1.007412
1800	-4.92	1795.08	8975.4	-904.92	-4524.6	1.008222
1900	-5.76	1894.24	9471.2	-955.76	-4778.8	1.009122
2000	-6.7	1993.3	9966.5	-1006.7	-5033.5	1.010084
2100	-7.72	2092.28	10461.4	-1057.72	-5288.6	1.011069
2200	-8.8	2191.2	10956	-1108.8	-5544	1.012048
2300	-10.04	2289.96	11449.8	-1160.04	-5800.2	1.013153
2400	-11.36	2388.64	11943.2	-1211.36	-6056.8	1.014268
2500	-12.82	2487.18	12435.9	-1262.82	-6314.1	1.015463
2600	-14.36	2585.64	12928.2	-1314.36	-6571.8	1.016661
2700	-16.11	2683.89	13419.45	-1366.11	-6830.55	1.018007
2800	-17.88	2782.12	13910.6	-1417.88	-7089.4	1.01928
2900	-19.88	2880.12	14400.6	-1469.88	-7349.4	1.020707
3000	-21.91	2978.09	14890.45	-1521.91	-7609.55	1.022071
3100	-24.02	3075.98	15379.9	-1574.02	-7870.1	1.023427
3200	-26.12	3173.88	15869.4	-1626.12	-8130.6	1.024689
3300	-27.92	3272.08	16360.4	-1677.92	-8389.6	1.025598

File : DataDV_CV.wb3

More Detailed Files : CVDVmz_37_1.wb3
CV DVmz_37_2.wb3

FIG. 17B

Fields between tubes
June 25/98

Inner	0.1 cm	Vinner	2000	
Outer	0.3	Vouter	0	

A 02260572 1999-01-29

		0.99903	regression (3 terms)
		1.12E-07	
		1.29E-10	

Radius	Field E	E^2	Mobility
0.1	18204.78	3.31E+08	1.043816
0.105	17337.89	3.01E+08	1.039745
0.11	16549.8	2.74E+08	1.036212
0.115	15830.25	2.51E+08	1.033126
0.12	15170.65	2.3E+08	1.030415
0.125	14563.83	2.12E+08	1.028019
0.13	14003.68	1.96E+08	1.025893
0.135	13485.03	1.82E+08	1.023996
0.14	13003.42	1.69E+08	1.022296
0.145	12555.02	1.58E+08	1.020768
0.15	12136.52	1.47E+08	1.019388
0.155	11745.02	1.38E+08	1.018138
0.16	11377.99	1.29E+08	1.017003
0.165	11033.2	1.22E+08	1.015967
0.17	10708.7	1.15E+08	1.015021
0.175	10402.73	1.08E+08	1.014154
0.18	10113.77	1.02E+08	1.013357
0.185	9840.424	9.68E+07	1.012622
0.19	9581.466	9.18E+07	1.011945
0.195	9335.787	8.72E+07	1.011318
0.2	9102.392	8.29E+07	1.010737
0.205	8880.383	7.89E+07	1.010197
0.21	8668.945	7.52E+07	1.009694
0.215	8467.342	7.17E+07	1.009226
0.22	8274.902	6.85E+07	1.008789
0.225	8091.015	6.55E+07	1.00838
0.23	7915.124	6.26E+07	1.007998
0.235	7746.717	6E+07	1.007638
0.24	7585.327	5.75E+07	1.007301
0.245	7430.524	5.52E+07	1.006984
0.25	7281.914	5.3E+07	1.006685
0.255	7139.131	5.1E+07	1.006404
0.26	7001.84	4.9E+07	1.006138
0.265	6869.73	4.72E+07	1.005887
0.27	6742.513	4.55E+07	1.005649
0.275	6619.922	4.38E+07	1.005424
0.28	6501.709	4.23E+07	1.005211
0.285	6387.644	4.08E+07	1.005009
0.29	6277.512	3.94E+07	1.004816
0.295	6171.113	3.81E+07	1.004633
0.3	6068.262	3.68E+07	1.00446

FIG. 17C

Ion Trajectory DV2500 5:1 Ratio 83kHz P1 CV 0

FIG. 18A
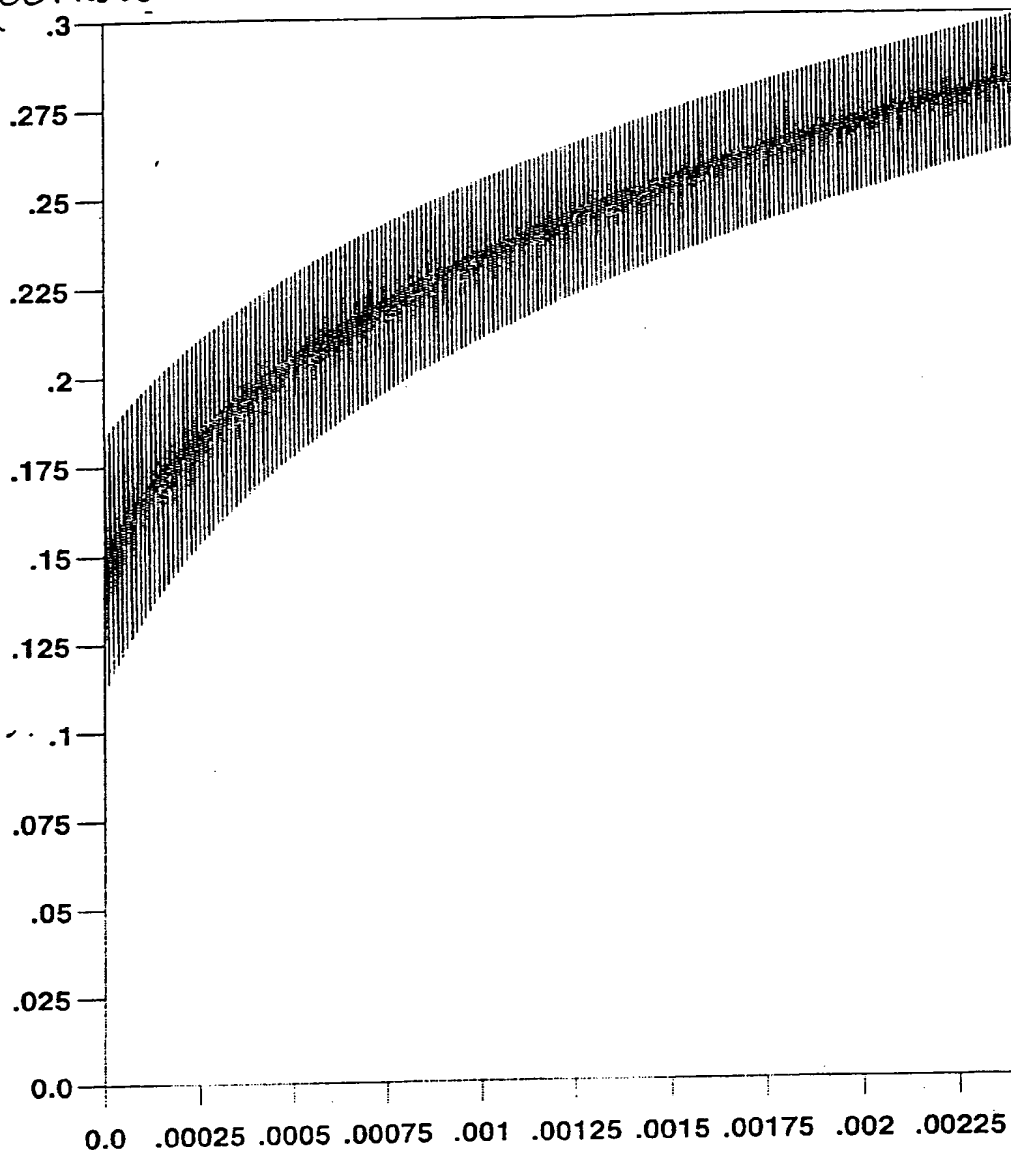
Ion Trajectory DV2500 5:1 Ratio 83kHz P1 CV 0

OUTER ELECTRODE

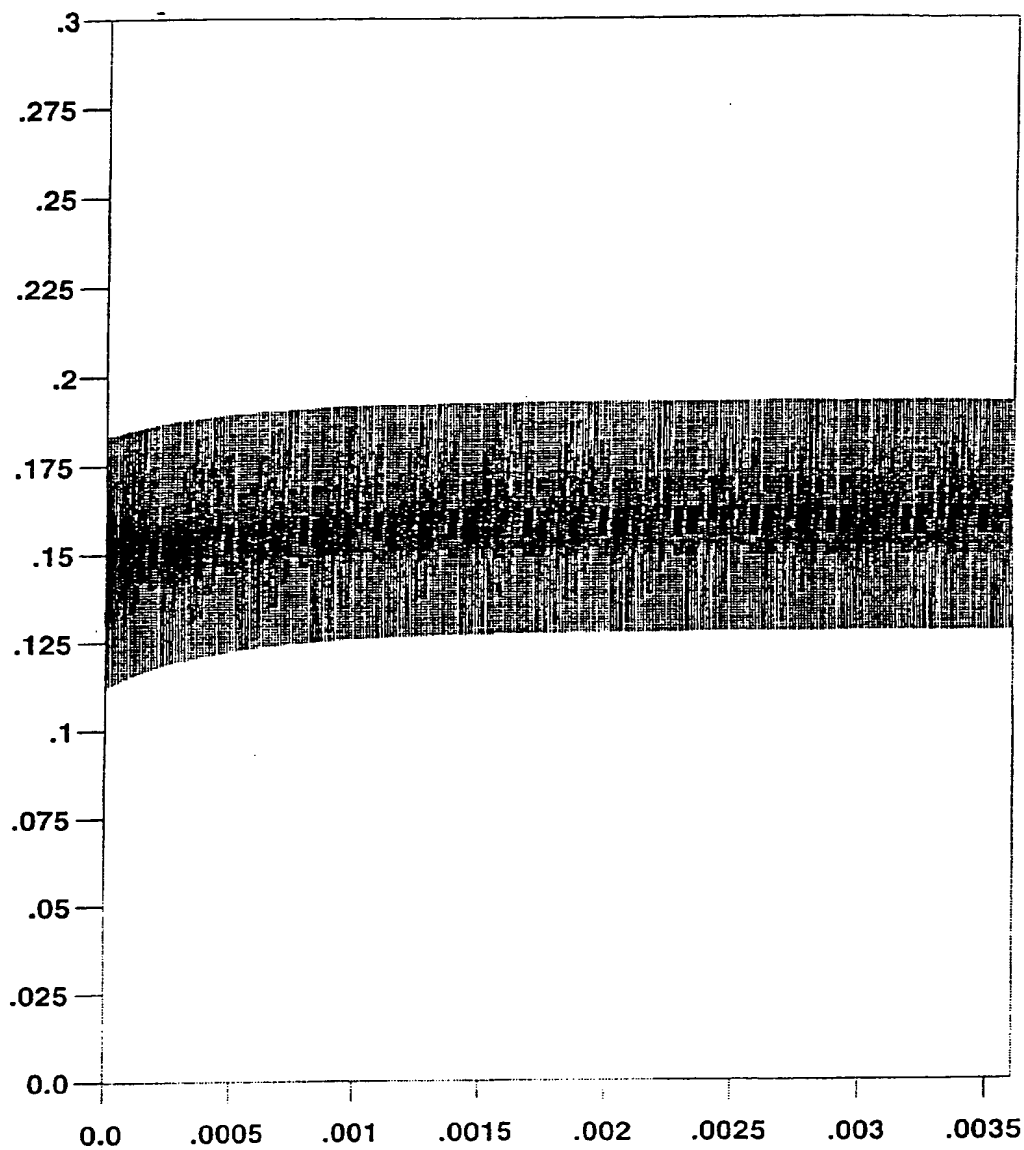Radial Distance (cm)

INNER ELECTRODE

Time (s)   FIG. 18B

Ion Trajectory DV2500 5:1 Ratio 83kHz P1 CV -11

FIG. 18C

Ion Trajectory DV2500 5:1 Ratio 83kHz P1 CV -11

FIG. 18D

Grid

54   GAS FLOW
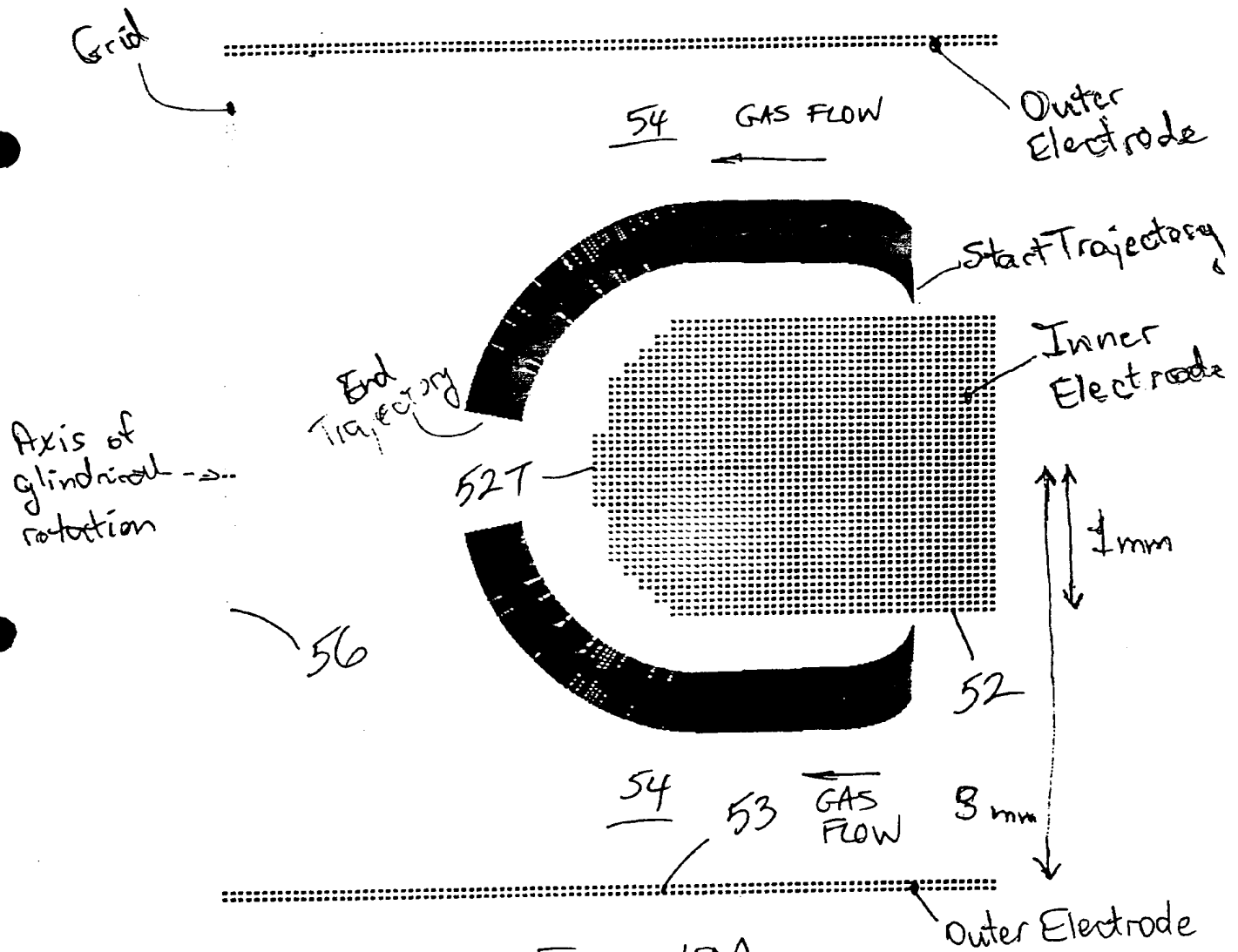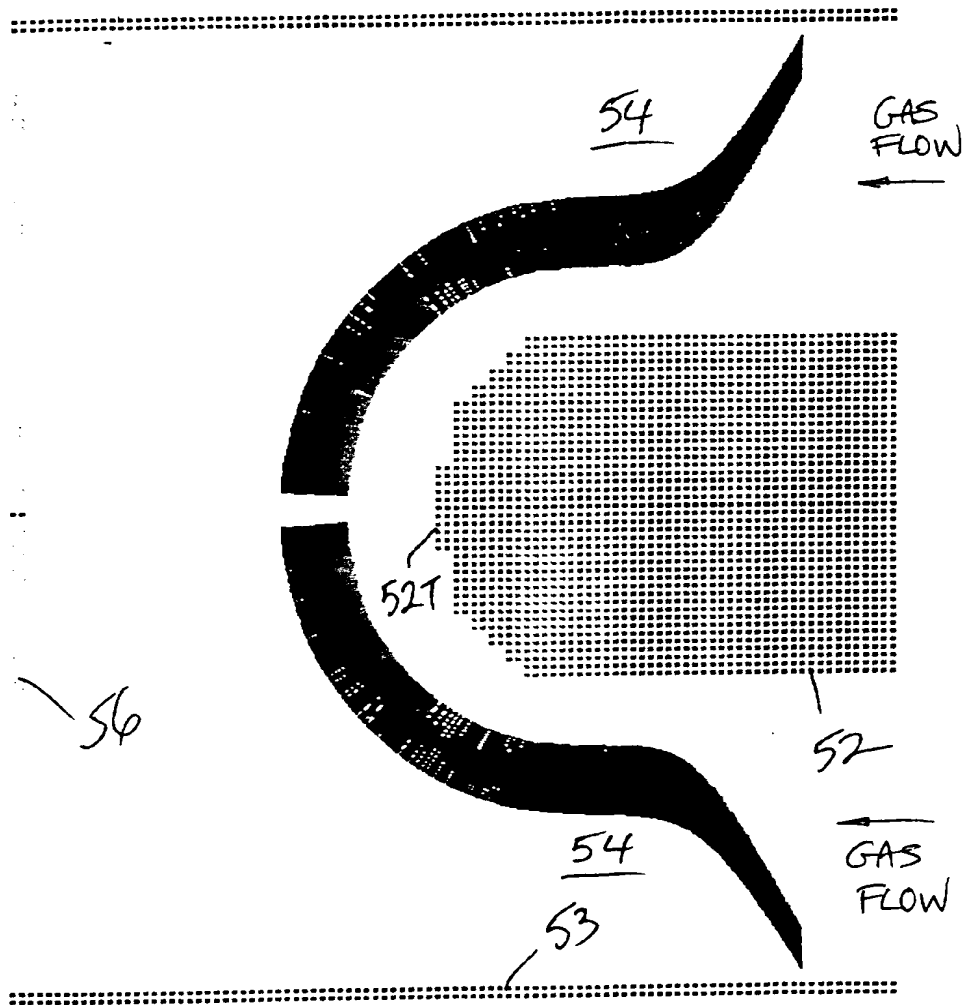
Outer
Electrode

Start Trajectory

Inner
Electrode

End
Trajectory

52T

Axis of
glindrical
rotation

1mm

56

52

54   53   GAS FLOW   8 mm

Outer Electrode

FIG. 19A

54

GAS
FLOW

52T

56

52

54

53

GAS
FLOW

FIG. 19B

54

GAS FLOW

56

52T

52

54

53

GAS FLOW

FIG. 19C

56

52T

52

53

GAS FLOW

GAS FLOW

FIG. 19D

FIG. 19E

$V_{OR} = -2.5$ volts

94

GAS FLOW

18A

92T

18

92

94

93

GAS FLOW

FIG. 19F

90

FIG. 19G

$V_{OR}=-7.5$ volts

94

GAS
FLOW

18A

92T

92

18

93

24

GAS
FLOW

A

FIG. 13H

90

V_{OR}=-15 volts

94   GAS
           FLOW

18A   92T

92

18

93   94   GAS
             FLOW

FIG. 19I

Gas Flow In

Focus Region

Gas Flow In

Trapping
Region

Gas Flow Out
through small
holes

Asymmetric
Waveform Generator

FIGURE 19J

FIG. 20A

FIG. 20B

Experimental Optimum DV,CV (H2O)H+ Ion
Regression Fit to Optimum is shown
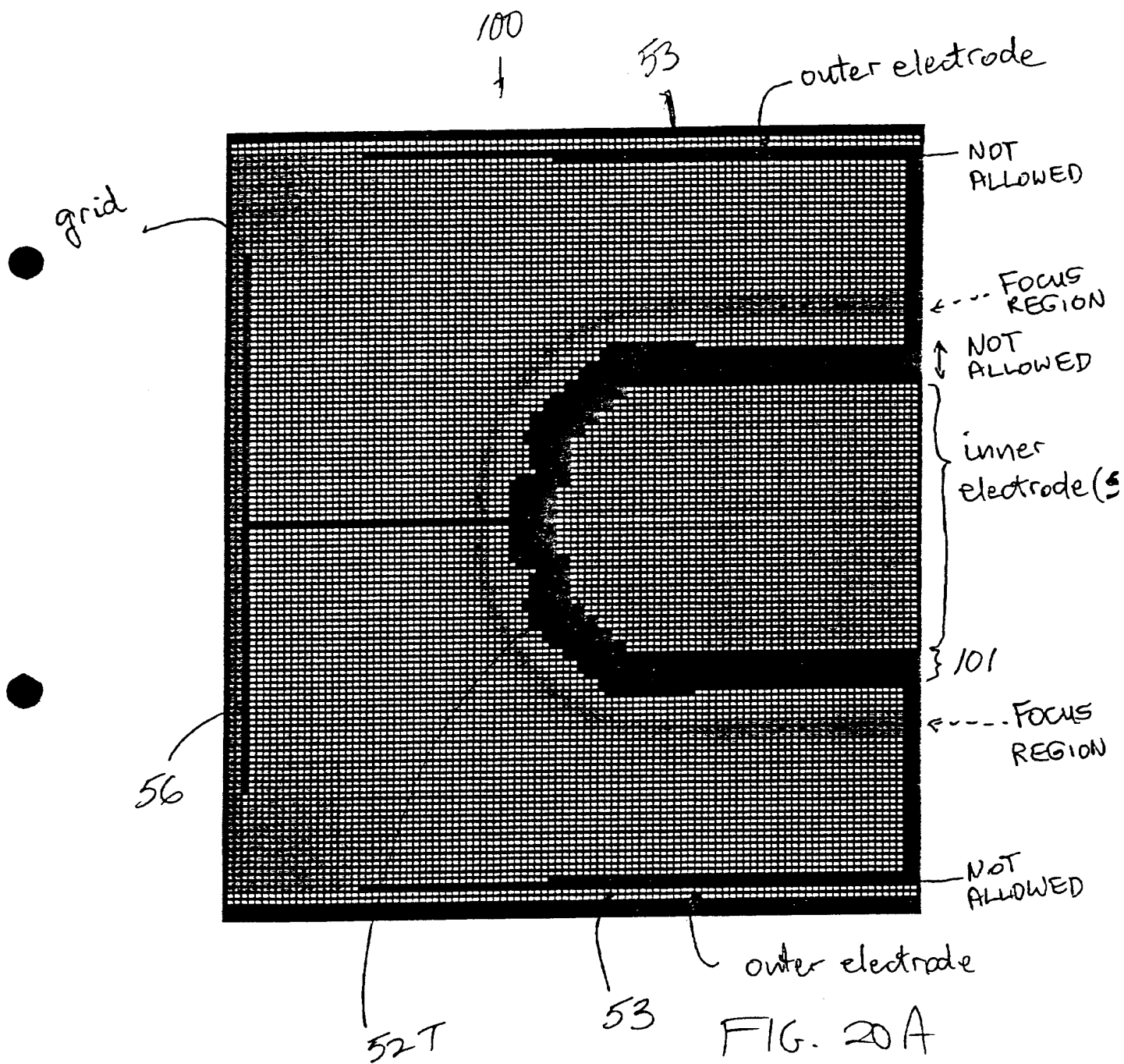

FIG. 21

FIG. 22A

Actual DV, CV Fields in FIS analyzer
DV2500,CV-12.82 radii= 0.7 and 0.9 cm

FIG . 22B

Comparison of Optimum/Actual E's
Actual DV2500,CV-12.82 rad=0.7 0.9 cm

FIG. 22C

Ions Traveling AGAINST
the gas flow direction because of the
dc field from the segments

Gas Flow In

Asymmetric
Waveform Generator

DC Offset Voltages for the
Segmented Inner Cylinder

DC Offset Voltages for the
Segmented Outer Cylinder

Not all of the segments in the outer
cylinder are shown

Not all of the electrical connections
to the segments are shown

The electronic means to add the dc
segment voltages to DV and CV is
not shown

FIG. 23

110

113

Ions that arrive in this segment cannot escape The Trap !

Outer FAIMS Electrode

112

Inner FAIMS Electrode

Outer Electrode dc voltages

+5 V   +2V   0 V   +2V   +5 V

112A   112B ⊕ ⊕   ⊕ 112C   112E
                        112 D

Inner Electrode final dc voltages

-7 V   -9 V   -12 V   -9 V   -7 V
113A   113B   113C   113D   113E

Conductors carry DV and CV and offset voltages for each segment on the inner electrode

Conductors carry offset voltages for each segment on the outer electrode

Asymmetric Waveform Generator

DC Offset Voltages for the Segmented Inner Cylinder

DC Offset Voltages for the Segmented Outer Cylinder

Not all of the electrical connections to the segments are shown

The electronic means to add the dc segment voltages to DV and CV is not shown
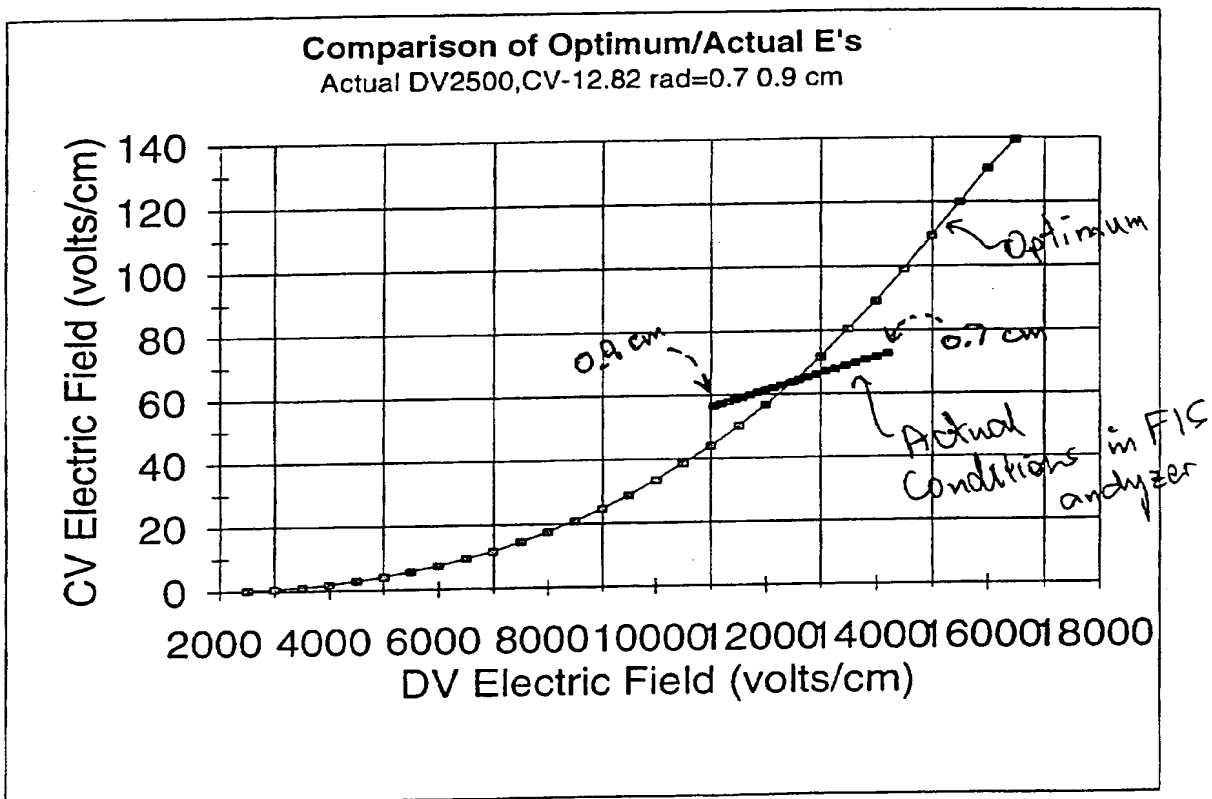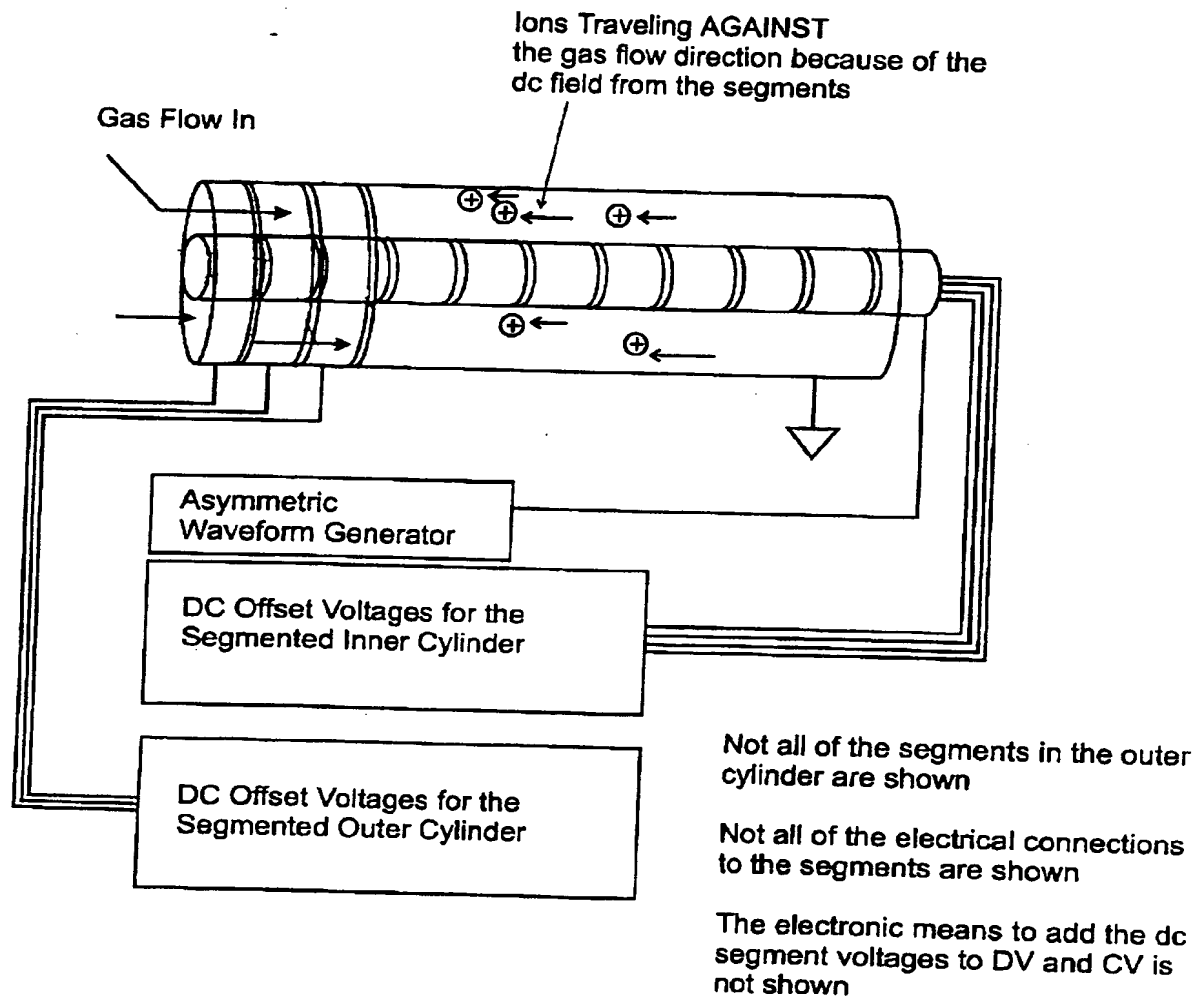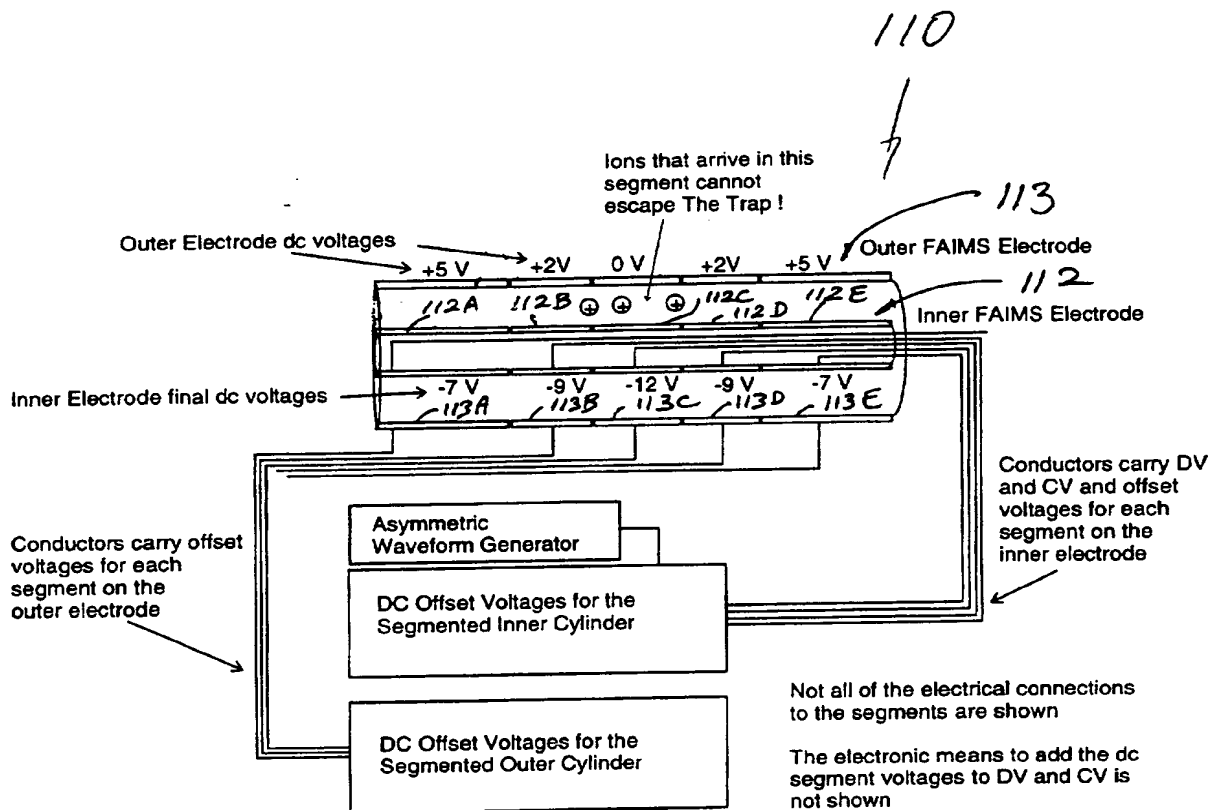
Typical Voltages for Inner and Outer Electrodes, Five Segments as shown in the Figure above

Outer Electrode	Inner Electrode DV	Inner Electrode CV	Inner Electrode Offset
+5	+2500	-12	+5
+2	+2500	-12	+2
+0	+2500	-12	+0
+2	+2500	-12	+2
+5	+2500	-12	+5

Example: inner electrode final applied dc voltage = CV+offset = -12 + 5 = -7 volts
Note: CV is still -12 since on that segment outer=+5, inner=-7, CV is difference = -12 volts

Seg_Trap_1.cdr

FIG. 24